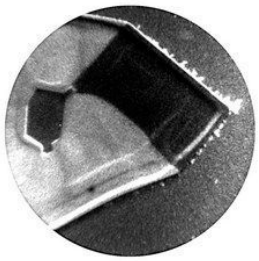

LEEM-PEEM 7
August 8-13, 2010
New York

Grand Hyatt Hotel New York
109 East 42nd Street at Grand Central Terminal,
New York, New York, USA 10017
Tel: +1 212 883 1234 Fax: +1 212 697 3772

FINAL PROGRAM

www.bnl.gov/leempeem7

SPONSORED BY:

IBM
SPECS Surface Nano Analysis GmbH
Center for Functional Nanomaterials BNL
National Synchrotron Light Source BNL
Elmitec GmbH
Omicron NanoTechnology GmbH
Focus GmbH
SmarAct GmbH

International Advisory Committee:

Michael Altman (Hong Kong)
Ernst Bauer (Arizona State)
Gary Kellogg (Sandia National Labs)
Takanori Koshikawa (Osaka, Japan)
Andrea Locatelli (Trieste, Italy)
Bene Poelsema (Twente, Netherlands)
Rudolf Tromp (IBM)

Distinguised Guest Lecturers:

Prof. Chuhei Oshima (Waseda University, Japan)
Prof. Phillip First (Georgia Institute of Technology)
Dr. Eli Rotenberg (Lawrence Berkeley National Laboratory)

Organizers:




Rudolf Tromp
IBM
rtromp@us.ibm.com

James Hannon
IBM
jbhannon@us.ibm.com

Jurek Sadowski
CFN
sadowski@bnl.gov

Peter Sutter
CFN
psutter@bnl.gov

Sunday August 8 – Grand Hyatt Hotel

1:00 pm: Tutorial on LEEM
Prof. Michael Altman
Hong Kong University

3:00 pm: Tutorial on (X)PEEM
Dr. Andreas Scholl
Lawrence Berkeley National Laboratory

The Tutorial will be held in the Broadway Room

11:00 am – 8:00 pm: Conference Registration and Welcome

8:00 pm – 10:00 pm

Welcome Reception

Grand Hyatt Hotel
Monday August 9 – Grand Hyatt Hotel

8:20 am – Welcome and Opening Remarks – R.M. Tromp

Morning Session: INSTRUMENTS AND METHODS
Chairs: T. Koshikawa, J. Falta

8:30 am: **Distinguished Guest Lecture**: **Single Atom Electron Sources**

Chuhei Oshima (Waseda University)

9:10 am: R. Yamaguchi, K. Terashima, K. Fukumoto, Y. Takada, M. Kotsugi, Y. Miyata, K. Mima, S. Komori, S. Itoda, Y. Nakatsu, M. Yano, N. Miyamoto, T. Nakamura, T. Kinoshita, Y. Watanabe, A. Manabe, S. Suga, S. Imada **;** Magnetic domain and chemical structures of Dy-doped Nd-Fe-B permanent magnet studied by PEEM and XMCD

9:30 am: Michael Horn von Hoegen; Ultrafast Electron Diffraction at Surfaces: From Ballistic heat Transport to Strongly Driven Transitions

9:50 am: : M. Kotsugi, M. Mizuguchi, T. Ohkouchi, T. Kojima, K. Takanashi, Y. Watanabe; Assignment of Local Magnetic Moment in L10-type FeNi Using Photo Electron Emission Microscopy (PEEM)

10:10 am: break

10:40 am: A. Scholl, A.T. Young, A. Doran, F. Yang, Y. Takamura, J. Wu, Z.Q Qiu, M. Burkhardt, S. Hossein, Q. He, R. Ramesh; Low Temperature Spectromicroscopy Using the Advanced Light Source PEEM-3

11:00 am: Müllerová, M. Hovorka and L. Frank: Scanning Transmission Low Energy Electron Microscopy

11:20 am: S.M. Schramm, A.B. Pang, M.S. Altman, R.M. Tromp: Image Formation in Aberration-Corrected LEEM and PEEM

11:40 am: R.M. Tromp, J.B. Hannon, A.W. Ellis, W. Wan, A. Berghaus, O. Schaff
A New Aberration-Corrected LEEM/PEEM Instrument

12:00 : break for lunch

Monday August 9 – Grand Hyatt Hotel

Afternoon Session: SURFACES
Chairs: A.K. Schmid, S.J. van der Molen

1:30 pm: E. Hilner, A.A. Zakharov, J.N. Andersen, E. Lundgren,A. Mikkelsen
Influence of Au Nano Particles on the Self-Propelled Motion of Mesoscopic Droplets

1:50 pm: W.X. Tang, D.E. Jesson, J. Tersoff; Surface Dynamics during Langmuir Decomposition of GaAs

2:10 pm: T.R.J. Bollmann, R. van Gastel, B. Poelsema
Stress Driven Growth and Substrate Interaction of Pb Islands on Ni(111)

2:30 pm: Nicola Ferralis, Farid El Gabaly, Andreas K. Schmid, Roya Maboudian, Carlo Carraro; Real-Time Observation of Reactive Spreading of Gold on Silicon

2:50 pm: E. Bussmann, F. Cheynis, F. Leroy, P. Müller; Dewetting of Silicon-on-Insulator thin films measured by Low Energy Electron Microscopy

3:10 pm: break

3:40 pm: J. Falta, Th. Schmidt, M. Speckmann, I. Heidman, J.I Flege, A. Locatelli, T.O. Menteş, M.A. Niño, P. Sutter; Tailoring of Vicinal Silicon Surface and Nanostructure Formation

4:00 pm: Ivan Ermanoski and G.L Kellogg; LEEM, LEED, and LEEM-IV investigations of iron oxide thin films on YSZ(001)

4:20 pm: Ivan Ermanoski, G.L Kellogg, N.C. Bartelt; Defect-Free Stripe Arrays on B-doped Si(001)

4:40 pm: K.L. Man, A.B. Pang, M.S. Altman; Adatom-Vacancy Mechanisms of Step Motion on the Si(111)-(1x1) Surface

5:00: End of today's program

Tuesday August 10 – Grand Hyatt Hotel

Morning Session 1: MAGNETISM
Chair: E. Bauer

8:30 am: Y. Kotani, T. Taniuchi, M. Osada, T. Sasaki, M. Kotsugi, Y. Watanabe, K. Ono Attogram X-ray Spectroscopy of Molecularly Thin Ferromagnetic Transition Metal Oxide Nanosheets

8:50 am: T. Koshikawa, M. Suzuki, M. Hashimoto, T. Yasue, Y. Nakagawa, A. Mano, N. Yamamoto, M. Yamamoto, T. Konomi, M. Kuwahara, S. Okumi, T. Nakanishi, X.G. Jin, T. Ujihara, Y. Takeda, T. Kohashi, T. Oshima, T. Saka, T. Kato, H. Horinaka, E. Bauer Dynamic Observation of Magnetic Domains with Novel Spin-polarized LEEM

9:10 am: K.M. Man, A. Pavlovska, M.S. Altman, E. Bauer, S.K. Lok, I.K. Sou, G. Wong, A. Locatelli, T.O. Menteş, M.A. Niño; Fe Nanowires on ZnS(100)

9: 30 am: Adrian Quesada, A.K. Schmid, G. Chen, J. Li, Y.Z. Wu; The Magnetic Stripe Phase in Fe/Ni/Cu(100): Reversible Transition and Domain Wall Spin Structure

9:50 am: A. Kaiser, C. Wiemann, S. Cramm, C. Tieg, C.M. Schneider; Layer-Specific Magnetization Dynamics in Spin-Valve Systems Revealed by Time-Resolved PEEM

10:10 am: M. Hjort, A.A. Zakharov, M.T. Borgström, R. Timm, J.N. Andersen, E. Lundgren, L. Samuelson, A. Mikkelsen; Combined PEEM, LEEM, and XPS Studies of III-V Semiconductor Nanowires

10:30 am: Break and poster session

12:00 am: Break for lunch

Tuesday August 10 – Grand Hyatt Hotel

Morning Session 2: Poster Session (Chair: J. Sadowski)

P1. A.M. Clausen, C.S. Ritz, C. Euaruksakul, K. Saenger, D. Savage, M.G. Lagally; Probing Local-Stressor Induced Conduction Band Changes in Si Nanoribbons and Membranes

P2. E. Starodub, N.C. Bartelt, K.F. McCarty; The Reaction of Oxygen with Graphene on Ir and Ru

P3. R. van Gastel, I. Sikharulidze, S. Schramm, J.P Abrahams, B. Poelsema, R.M. Tromp, S.J. van der Molen; Medipix 2 Detector Applied to Low Energy Electron Microscopy

P4. A. Locatelli, T.O. Menteş, M.A. Niño, E. Bauer; Space Charge in XPEEM under Micro-focused Illumination with Synchrotron Radiation

P5. F. Nickel, A. Kaiser, I. Krug, S. Cramm, C. Wiemann, A. Schmid, A. Berghaus, O. Schaff, and C.M. Schneider; Commissioning af the New Aberration-Corrected, Energy-Filtered PEEM/LEEM Endstation at BESSY

P6. H. Setoyama, D. Yoshimura, T. Okajima; Installation and Obtained Performance of PEEM System at the BL10 of SAGA-LS

P7. S.M. Kennedy, C.X. Zheng, W.X. Tang, D.M. Paganin, D.E. Jesson; Laplacian and Caustic Imaging of Surface Topography in Mirror Electron Microscopy

P8. R.M. Tromp; Aberrations of a Cathode Objective Lens

P9. B. Borkenhagen, H. Döscher, G. Lilienkam, Th. Hannappel, W. Daum; Anit-Phase Domain Inspection of III-V on Silicon by Low Energy Electron Microscopy

P10. H.M. Ghomi, U. Lanke, A. Odeshi; XPEEM Investigation of Adiabatic Shear Bands in Metallic Alloys

P11. J.I. Flege, A. Meyer, B. Kaemena, S. Senanayake, F. Alamgir, F. Falta; In-situ Characterization of Bimetallic Oxidation and Oxide Thin-Film Growth using Intensity-Voltage Low Energy Electron Microscopy

P12. T. Nakagawa, T. Yokoyama; Magnetic Domain Imaging by Laser PEEM_ Two Photon Photoemission and Energy Dependence

P13. U.D. Lanke, T. Walker, V. Olorunda, M. Stauffer, A. Odeshi, M. Quann, A. Trevors, S. Mason, A. O'Reilly, P. MacDonald, T. Saulnier, A. Riebel, J. d'Entremont, E.Flett, K. Cripps; Detection of Magnetic Circular Dichroism in an Extraterrestial Object_ X-ray Photo Emission Electron Microscopy Study of an Iron Meteorite

P14. Q. Wu, Y.R. Niu, R. Zdyb, A. Pavlovska, E. Bauer, M.S. Altman; SPLEEM Investigations of Fe Films on the W(111) Surface

P15. Shuaihua Ji, J. B. Hannon, R. M. Tromp, A. W. Ellis, M. C. Reuter and F. M. Ross; Surface Electrochemical Potential Mapping of Graphene on SiC(0001)

P16. S. Oida, F.R. McFeely, J.B. Hannon, R.M. Tromp, M. Copel, Z. Chen, Y. Sun, D.B. Farmer, J. Yurkas; Decoupling Graphene from SiC by Oxidation

P17. Stephen Christensen, Brian Haines, Uday Lanke, Stephen Urquhart; Secondary Electron Emission Microscopy and Partial - Yield X - ray Absorption Spectromicroscopy with an Energy Filtered PEEM Microscope

P18. S. Günther, M. Kronseder, G. Woltersdorf, C.H. Back; Threshold photoemission magnetic circular dichroism of Ni(001) films: theory and experiment

P19. Hongwen Liu, N. Fukui, H.T. Yuan, L. Zhang, Y. Iwasa, T. Hitosugi, M.W. Chen, T. Hashizume, Q.K Xue; Growth of topological insulator Bi2Te3 ultrathin films on Si(111) investigated by LEEM

P20. W. Swiech, E Samman and C. P. Flynn; Pulse-probe studies using delayed LEEM and LEED following an ion beam pulse

P21. R. Yamaguchi, K. Terashima, K. Fukumoto, Y. Takada, M. Kotsugi, Y. Miyata, K. Mima, S. Komori, S. Itoda, Y. Nakatsu, M. Yano, N. Miyamoto, T. Nakamura, T. Kinoshita, Y. Watanabe, A. Manabe, S. Suga, S. Imada **;** Magnetic domain and chemical structures of Dy-doped Nd-Fe-B permanent magnet studied by PEEM and XMCD

Tuesday August 10 – Grand Hyatt Hotel

Afternoon Session 1: LASER BASED PEEM
Chair: M. Horn von Hoegen

1:30 pm: Erik Mårsell, T. Fordell, M. T. Borgström, A. L'Huillier and A. Mikkelsen; PEEM studies of surface plasmons in nanostructures using femtosecond and attosecond IR/XUV laser pulses

1:50 pm: A.Höfer, S. Förster, K. Duncker, and W. Widdra; Laser - excited PEEM study of the temperature dependent ferroelectric domain structures of BaTiO3(001)

2:10 pm: T. Taniuchi, K. Isogai, Y. Kotani, T. Togashi, H. Akinaga, K. Ono, M. Oshima, S. Shin; Measurement System of UV-PEEM using Wavelength Tunable Femto-Second Laser

2:30 pm: N.M. Buckanie, P. Kirschbaum, S. Sindermann, F.-J. Meyer zu Heringdorf Interaction of Surface Plasmon Polaritons with Ag Islands as Imaged in Two Photon Photoemission PEEM

2:50 pm: Break and Continuation of Poster Session

4:30 pm: End of program for today

Evening Options:

Blue Note

Wednesday August 11 – IBM T.J. Watson Research Center

7:20 am: Leave Hyatt Hotel by Bus (Breakfast on the Bus)
9:00 am: Arrive at T.J. Watson Research Center

9:30 am: Welcome by Director of Physical Sciences Supratik Guha

Morning Session: GROWTH AND THIN FILMS
Chair: Th. Schmidt

9:40 am: B. Poelsema, G. Hlawacek, F.S. Khokhar, R. van Gastel, C. Teichert; Organic Semiconductor Growth on Graphene Studied by LEEM and μLEED

10:00 am: . A. Al-Mahboob, Y. Tsuruma, J.T. Sadowski, Y. Fujikawa, K. Saiki, T. Hashizume, T. Sakurai, P. Sutter; The Nucleation and Anisotropic Growth of Pn on SiO_2 and FET Structures

10:20 am: M. Vaughn, K.D. Jamison, M.E. Kordesch; Thermionic Electron Emission Microscopy of Ba, Sc, Y, Zr, To and Mg Oxide Multilayers on Tungsten

10:40 am: A. Sala, H. Marchetto, Th. Schmidt, H.-J. Freund; LEEM/LEED Investigation of Fe_3O_4 Thin Film Growth on a Pt(111) Substrate: Morphology and Atomic Termination

11:00 am: T.O. Menteş, A. Locatelli, M.A. Niño, E. Bauer, A. Pavlovska, M. Lewandowski, I.M.N. Groot, S. Shaikhutdinov, H.-J. Freund; The System $Au/Fe_2O_3/Pt(111)$

11:20: I. Krug, N. Barrett, A. Petraru, O. Renault, K. Rahmanizadeh, G. Bihlmayer, L. LeGuyader, A. Besmehn, H. Kohlstedt, C.M. Schneider; Electronic vs. Defect-induced Self-stabilization of Ferroelectric Polarization in Thin PZT Films

11:40 am: Break for Lunch

Wednesday August 11 – IBM T.J. Watson Research Center

Afternoon Session: ELECTRONIC STRUCTURE
Chair: A. Locatelli

1:00 pm: Distinguished Guest Lecturer: Dr. E. Rotenberg (Lawrence Berkeley National Laboratory)
(title to be filled in)

1:40 pm: C. Mathieu, N. Barrett, Y. Mi, O. Renault, N. Weber, B. Vilquin; Recent Advances in Bandstructure Imaging by k-PEEM

2:00 pm: N.B. Weber, M. Escher, M. Merkel, K. Winkler; k-Space Imaging in Photoelectron Microscopy: Comparison of Band-pass and High-pass Energy Filter Approaches

2:20 pm: A.A. Zakharov, C. Virojanadara, S. Watcharinyanon, R. Yakimova, L.I. Johansson; 3D (k_x-k_y-E) Band Mapping by using X-ray Photoelectron Emission Microscope

2:40 pm: Break and Conference Photograph

3:20 pm: JEOPARDY (Erik Brown)

4:10 pm: BLUE GENE (Ruud Haring)

3:20 pm: Group 1 Lab Tours
4:10 pm: Group 2 Lab Tours

Lab Tours:

IBM LEEM-II (Jim Hannon)

IBM/SPECS Aberration Corrected LEEM (Ruud Tromp)

In-Situ UHV-TEM (Frances Ross)

5:00 pm – 5:45 pm Selection LEEMPEEM 2012

5:45 pm: End of Scientific Program for Today.

Wednesday August 11 Evening – Crabtree Kittle House

11 Kittle Road
Chappaqua, NY 10514-1800
(914) 666-8044

CONFERENCE BANQUET

6:30 pm: Cocktails and Jazz

7:30 – 10:00 pm: Conference Banquet

10:30 pm: Return to Grand Hyatt New York

Thursday August 12 – Grand Hyatt Hotel

Morning Session: **GRAPHENE**
Chairs: B. Poelsema, M.Altman

8:20 am: Distinguished Guest Lecturer: Dr. Phillip N First; STM Studies of Graphene Thin Films

9:00 am: Qiang Fu, Yi Cui, Hui Zhang, Xinhe Bao; Dynamic Characterization of Graphene Growth on Ru(0001)

9:20 am: A.T. N'Diaye, R. van Gastel, A.J. Martínez-Galera, J. Coraux, H. Hattab, D. Wall, F.-J. Meyer zu Heringdorf, M. Horn-von Hoegen, J.M. Gómez-Rodríguez, B. Poelsema, C. Busse, Th. Michely; Steering the Growth and Watching the Strain of Epitaxial Graphene on Iridium(111)

9:40 am: P. Sutter, J. Sadowski, E. Sutter; Graphene on Transition Metals – Growth and Interface Physics

10:00 am: J. Sun, J.B. Hannon, R.M. Tromp, P. Johari, A.A. Bol, V.B. Shenoy, K. Pohl; Spatially Resolved Structure and Electronic Properties of Graphene on Polycrystalline Ni

10:20 am: Break

10: 50 am: A.A. Zakharov, K.V. Emtsev, U. Starke; Decoupling Epitaxial Graphene from SiC(0001) Surface by a Germanium Buffer Layer

11:10 am: S. Nie, J.M. Wofford, N.C. Barlelt, K.F. McCarty, O.D. Dubon; Real-time Analysis of Graphene Growth on Polycrystalline Copper Foils

11:30 am: K. McCarty, A.L. Walter, E. Starodub, S. Nie, K. Thürmer, K. Horn, A. Bostwick, N.C. Bartelt, E. Rotenberg; Second-layer Graphene on Ir(111) –Relating Growth Mechanism to Physical and Electronic Structure

11:50 am: T. Ohta, N.C. Bartelt, S. Nie, K. Thürmer, G.L. Kellogg; The Role of Carbon Surface Diffusion on the Growth of Epitaxial Graphene on SiC

12:10 pm: FINAL REMARKS AND CONCLUSION

Thursday August 12 - BROOKHAVEN NATIONAL LABORATORY
CENTER FOR FUNCTIONAL NANOMATERIALS
NATIONAL SYNCHROTRON LIGHT SOURCE

Immediately after the conclusion of the formal LEEM-PEEM 7 program, there will be an opportunity to visit the Center for Functional Nanomaterials (CFN) as well as the National Synchrotron Light Source (NSLS) in Brookhaven, NY. Both facilities, under the umbrella of the United States Department of Energy, feature state-of-the-art LEEM and PEEM capabilities, in addition to numerous other sample processing and characterization capabilities. CFN is housed in a brand-new, spacious, and well-equipped building near NSLS, and offers users (under an open application user program) ample opportunities for interaction and unique experiments. NSLS has long been a powerhouse in the international world of synchrotron radiation, and with construction of NSLS-II, a new and powerful third generation synchrotron facility under way, Brookhaven will continue to be a much sought-after location for cutting edge science.

PLEASE REGISTER ON MONDAY IF YOU WANT TO JOIN THIS VISIT!

Thursday August 12 :VISIT TO CNF/BNL AGENDA

12:45 pm	Depart from Grand Hyatt Hotel, NYC	
2:30 pm	Welcome and Overview of CFN	Emilio Mendez
2:40 pm	Overview of NSLS and NSLS-II	Chi-Chang Kao
2:50 pm	Group Photo and Coffee Break	
3:15 pm	Tour of CFN	
4:15 pm	Tour of NSLS	
5:15 pm	Adjourn	
7:00 pm	Arrive at Grand Hyatt Hotel, NYC	

Friday August 13 – IBM T.J. Watson Research Center

LEEM/PEEM Tutorial: Experimental Session

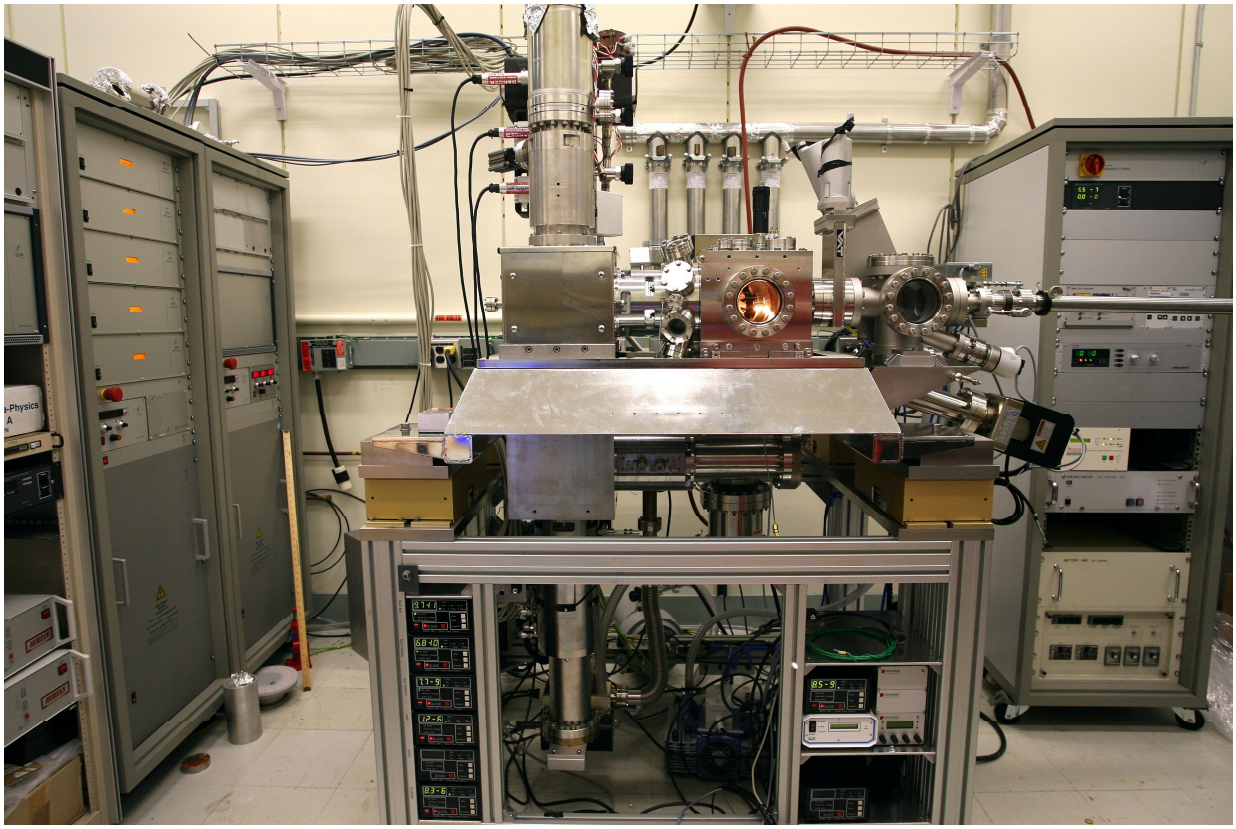

Rudolf M. Tromp
James B. Hannon

Grand Hyatt Hotel
Monday August 9 – Grand Hyatt Hotel

8:20 am – Welcome and Opening Remarks – R.M. Tromp

Morning Session: INSTRUMENTS AND METHODS
Chairs: T. Koshikawa, J. Falta

8:30 am: **Distinguished Guest Lecture**: **Single Atom Electron Sources**

Chuhei Oshima (Waseda University)

9:10 am: R. Yamaguchi, K. Terashima, K. Fukumoto, Y. Takada, M. Kotsugi, Y. Miyata, K. Mima, S. Komori, S. Itoda, Y. Nakatsu, M. Yano, N. Miyamoto, T. Nakamura, T. Kinoshita, Y. Watanabe, A. Manabe, S. Suga, S. Imada **;** Magnetic domain and chemical structures of Dy-doped Nd-Fe-B permanent magnet studied by PEEM and XMCD

9:30 am: Michael Horn von Hoegen; Ultrafast Electron Diffraction at Surfaces: From Ballistic heat Transport to Strongly Driven Transitions

9:50 am: : M. Kotsugi, M. Mizuguchi, T. Ohkouchi, T. Kojima, K. Takanashi, Y. Watanabe; Assignment of Local Magnetic Moment in L10-type FeNi Using Photo Electron Emission Microscopy (PEEM)

10:10 am: break

10:40 am: A. Scholl, A.T. Young, A. Doran, F. Yang, Y. Takamura, J. Wu, Z.Q Qiu, M. Burkhardt, S. Hossein, Q. He, R. Ramesh; Low Temperature Spectromicroscopy Using the Advanced Light Source PEEM-3

11:00 am: Müllerová, M. Hovorka and L. Frank: Scanning Transmission Low Energy Electron Microscopy

11:20 am: S.M. Schramm, A.B. Pang, M.S. Altman, R.M. Tromp: Image Formation in Aberration-Corrected LEEM and PEEM

11:40 am: R.M. Tromp, J.B. Hannon, A.W. Ellis, W. Wan, A. Berghaus, O. Schaff
A New Aberration-Corrected LEEM/PEEM Instrument

12:00 : break for lunch

Single-Atom Electron Sources

Chuhei Oshima

Department of Applied Physics, Waseda University, 3-4-1 Okubo, Shinjuku-ku Tokyo 169-0072, Japan

coshima@waseda.jp

Here, I talk about present situation of a practical single-atom electron source. Because of the collimated emission from a single atom at the top of the nano-pyramids, single-atom electron sources processes the excellent characteristic features of electron emission as follows,

1) High brightness; we estimated to be 10^{10} A/cm^2/str. (Ep =1-2keV and I_T=10nA).
2) Highly collimated electron beam; the emission angle of ±2 degree (FWHM).
3) Highly spatial coherency owing to the extremely narrow area.
4) Demountable character; the electron source can be transfer- red to one chamber to the others through air without fatal damage.

In comparison with the conventional nano-tips or ultra-sharp tips, in addition, three excellent characters are recognized, because of their thermodynamically stable atomic structures.

1) The unique relation between the emission direction and crystal orientation. One can control the direction precisely.
2) Repairing function; if the tip apex is broken or modified by ion bombardment and chemisorptions, the heat treatment recovers repeatedly the apex because of thermodynamically stable character.
3) The atom located at the top of the apex emits the electron currents of 20 nA-1μA.

On the basis of those emission properties of the single-atom electron source, we tried to develop a practical electron gun. The research subjects are as follows,

1) Clarification of fundamental emission characters (energy widths of the beam, spatial coherence, etc.).
2) Clarification of the lifetime and enlargement.
3) Development of beam alignment technique and the evaluation method.
4) Decreasing noise (mechanical vibration, electro- magnetic noise, fluctuations of potentials supplied with controllers
5) Application of the gun to electron microscope.

The results are as follows:

1) The life time of 500hr at emission current of an order of 10nA, which corresponds to the brightness of 10^{10}A/cm.str. (1.5kV).
2) The accuracy of beam alignment of 0.2 degree,
3) A permalloy gun chamber with a base pressure of 1 x 10^{-9}Pa.

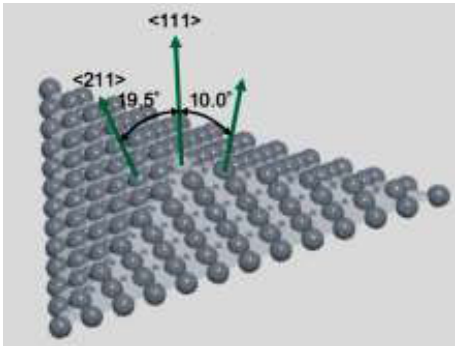

Fig.1 Schematic diagram of atomic structure of a nano-pyramids. The collimated electron beam is emitted from the single atom at the top.

Magnetic domain and chemical structures of Dy-doped Nd-Fe-B permanent magnet studied by PEEM and XMCD

R. Yamaguchi[a], K. Terashima[a], K. Fukumoto[b,c d], Y. Takada[c], M. Kotsugi[b], Y. Miyata[a], K. Mima[a], S. Komori[e,f], S. Itoda[e], Y. Nakatsu[e], M. Yano[e,f], N. Miyamoto[f], T. Nakamura[b], T. Kinoshita[b], Y. Watanabe[b], A. Manabe[f], S. Suga[e], S. Imada[e,a]

[a] *Department of Physical Sciences, Ritsumeikan University, Kusatsu, Shiga 525-8577, Japan*

[b] *Japan Synchrotron Radiation Research Institute (JASRI), Sayo, Hyogo 679-5198, Japan*

[c] *Toyota Central Research & Development Laboratories, Inc., Nagakute, Aichi 480-1192, Japan*

[d] *Department of Materials Science, Tokyo Institute of Technology, Meguro-ku, Tokyo, 152-8550, Japan*

[e] *Department of Materials Physics, Osaka University, Toyonaka, Osaka 560-8531, Japan*

[f] *Toyota Motor Corporation, Toyota, Aichi 471-8571, Japan*

Permanent magnet is becoming much more important than ever particularly as a main part of motor used for hybrid and electric cars. Especially, tolerance to higher temperatures is important in development of permanent magnets. It has been known that Dy-doping makes Nd-Fe-B magnet much more tolerant to heat. It is expected that formation of reversed domains is suppressed by Dy doping. In order to reveal the mechanism for this, it is necessary to observe the formation of reversed domains focusing on the relation between the chemical structure and the magnetic domain structure.

Reversed domains are expected to be formed first on the surface of the permanent magnet. Therefore, photoelectron emission microscope (PEEM) is a powerful tool for the study of reversed domains. Combination of PEEM with monochromatized synchrotron radiation enables x-ray photoabsorption spectromicroscopy, by which chemical distribution on the surface can be measured. Further combination of PEEM with circularly polarized synchrotron radiation enables x-ray magnetic circular dichroism (XMCD) microscopy, by which magnetic domain structure can be observed.

The strong stray magnetic field produced by a magnetized permanent magnet sample, however, has so far disabled the observation by PEEM. In this study, the permanent magnet sample has been attached to a yoke without gaps, so that the stray field on the surface of the sample was reduced to less than 10 gauss. This has enabled the observation of the magnetic domain structure of the fully magnetized Nd-Fe-B magnet by PEEM. Experiments have been performed at BL17SU and BL25SU in SPring-8.

The magnetic domain structures of surfaces parallel to the c axis of $Nd_2Fe_{14}B$ grains in the samples have been studied. We first compared, at the room temperature, the sample without and with Dy doping. On the sample without Dy doping, the observed reversed domains were connected across several grains in the direction of c axis. On the other hand, on the Dy doped sample, the total area of the reversed domains as well as the size of each reversed domain was smaller than those of non-doped sample. More importantly, each reversed domain tended to be confined within a grain. Next, the effect of heat on the Dy doped sample has been studied. When the temperature was raised, the reversed domains became longer in the c axis, growing across grains. Above T = 80 °C, the total area of the reversed domains increased drastically, and the shapes of the reversed domains became much wider and became interconnected. The relation between these changes in domain structures and the chemical distribution will be discussed.

Ultrafast Electron Diffraction at Surfaces: From Ballistic Heat Transport to Strongly Driven Phase Transitions

Michael Horn von Hoegen
Department of Physics, University of Duisburg-Essen, 47057 Duisburg, Germany
horn-von-hoegen@uni-due.de

Abstract

The multitude of possible processes that can occur at surfaces cover many orders of magnitude in the time domain. While large scale growth and structure formation, for instance, happens on a timescale of minutes and seconds, diffusion is already much faster, but can still be observed by PEEM or LEEM. Many other processes as chemical reactions, phonon dynamics, nanoscale heat transport, or phase transitions, however, take place on the femto- and picosecond timescale and are yet way to fast for imaging techniques.

In order to study such ultrafast processes at surfaces we have combined modern surface science techniques with fs laser pulses in a pump probe scheme. We use a reflection high energy electron diffraction (RHEED) setup with grazing incident electrons of $7 - 30$ keV to ensure surface sensitivity [1,2]. Utilizing the Debye Waller effect the cooling of vibrational excitations in monolayer adsorbate systems or the nanoscale heat transport through a heterofilm interface is studied on the lower ps-time scale [3-5]: the cooling of ultrathin Bi(111) films on Si(001) is dominated by a pronounced non-equilibrium distribution in the phonon system resulting in a strongly reduced cooling rate.

In order to demonstrate the huge potential of this technique I will shortly present examples for the dynamics of strongly driven structural phase transitions at surfaces upon excitation with a fs-laser pulse: the famous order-disorder phase transition from c(4x2) to (2x1) on Si(001) at 200 K and the Indium induced Peierls-like transition from c(8x2) to (4x1) on Si(111) at 80 K which is additionally accompanied by the formation of a charge density wave [6].

[1] A. Janzen, B. Krenzer, P. Zhou, D. von der Linde, and M. Horn-von Hoegen, Surf. Sci. **600**, 4094 (2006)
[2] A. Janzen, B. Krenzer, O. Heinz, P. Zhou, D. Thien, A. Hanisch, F.-J. Meyer zu Heringdorf, D. von der Linde, and M. Horn-von Hoegen, Rev. Sci. Inst. **78**, 013906 (2007)
[3] B. Krenzer, A. Janzen, P. Zhou, D. von der Linde, and M. Horn-von Hoegen, New J. Phys. **8**, 190 (2006)
[4] A. Hanisch, B. Krenzer, T. Pelka, S. Möllenbeck, and M. Horn-von Hoegen, Phys. Rev. B **77**, 125410 (2008)
[5] B. Krenzer, A. Hanisch-Blicharski, P. Schneider, Th. Payer, S. Möllenbeck, O. Osmani, M. Kammler, R. Meyer and M. Horn-von Hoegen, Phys. Rev. B **80**, 024307 (2009)
[6] S. Möllenbeck, A. Hanisch-Blicharski, P. Schneider, M. Ligges, P. Zhou, M. Kammler, B. Krenzer, and M. Horn-von Hoegen, MRS-Proceedings (accepted)

Assignment of local magnetic moment in $L1_0$-type FeNi using photoelectron emission microscopy (PEEM)

M. Kotsugi[a], M. Mizuguchi [b], T. Ohkouchi[a], T. Kojima [b], K. Takanashi [b], Y. Watanabe[a]

[a] *Japan Synchrotron Radiation Research Institute (JASRI), 1-1-1 Sayo, Koto, Hyogo 679-5198, Japan*

[b] *Tohoku Univ., 2-1-1, Katahira, Aoba-ku, Sendai 980-8577, Japan*

Magnetic anisotropy energy is the key property to improve the areal density in widespread applications. For the ecological viewpoint in these days, a rare-metal-free $L1_0$-ferromagnet composed of abundant Fe and Ni is newly attracting much attentions [1, 2]. The magnetic anisotropy energy of $L1_0$-FeNi shows 3.2×10^5 J/m^3, which is entirely larger value compare to common FeNi alloys. However, the mechanism to obtain perpendicular magnetization has never been addressed yet.

Here, we investigate the magnetic domain structure using photoelectron emission microscopy (PEEM) in the connection to magnetic circular dichroism (MCD). Microscopic magnetic domain structure is discussed in the association with macroscopic property. Although $L1_0$-FeNi phase has been derived from iron meteorite, the application of molecular beam epitaxy (MBE) recently opens a possibility for the synthetic fabrication of single crystalline $L1_0$-FeNi film.

Experiment was performed using a Spectroscopic Photoemission and low energy electron microscope (SPELEEM) of BL17SU in SPring-8. High-resolution magnetic domain structure was obtained at Fe L_3 absorption edge for various incident angle of synchrotron radiation. It reveals a stripe magnetic domain structure. Angular distribution of magnetic domain images is used to acquire the 3 dimensional components of magnetic moment by quantitative analysis with pixel-by-pixel manner. Figure 1a,b shows the decomposed in-plane and out-of-plane component in the magnetic domain structure. Figure 1c shows the line profile of Figure 1b, showing a slight increase in out-of-plane component. It suggests that the magnetic moment in the narrow magnetic domain obtains out-of-plane component.

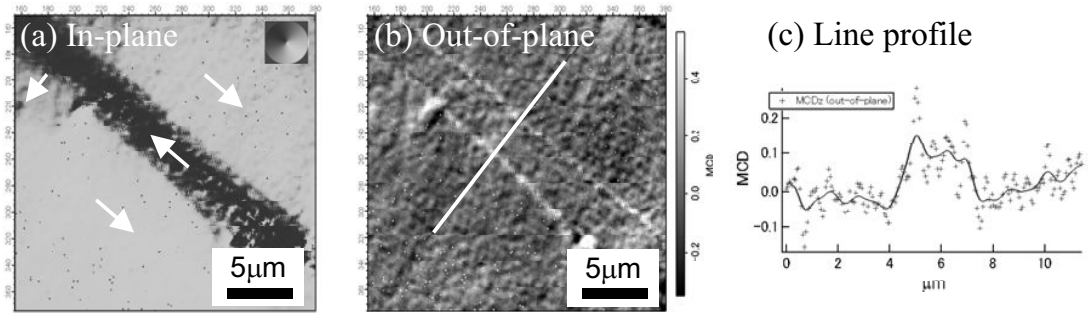

Fig. 1: Decomposed magnetic domain structures of $L1_0$-FeNi. (a) In-plane and (b) out-of-plane component of microscopic magnetic moment. (c) Line profile crossing narrow magnetic domain shows obvious out-of-plane component.

[1]M. Kotsugi et al. APEX 3 (2010) 13001 [2] T. Shima et al. JMMM 310 (2007) 2213

Low Temperature Spectromicroscopy Using the Advanced Light Source PEEM-3

A. Scholl[1], A.T. Young, A. Doran, F. Yang, Y. Takamura, J. Wu, Z.Q Qiu, M. Burkhardt, S. Hossein, Q. He, R. Ramesh

[1]Lawrence Berkeley National Laboratory, 1 Cyclotron Road, Berkeley CA 94720, USA

Magnetic materials, in particular oxides, possess rich phase diagrams as function of temperature and doping or composition. Antiferromagnetic phases, ferro-, and ferrimagnetic phases can coincide with charge, orbital order and, in some materials, multiferroic properties. X-ray Photoemission Electron Microscopy using dichroism contrast images the magnetic domain structures of such systems with element specificity, which can be correlated to the crystal structure and also the interface exchange coupling in multilayer systems.

We will show first results using the new liquid He cooled sample stage and give an overview over the performance and capabilities of the PEEM-3 microscope. Samples can be cooled down to temperatures of 30 K and heated up to 1000 K and higher. The manipulator allows us to apply low magnetic field pulses and also current pulses down to 30 ns in length. Using x-rays the spatial resolution of the microscope is mostly limited by chromatic aberrations. Multi-line patterns of 25 nm width were resolved. The sample loading system is fully automated and remote operation of all functions of the microscope is possible.

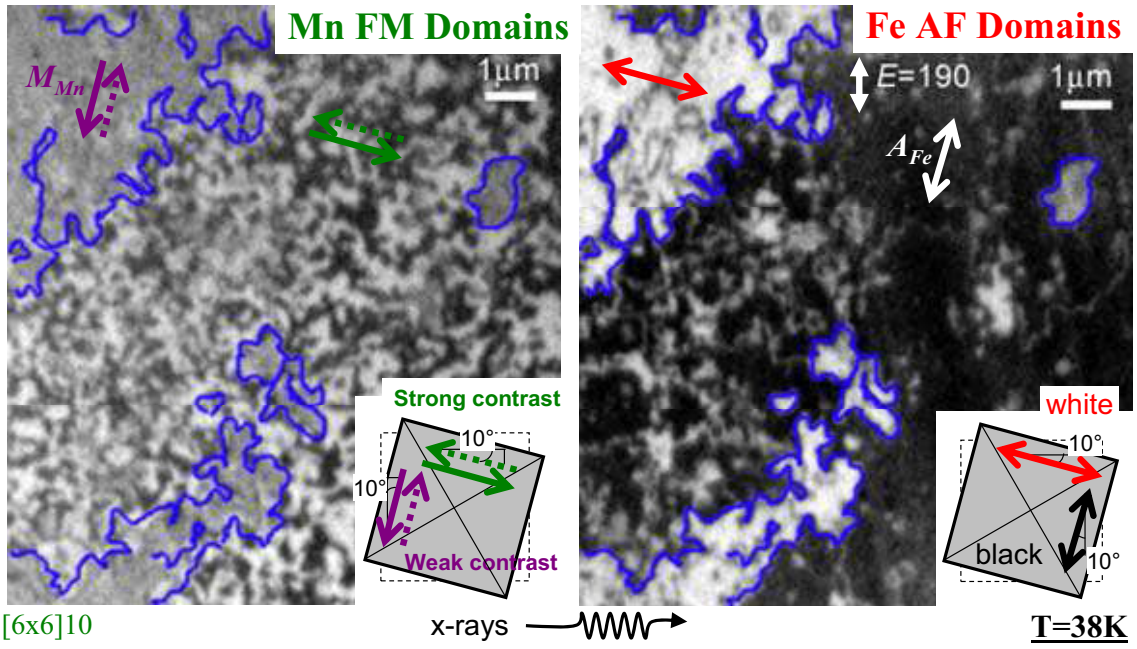

As an example the ferromagnetic and antiferromagnetic domain structures of a LSMO/LSFO multilayer are shown at 38 K.

SCANNING TRANSMISSION LOW ENERGY ELECTRON MICROSCOPY

I. Müllerová*, M. Hovorka and L. Frank

Institute of Scientific Instruments ASCR, v.v.i., Královopolská 147, 612 64 Brno, Czech Republic, *e-mail: ilona@isibrno.cz

The standard scanning electron microscope (SEM) and the low energy electron microscope (LEEM) examine surface structures using reflected electrons. The cathode lens (CL) principle with negatively biased sample, used in emission microscopes, was introduced in the SEM in order to work at arbitrarily low energy [1]. Anode of the CL, inserted to above the sample, consists of a one channel scintillation detector with a small central bore (0.3mm) and collects reflected electrons accelerated in the CL field. Another detector, based on the PIN structure, is positioned below the sample and acquires signal transmitted through thin foils and similarly accelerated. In the very low energy range we rely on the inelastic mean free path of electrons steeply extending below about 50 eV, and hence on increased penetrability of electrons, at last through crystallinic layers. One of the demonstration experiments was done on a sample of overlapped graphene layers with some single layer islands, deposited on a supporting grid. Micrographs in the total transmitted signal at very low energies exhibit a very high thickness contrast, obviously sensitive to individual atomic layers. The energy dependence of the transmitted signal achieves the maximum transmissivity at 5 eV. The reflected electron micrographs are useful to navigation and enable one to distinguish the thinnest areas from empty holes. Similar results have been obtained with a 3 nm foil of gold [2].

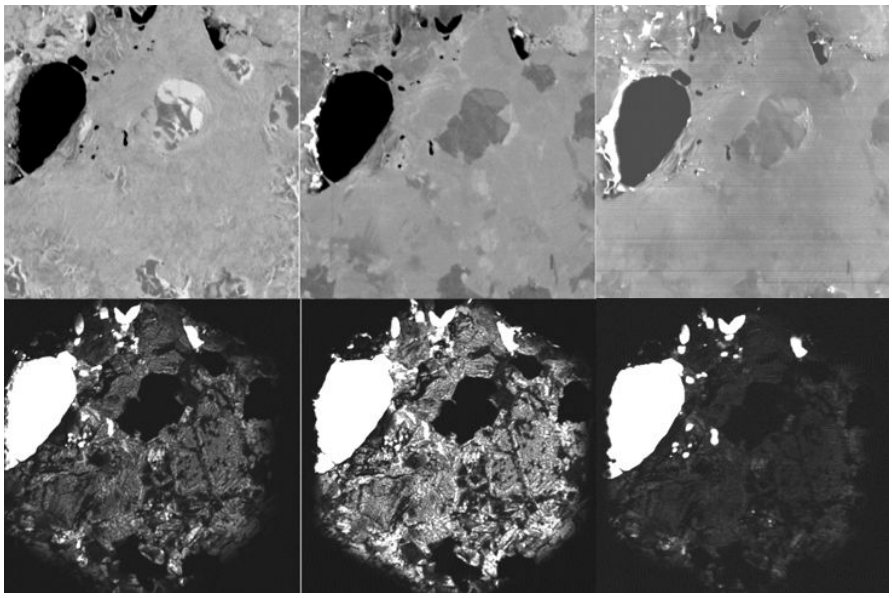

Figure Graphene deposited on a supporting grid, shown in the reflected mode (upper row) and in the transmitted signal (lower row). Primary beam energy was 6 keV, landing energies from the left: 11 eV, 5 eV and 3 eV. Sample was provided by A. Geim, Uni. Manchester.

References:
[1] Müllerová I. and Frank L., Adv. Imaging & Electron Phys. **128** (2003) 309-443.
[2] Müllerová I. et al., Materials Trans. **51** (2010) 265-270.
The work is supported by the GAASCR project no: IAA100650902 and the EU STREP project no. 028326 (SIBMAR, http://sibmar.org/index.html)

Image Formation in Aberration-Corrected LEEM and PEEM

S.M. Schramm[1], A.B. Pang[3], M.S. Altman[3], R.M. Tromp[1,2]

1 - Leiden University, Leiden Institute of Physics, P.O. Box 9504, NL-2300RA Leiden, The Netherlands
2 - IBM Research Division, T. J. Watson Research Center, P.O. Box 218, Yorktown Heights, NY 10598, United States
3 - Department of Physics, Hong Kong University of Science and Technology, Clear Water Bay, Kowloon, Hong Kong

We present results of wave-optical calculations of image formation in standard and aberration-corrected Low Energy Electron Microscopy (LEEM) and Photo Electron Emission Microscopy (PEEM). Our approach is based on the Contrast Transfer Function (CTF) formalism used in Transmission Electron Microscopy (TEM). The CTF formalism used in TEM takes only the lowest order geometric and chromatic aberrations into account. We extend this formalism such that it considers geometric and chromatic aberration coefficients up to fifth order. Therefore, we are able to apply it to study the image formation also in Aberration-Corrected LEEM instruments like the FE-LEEM P90 developed by IBM/SPECS [1]. We use the extended CTF formalism to calculate image contrast and resolution of 1-dimensional and 2-dimensional pure phase, pure amplitude (see Figure 1), and mixed phase and amplitude objects. In addition, we derive optimum defocus values which optimize the resolution of arbitrary objects in standard and aberration-corrected LEEM equivalent to the Scherzer defocus for weak phase objects in TEM. Finally, we adapt our CTF approach to consider the case of PEEM, i.e. incoherent imaging. We show that the optimum resolution of the aberration-corrected FE-LEEM P90 system is r=1nm for LEEM and r=2.6nm for PEEM [2].

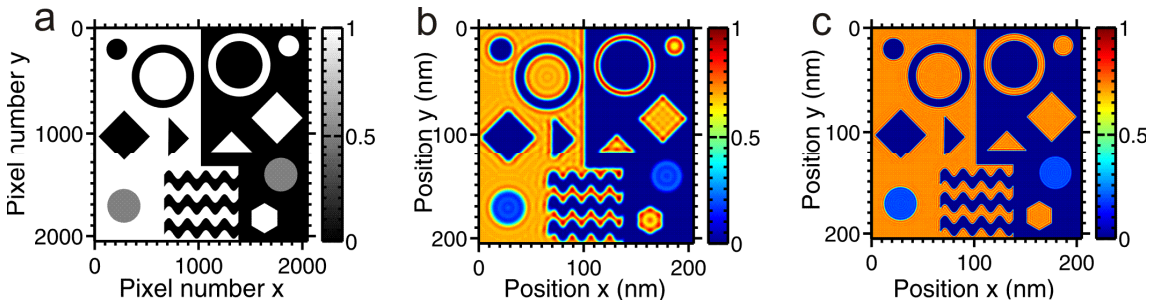

Figure 1: (a) Amplitude object image of different shapes. The phase is constant over the entire object $\phi = 0$. (b) Image contrast of the object in (a) with a size of 0.1nm per pixel for standard LEEM. (c) Image contrast of the object in (a) with a size of 0.1nm per pixel for aberration-corrected LEEM. All images are calculated for a starting electron energy of $E = 10eV$, an energy spread of $\Delta E = 0.25eV$, at in-focus condition.

[1] R.M. Tromp, J.B. Hannon, A.W. Ellis, W. Wan, A. Berghaus, O. Schaff, Ultramicroscopy **110** (2010), 852

[2] S. Schramm, R.M. Tromp, A.B. Pang, M.S. Altman, *to be published*

A NEW ABERRATION –CORRECTED LEEM/PEEM INSTRUMENT

R.M. Tromp[1], J.B. Hannon[1], A.W. Ellis[1], W. Wan[2], A. Berghaus[3], O. Schaff[3]

[1] IBM T.J. Watson Research Center, PO Box 218, Yorktown Heights, NY 10598, USA
[2] Lawrence Berkeley National Lab, 1 Cyclotron Road, Berkeley, CA 94720, USA
[3] SPECS GmbH, Voltastrasse 5, D-13355 Berlin, Germany

We describe a new aberration-corrected Low Energy Electron Microscope (LEEM) and Photo Electron Emission Microscope (PEEM), equipped with an in-line electron energy filter. The chromatic and spherical aberrations of the objective lens are corrected with an electrostatic electron mirror that provides independent control over the chromatic and spherical aberration coefficients C_c and C_3, as well as the mirror focal length, to match and correct the aberrations of the objective lens. For LEEM (PEEM) the theoretical resolution is calculated to be ~ 1.5 nm (~ 4 nm). Unlike previous designs, this instrument makes use of two magnetic prism arrays to guide the electron beam from the sample to the electron mirror, removing chromatic dispersion in front of the mirror by symmetry. The aberration correction optics was retrofitted to an uncorrected instrument with a base resolution of 4.1 nm in LEEM. Initial results in LEEM show an improvement in resolution to ~2 nm. Performance of the mirror optics conforms very closely to theory.

R.M. Tromp, J.B. Hannon, A.W. Ellis, W. Wan, A. Berghaus, O. Schaff, Ultramicroscopy **110** (2010) 852

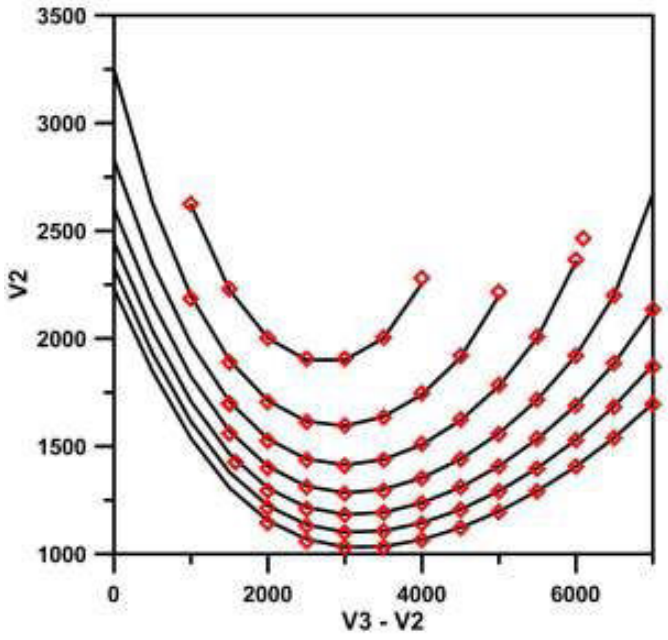

Comparison of experimental mirror focusing potentials (red diamonds) with theory

Monday August 9 – Grand Hyatt Hotel

Afternoon Session: SURFACES
Chairs: A.K. Schmid, S.J. van der Molen

1:30 pm: E. Hilner, A.A. Zakharov, J.N. Andersen, E. Lundgren,A. Mikkelsen
Influence of Au Nano Particles on the Self-Propelled Motion of Mesoscopic Droplets

1:50 pm: W.X. Tang, D.E. Jesson, J. Tersoff; Surface Dynamics during Langmuir Decomposition of GaAs

2:10 pm: T.R.J. Bollmann, R. van Gastel, B. Poelsema
Stress Driven Growth and Substrate Interaction of Pb Islands on Ni(111)

2:30 pm: Nicola Ferralis, Farid El Gabaly, Andreas K. Schmid, Roya Maboudian, Carlo Carraro; Real-Time Observation of Reactive Spreading of Gold on Silicon

2:50 pm: E. Bussmann, F. Cheynis, F. Leroy, P. Müller; Dewetting of Silicon-on-Insulator thin films measured by Low Energy Electron Microscopy

3:10 pm: break

3:40 pm: J. Falta, Th. Schmidt, M. Speckmann, I. Heidman, J.I Flege, A. Locatelli, T.O. Menteş, M.A. Niño, P. Sutter; Tailoring of Vicinal Silicon Surface and Nanostructure Formation

4:00 pm: Ivan Ermanoski and G.L Kellogg; LEEM, LEED, and LEEM-IV investigations of iron oxide thin films on YSZ(001)

4:20 pm: Ivan Ermanoski, G.L Kellogg, N.C. Bartelt; Defect-Free Stripe Arrays on B-doped Si(001)

4:40 pm: K.L. Man, A.B. Pang, M.S. Altman; Adatom-Vacancy Mechanisms of Step Motion on the Si(111)-(1x1) Surface

5:00: End of today's program

Influence of Au Nano Particles on the Self-Propelled Motion of Mesoscopic Droplets

E. Hilner[1], A.A. Zakharov[2], J. N. Andersen[1], E. Lundgren[1] and A. Mikkelsen[1]

1. Dep. of Physics, Lund University, Sweden, 2. MAX lab, Lund University, Sweden

One very interesting observation for droplets on surfaces is so called self-propelled motion, which is found in many different types of materials systems [1, 2]. Self-propelled droplet motion have recently been reported for Ga droplets on GaAs(001) [3] and GaP(111)B [4]. Droplets in both cases move in straight lines leaving a trail behind them on the surface. We have found that by depositing a small amount of Au nano particles (50 nm, ~1/μm²) on the GaP(111)B surface before annealing we can change the droplet dynamics completely.

We have used Spectroscopic PhotoEmission and Low Energy Electron Microscopy (SPELEEM) and Scanning Tunneling Microscopy (STM) to acquire dynamical, chemical and structural information about the system from the micron to atomic scale. The influence of the Au nanoparticles on the GaP(111)B substrate as starting points for de-oxidation is explored. The complex dynamics of the Ga droplets and the Au nanoparticles are described: Micrometer sized Ga droplets form and move by self-propulsion perpendicular to and up the surface steps of clean GaP(111)B upon annealing[4]. However adding Au nanoparticles to the surface leads to a dramatic change and the droplets now move much more randomly although still with an average direction up the surface steps. We find that the presence of Au particles change the morphology of the substrate in their vicinity by inducing a more rapid evaporation of pyramid shaped crystallites present on GaP(111)B. Because the motion of Ga droplets is intimately connected to the surface morphology this in turn leads to a randomization of the droplet motion. Finally we can explore droplet coalescence, and find that there is an upper droplet size limit.

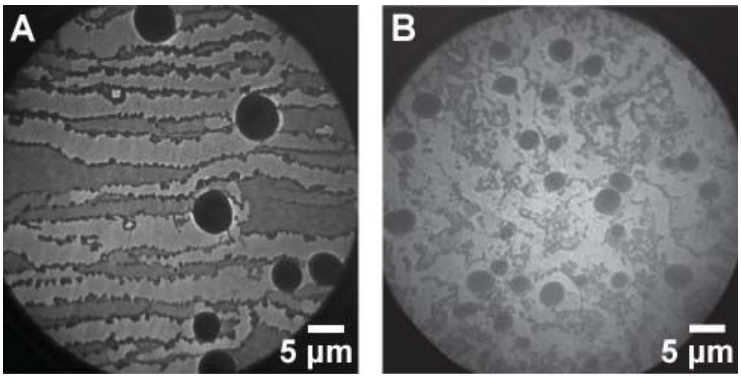

Figure 1: A) Ga droplets with trails on the clean GaP(111)B surface. The droplets moves in straight lines. B) Ga droplets on a GaP(111)B where gold nano particles were deposited. The Ga droplets move more randomly.

[1] A. K. Schmid, N. C. Bartelt and R. Q. Hwang, R. Q. , Science 290, 1561 (2000)
[2] H. Linke et al. , Phys. Rev. Lett. 96, 154502 (2006)
[3] J. Tersoff, D. E. Jesson and W. X. Tang, Science 324, 236 (2009)
[4] E. Hilner, et al, Nano Lett. 9(7), 2710 (2009)

Surface Dynamics during Langmuir Decomposition of GaAs

W. X. Tang[1], D. E. Jesson[1] and J. Tersoff[2]
[1]School of Physics, Monash University, Victoria 3800, Australia
[2]IBM Research Division, T. J. Watson Research Center, Yorktown Heights, NY10598, USA

With the aim of studying III-V surface dynamics we have developed a III-V low energy electron microscope (LEEM) which combines surface electron microscopy with a III-V MBE system equipped with an As cracker source as well as Ga and In effusion cells. The lens region is surrounded by a specially designed cooling shroud to reduce As pressure during deposition. In this paper, we will present our recent studies of Langmuir (free) evaporation of GaAs (001).

Above the so-called congruent evaporation temperature T_c, As preferentially evaporates from the surface leaving behind Ga rich liquid droplets. Real-space movies of this decomposition reveal several remarkable phenomena. Firstly, we find that droplets actually move during evaporation driven by a disequilibrium between the droplet and the surrounding surface [1]. Consequently at T_c, when the surface and the droplets are in equilibrium, the motion stops (see Fig.1). In addition, striking bursts of 'daughter' droplet nucleation occur during the coalescence of large 'parent' droplets. These observations imply a morphology dependent T_c and we will demonstrate how this new concept can be used to write nanostructures [2]. We will also show how T_c can be manipulated by varying the As flux, which has important technological implications.

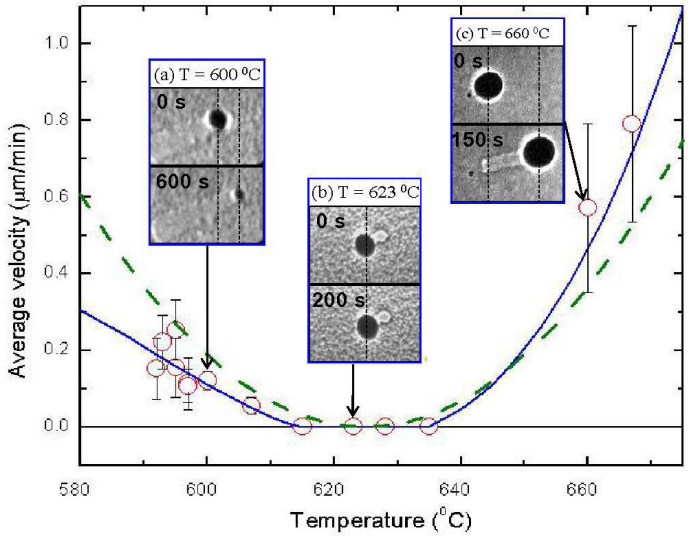

Fig. 1 Average droplet velocity v temperature. The inset panels (a-c) show mirror electron microscope images of Ga droplets at two different times for a given temperature. The vertical lines act as reference markers to compare droplet size and position.

[1] J. Tersoff, D. E. Jesson and W. X. Tang, Science, **324** (2009) 236.
[2] J. Tersoff, D. E. Jesson and W. X. Tang, Physics Review Letters (In Press)

Stress driven growth and substrate interaction of Pb islands on Ni(111)

T.R.J. Bollmann,[1] R. van Gastel,[1] and B. Poelsema[1]

[1] *University of Twente, MESA$^+$ Institute for Nanotechnology, P.O. Box 217, NL-7500AE Enschede, The Netherlands*

Low Energy Electron Microscopy (LEEM) allows real-time imaging of epitaxial growth of metals on metal substrates. We have used LEEM in combination with μLEED to study the structure, size and height evolution of Pb islands on top of a Pb wetting layer on a Ni(111) surface, as well as the diffusion of islands across steps during epitaxial growth at elevated temperatures. Pb islands diffusing across nickel steps show remarkable self-organization in that they can half their surface area by doubling their layer in height. Concerted rapid coarsening of (larger) Pb islands within seconds is also observed. In both cases mass transport of Pb leads to new island equilibrium shapes with increased uniform (integer) heights. We present a systematic LEEM investigation of the effects that play a role in the area versus height evolution of Pb islands at elevated temperatures. The results are discussed in view of stress driven growth.

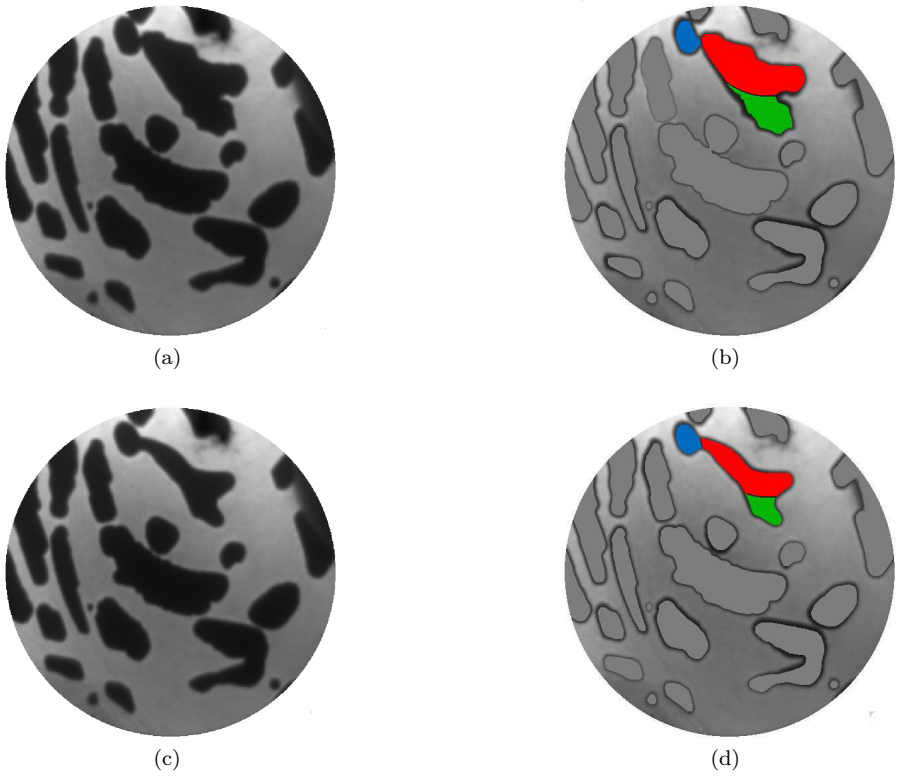

Fig. 1: (a) and (c) LEEM images of two islands crossing a step edge in downward direction. Sample temperature is 476K, FoV 15μm @ 20.0eV electron energy. Time between successive images is 26 seconds. (b) and (d) Automatic thresholded equivalents of image (a) and (c).

Real-Time Observation of Reactive Spreading of Gold on Silicon

Nicola Ferralis[1], Farid El Gabaly[2], Andreas K. Schmid[3], Roya Maboudian[1] and Carlo Carraro[1]

[1] Department of Chemical Engineering, University of California, Berkeley, CA 94720,
[2] Sandia National Laboratories, Livermore, Ca 9455
[3] National Center for Electron Microscopy, Lawrence Berkeley National Laboratory, Berkeley, CA 94720

The spreading of a bilayer gold film propagating outward from gold clusters, which are pinned to clean Si(111), is imaged in real time by low-energy electron microscopy. By monitoring the evolution of the boundary of the gold film at fixed temperature, a linear dependence of the spreading radius on time is found. The measured spreading velocities in the temperature range of 800 < T < 930 K varied from below 100 pm/s to 50 nm/s (Fig.1). We show that the spreading rate is limited by the reaction to form Au silicide, and the spreading velocity is likely regulated by the reconstruction of the gold silicide that occurs at the interface. [1]

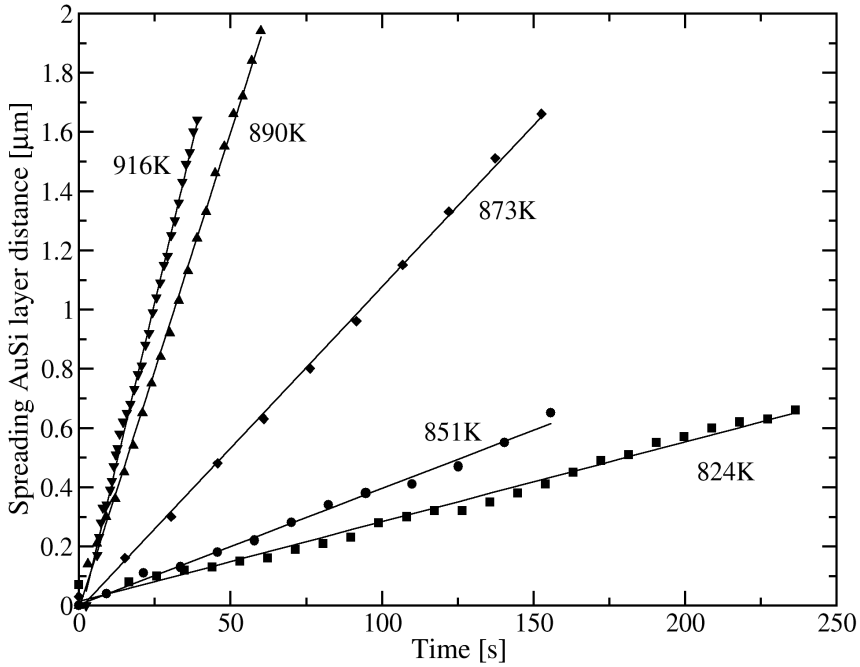

Fig. 1. Gold-silicide spreading velocities are measured at different temperatures. The persistence of linear time evolution of the spreading of the silicide layer, incompatible with diffusive spreading, indicates that reaction-limited kinetics endure over a wide temperature range.

[1] N. Ferralis, F. El Gabaly, A.K. Schmid, R. Maboudian, C. Carraro, Phys. Rev. Lett. 103 (2009), 256102.

Dewetting of Silicon-On-Insulator thin films measured by Low-Energy Electron Microscopy

E. Bussmann, F. Cheynis, F. Leroy, P. Müller

CINaM, CNRS UPR 3118, Campus de Luminy, Case 913, 13288 Marseille cedex 9, France
(corresponding author: cheynis@cinam.univ-mrs.fr)

Thin-film dewetting is a process by which an initially continuous film spontaneously agglomerates in 3D islands, which in some cases exhibit self-organization. A detailed understanding of the dewetting mechanisms is thus crucial to avoid this agglomeration or to engineer arrays of nanostructures with controlled properties. Silicon-on-Insulator (SOI) films are promising materials for microelectronics. However, when annealed at typically >700°C under UHV conditions, the Si(001) film spontaneously dewets and transforms into an assembly of nano-sized islands. Previous *ex-situ* studies of dewetted SOI films have provided a qualitative description of the dewetting process [1-4]. However, the dewetting dynamics, as well as the thermodynamic driving forces (atomistic mechanisms at work), remain largely unknown. In this work performed on an Elmitec GmbH LEEM/PEEM III recently installed at the CINaM, we simultaneously measure the dewetting dynamics and the motion of surface atomic-steps (surface self-diffusion) using dark-field LEEM imaging [Fig. 1(a)]. The dewetted structures are then characterized by *ex-situ* AFM measurements [Fig. 1(b)].

In experiments, the following scenario is observed: **(i)** dewetting voids nucleate at defects in the Si(001) layer forming **(ii)** small squares due to the fourfold symmetry of the surface. In this initial stage, the area of the opening voids grows linearly with time and a thickening rim forms surrounding the dewetted area. **(iii)** As dewetting progresses, the rim exhibits an instability that leads to the formation of elongated Si fingers. **(iv)** These fingers in turn undergo a Plateau-Rayleigh instability, giving rise to 3D Si nano-islands. Once the first fingers are formed, the void Area~t^2.

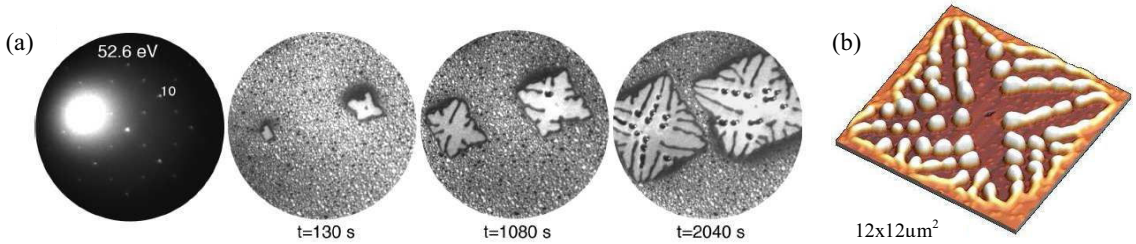

Fig. 1: (a) LEED/LEEM images of the dewetting of a 22 nm-thick SOI film (T = 870 °C, FOV 25 µm, E = 7.8 eV). (b) AFM image of the SOI dewetting.

Beyond the real-time measurements of the morphological evolution of SOI dewetting, our experimental data are compared to a simple analytical model (based on mass-conservation, surface diffusion phenomena and 2D nucleation on the top of the rim) and to Kinetic Monte Carlo simulations. These approaches unambiguously show that the SOI dewetting process is surface-diffusion-limited and driven by surface and interface free-energy-minimization.

[1] D. T. Danielson *et al.*, J. Appl. Phys. 100, 83507 (2006).
[2] R. Nuryadi *et al.*, J. Vac. Sci. Technol. B, 20(1), 167 (2002).
[3] B. Yang *et al.*, Phys. Rev. B 72, 135413 (2005).
[4] E. Dornel *et al.*, Phys. Rev. B 73, 115427 (2006).

Tailoring of vicinal silicon surface and nanostructure formation

J. Falta[1], Th. Schmidt[1], M. Speckmann[1], I. Heidmann[1], J. I. Flege[1], A. Locatelli[2], T. O. Menteş[2], M. A. Niño[2], P. Sutter[3]

[1] *Institute of Solid State Physics, University of Bremen, Otto-Hahn-Allee 1, 28359 Bremen, Germany*
[2] *Sincrotrone Trieste, Strada Statale 14, km 163.5, 34149 Basovizza/Trieste, Italy*
[3] *Center for Functional Nanomaterials, Brookhaven National Laboratory, Upton, NY 11973, USA*

The fabrication of nanostructures on silicon is of high technological relevance, e. g., for opto-electronic or high-speed devices. In this context, Ge nanowires and Ge quantum dots are of special interest [1–4]. Vicinal silicon surfaces can be modified to show a regular pattern by the use of metal adsorbants. We have performed systematic studies of the impact of adsorption of gallium and silver on the surface morphology of Si(113), Si(112) and Si(111). Subsequent germanium deposition leads to the formation of Ge nanostructures varying in density, size and shape. The experiments have been performed at the LEEM/PEEM endstations of the nanospectroscopy beamline at the ELETTRA Synchrotron Light Source in Trieste, Italy and at the beamline U5UA at the National Synchrotron Light Source at Brookhaven National Laboratory.

On Si(111), the intial adsorption of Ga induces the decoration of step edges and domain boundaries. This chemical pattern leads to an alignment of nanoscale 3D islands during subsequent Ge growth (see Fig. 1 (a)) [5]. A step-edge decoration is also observed in case of Ag deposition on Si(111), however, Ge growth leads to a redistribution of Ag all over the surface and, thus, to a Ge growth similar to that on bare Si(111) [6]. For an entirely Ag covered Si(111)-$\sqrt{3}\times\sqrt{3}$-R30° surface, huge and flat Ge islands are observed (cf. Fig. 2 (a)).

Upon Ga deposition, the stable Si (113) surface decomposes into a regular array of (112) and (115) facets with tunable periodicity which can be used as tailored substrate for the preparation of a dense array of small Ge islands (see Fig. 1 (b)). Contrarily, adsorption of Ga on Si(112) stabilizes the intrinsically faceted substrate and leads to a smooth surface. Under appropriate growth conditions, subsequent Ge deposition leads to the formation of nanoscale Ge wires (see Fig. 1 (c)) [7].

On Si(113), Ag as a Ge growth modifier acts similarly as compared to Ga. The surface becomes decompresed into (111) and (115) facets. Again, this morphological change leads to the growth of elongated nanoscale Ge islands that are aligned at the substrate facets (see Fig. 2 (b)) [8]. (111) and (113) substrate facets are observed after Ag deposition onto Si(112), giving rise to a very similar Ge island morphology (cf. Fig. 2 (c)).

In addition to the LEEM experiments, complementary XPEEM, SPA-LEED and x-ray diffraction were used to study, e. g., the Ge/Si intermixing, the strain state, and defect structure of the Ge nanostructures. The results will be discussed to elucidate the underlying mechanisms that lead to the observed morphologies, like strain relaxation and diffusion and their anisotropy.

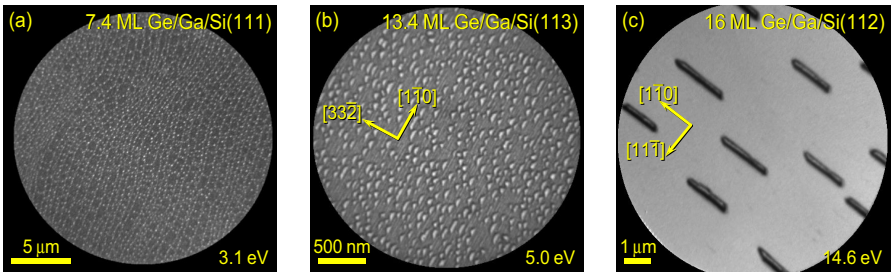

Figure 1: Morphology and alignment of Ge islands grown after pre-adsorption of Ga on (a) Si(111), (b) Si(113), and (c) Si(112).

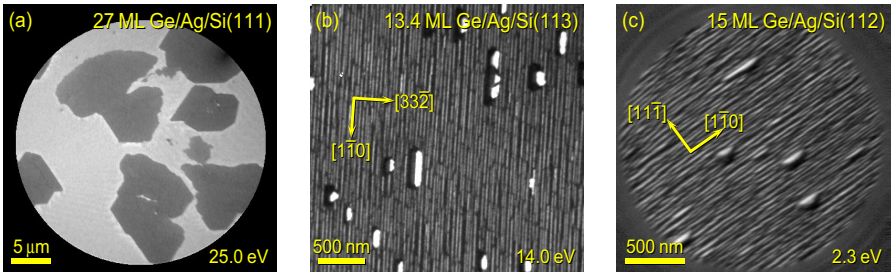

Figure 2: Morphology and alignment of Ge islands grown after pre-adsorption of Ag on (a) Si(111), (b) Si(113), and (c) Si(112).

References

[1] G. Abstreiter *et al.*, Semicond. Sci. Technol. **11**, 1521 (1996).
[2] J. Konle, H. Presting, H. Kibbel, K. Thinke, and R. Sauer, Sol.-State Electron. **45**, 1921 (2001).
[3] D. A. B. Miller, Proc. IEEE **97**, 1166 (2009).
[4] X. Sun, J. Liu, L. C. Kimerling, and J. Michel, Appl. Phys. Lett. **95**, 011911 (2009).
[5] Th. Schmidt *et al.*, Phys. Rev. Lett. **98**, 066104 (2007).
[6] Th. Schmidt, M. Speckmann, J. Falta, T. O. Menteş, M. A. Niño, and A. Locatelli, e-J. Surf. Sci. Nanotechn. **8**, 221 (2010).
[7] Th. Schmidt *et al.*, phys. stat. sol. (a) **206**, 1718 (2009).
[8] M. Speckmann, Th. Schmidt, A. Locatelli, T. O. Menteş, M. A. Niño, and J. Falta, phys. stat. sol. RRL **3**, 305 (2009).

LEEM, LEED, and LEEM-IV investigations of iron oxide thin films on YSZ(001)

Ivan Ermanoski and G. L. Kellogg

Sandia National Laboratories*, Albuquerque, New Mexico 87185

Email: glkello@sandia.gov

The iron oxide (Fe_xO_y) – yttria-stabilized zirconia (YSZ) system is currently used as a working material for solar thermochemical splitting of H_2O and CO_2 [1], but little fundamental information is available concerning the structure and composition of the mixed oxides. To address this deficiency, we are using low energy electron microscopy (LEEM), low energy electron diffraction (LEED) and LEEM-intensity vs. voltage (LEEM-IV) measurements to characterize the initial stages of Fe_xO_y growth on YSZ(100). The substrates are prepared by heating single-crystal YSZ wafers in air to 1400ºC followed by vacuum annealing in the LEEM. Thin films of iron oxide are grown by Fe deposition in ~10^{-6} Torr O_2 at temperatures in the range of 600-1000ºC. Figure 1 shows (a) a LEEM image, (b) a LEED pattern, and (c) a LEEM-IV curve associated with a film growing at 600ºC. Continued deposition results in the development of three distinct LEED patterns with 12-fold symmetry, and one pattern with 4-fold symmetry. Dark-field imaging shows a complicated domain structure where each of the 12-fold patterns corresponds to two or four rotationally equivalent domains. We are using LEED to determine the oxide composition (hematite, magnetite, wüstite) and surface structure, both of which depend on the layer thickness, substrate temperature, and background oxygen pressure. Future LEEM experiments will explore the intermixing between the iron oxide film and the YSZ substrate.

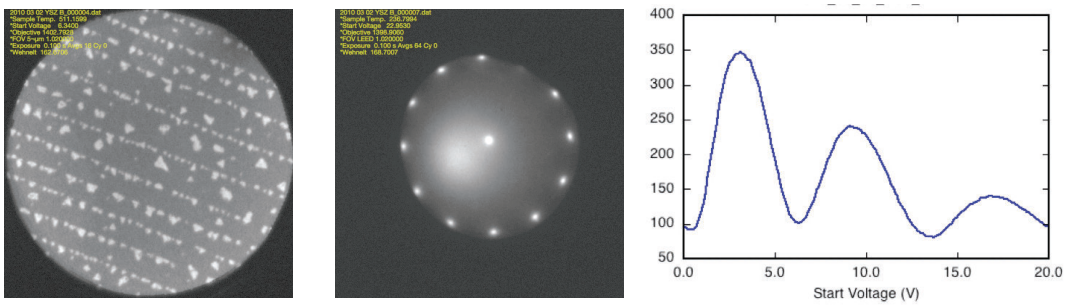

(a) (b) (c)

Fig. 1 (a) LEEM image of a iron oxide film grown on a YSZ(100) substrate after 90 min of deposition, 5 μm field of view. (b) LEED pattern from the surface shown in (a). (c) LEEM-IV curve showing quantum-size oscillations associated with the iron oxide film.

*Sandia National Laboratories is operated by Sandia Corporation, a wholly owned subsidiary of Lockheed Martin Company, for the U.S. DOE's NNSA under contract DE-AC0494AL85000. Funding for this work was provided through Sandia's LDRD Office.

[1] Diver, R.B., Miller, J.E., Allendorf, M.D., Siegel, N.P., Hogan, R.E., Journal of Solar Energy Engineering, **130** (2008) 041001.

Defect-Free Stripe Arrays on B-doped Si(001)

Ivan Ermanoski[1], G. L. Kellogg[1] and N. C. Bartelt[2]

[1]Sandia National Laboratories, Albuquerque, New Mexico 87185
[2]Sandia National Laboratories, Livermore, California 94551

Email: iermano@sandia.gov

We have used low energy electron microscopy (LEEM) to study in real time the self-assembly of periodic stripe arrays on the atomically flat Si(001) with high boron doping. Stripes are extremely elongated vacancy or adatom islands of single atomic step height, confined in micrometer-sized etched pits. "Perfect" arrays of many parallel, straight, and uniform stripes were formed by using Si deposition to prevent sublimation-induced defect formation, and to allow time for ordering via surface diffusion (Fig. 1). Si deposition allows observation of stripe evolution over the course of hours, with no net loss or gain of Si from the area of interest. Equilibrium stripes are very uniform in width and periodicity. At high temperature, arrays are stable when the area fractions of vacancy (θ_v) or adatom stripes (θ_a) are ~½, consistent with stress domain theory predictions. Stripe formation and ordering mechanisms include spontaneous nucleation and growth of new stripes, longitudinal splitting, as well as coarsening due to surface diffusion. Stripe periodicity depends on temperature (Fig. 2), allowing for control of this property. Stripes are stable in a range of ~150°C, outside of which they assume the familiar shape of elongated islands. Stripe order can be preserved to room temperature by quenching.

Work supported by the U.S. DOE, Office of BES, DMSE. Sandia National Laboratories is a multi-program laboratory operated by Sandia Corporation, a wholly owned subsidiary of Lockheed Martin Company, for the U.S. DOE's NNSA under Contract No. DE-AC04-94AL85000.

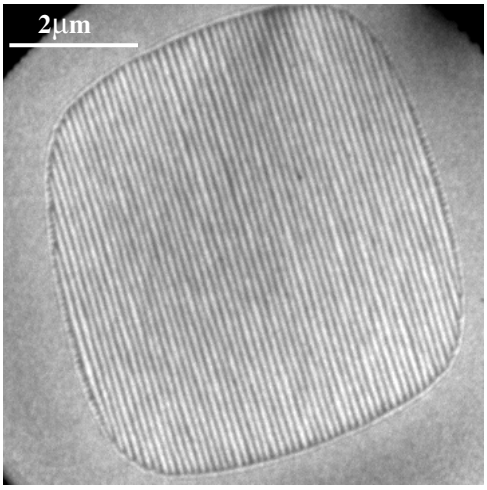

Fig. 1. A 917ºC LEEM image of an array of perfectly ordered stripes (bright areas) formed at the atomically flat bottom of an etched pit (interleaved dark areas). The surrounding gray area is highly stepped.

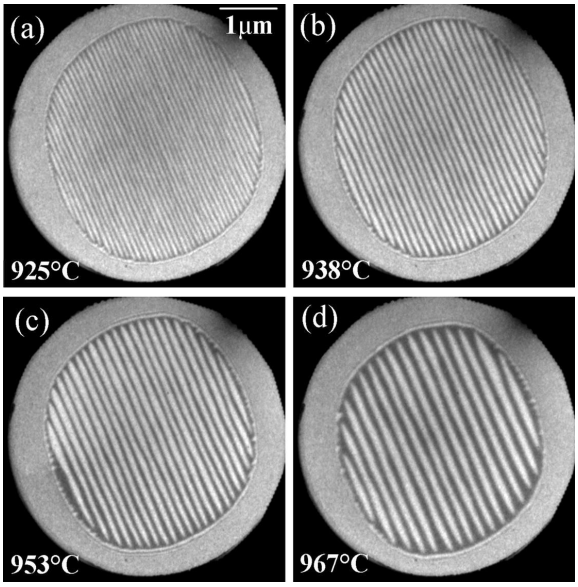

Fig. 2. (a)-(d) LEEM images of stripe arrays formed at several temperatures in the same pit.

Adatom-Vacancy Mechanism of Step Motion on the Si(111) (1x1) Surface

K.L. Man, A.B. Pang and M.S. Altman
Department of Physics, Hong Kong University of Science and Technology, Clear Water Bay, Kowloon, Hong Kong

The topography of a crystalline surface is defined at the shortest vertical length scale by the shapes and positions of discrete atomic steps, i.e., the step morphology. Dramatic changes of step morphology are often produced when mass transport to and from steps causes them to move during growth, sublimation and coarsening. In the present work, we have investigated mass transport and step motion kinetics on the Si(111) (1x1) surface. Interest in this surface is motivated by intriguing electromigration-induced step morphological evolution behavior that produces step bunching, step meandering and regular step arrangements depending upon the sample temperature [1,2]. We studied step motion kinetics by examining complementary two-dimensional island and vacancy island coarsening behavior using low energy electron microscopy (fig. 1). The areas of decaying islands and vacancy islands decrease according to power laws in time, $A(t) = A_0 \cdot (t_0 - t)^{\alpha}$, where $A(t)$ is the area of the island or vacancy island at time t, A_0 is the initial area, t_0 is the total decay time until the island or vacancy island disappears, and α is the decay exponent. Our studies revealed a significant difference between island and vacancy island decay times although the decay exponents are nearly identical at 1163K (fig. 2). The decay times and exponents also diverge with increasing temperature. Results of continuum kinetic modeling will be presented that demonstrate how these observations signal the participation of both adatoms and vacancies in mass transport, together with significant mutual annihilation of the two mass transporting species. This new insight may help to explain the inexplicable variety of electromigration-induced step morphologies on the Si(111) (1x1) surface. Involvement of both vacancies and adatoms in mass transport may also be more common than previously thought on other surfaces.

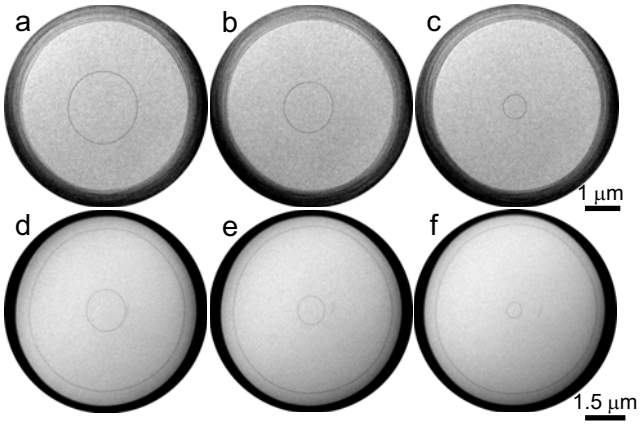

Fig. 1: LEEM images of (a)-(c) island decay and (d)-(f) vacancy island decay on the Si(111) (1×1) surface at 1163K..

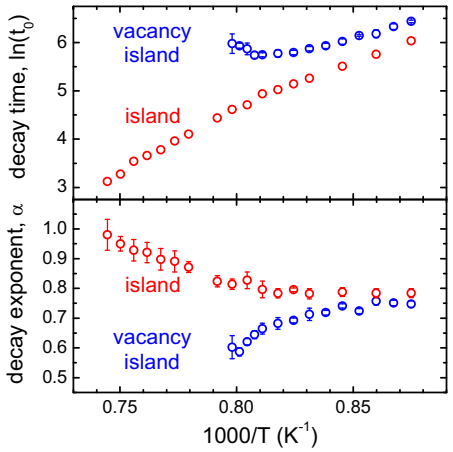

Fig. 2: Temperature dependence of island and vacancy island decay time and decay exponent on Si(111) (1x1).

References

[1] A.V. Latyshev, A.B. Krasilnikov, A.L. Aseev, L.V. Sokolov, and S.I. Stenin, Surf. Sci. **254**, 90 (1991).

[2] K.Yagi, H. Minoda, and M. Degawa, Surf. Sci. Rept. **43**, 45 (2001).

Tuesday August 10 – Grand Hyatt Hotel

Morning Session 1: MAGNETISM
Chair: E. Bauer

8:30 am: Y. Kotani, T. Taniuchi, M. Osada, T. Sasaki, M. Kotsugi, Y. Watanabe, K. Ono Attogram X-ray Spectroscopy of Molecularly Thin Ferromagnetic Transition Metal Oxide Nanosheets

8:50 am: T. Koshikawa, M. Suzuki, M. Hashimoto, T. Yasue, Y. Nakagawa, A. Mano, N. Yamamoto, M. Yamamoto, T. Konomi, M. Kuwahara, S. Okumi, T. Nakanishi, X.G. Jin, T. Ujihara, Y. Takeda, T. Kohashi, T. Oshima, T. Saka, T. Kato, H. Horinaka, E. Bauer Dynamic Observation of Magnetic Domains with Novel Spin-polarized LEEM

9:10 am: K.M. Man, A. Pavlovska, M.S. Altman, E. Bauer, S.K. Lok, I.K. Sou, G. Wong, A. Locatelli, T.O. Menteş, M.A. Niño; Fe Nanowires on ZnS(100)

9: 30 am: Adrian Quesada, A.K. Schmid, G. Chen, J. Li, Y.Z. Wu; The Magnetic Stripe Phase in Fe/Ni/Cu(100): Reversible Transition and Domain Wall Spin Structure

9:50 am: A. Kaiser, C. Wiemann, S. Cramm, C. Tieg, C.M. Schneider; Layer-Specific Magnetization Dynamics in Spin-Valve Systems Revealed by Time-Resolved PEEM

10:10 am: M. Hjort, A.A. Zakharov, M.T. Borgström, R. Timm, J.N. Andersen, E. Lundgren, L. Samuelson, A. Mikkelsen; Combined PEEM, LEEM, and XPS Studies of III-V Semiconductor Nanowires

10:30 am: Break and poster session

12:00 am: Break for lunch

Attogram x-ray spectroscopy of molecularly thin ferromagnetic transition metal oxide nanosheets

Y. Kotani[1,2], T. Taniuchi[2], M. Osada[3], T. Sasaki[3], M. Kotsugi[4], Y. Watanabe[4], and K.Ono[1]

[1] *IMSS, High Energy Accelerator Research Organization, Tsukuba, Ibaraki 305-0801, Japan*

[2] *ISSP, The University of Tokyo, Kashiwa, Chiba 277-8581, Japan*

[3] *MANA, National Institute for Materials Science, Tsukuba, Ibaraki 305-0044, Japan*

[4] *SPring-8 /JASRI, Kouto 1-1-1, Sayo, Hyogo 679-5198, Japan*

Recent developments in nanomaterials require the investigation of local electronic structures of individual nanostructures, which is essential in understanding their unique physical properties. Photoelectron emission microscopy (PEEM) provides some clues to answer this issue, as it provides a simple probe of local electronic structures of nanomaterials for attogram (= 10^{-18} g) samples with high spatial resolution (< 50 nm). In this study, we utilized PEEM to characterization for local electronic structures of molecularly thin ferromagnetic nanosheets ($Ti_{1-x}Co_xO_2$, $Ti_{1-y}Fe_yO_2$ and $Ti_{1-x-y}Co_xFe_yO_2$). Ferromagentic nanosheets are a new class of two-dimensional (2D) nanomaterials prepared by delaminating layered oxides into their single-molecular-thick sheets. These 2D nanosheets with a thickness of less than 1 nm and lateral dimensions up to a few mm are the thinnest self-standing 2D nanostructures, which make an important testing ground for attogram x-ray spectroscopy.

In $Ti_{1-x}Co_xO_2$ nanosheets, we found that PEEM measurements allow not only a determination of the local electronic structure of 1-nm-thick nanosheets but also a characterization of the stacking structures on chemical states. By analyzing the nanoscale x-ray absorption and photoemission spectra, the chemical state of doped Co ions in individual Co-doped nanosheet was found to be Co^{2+} state, which is consistent with previous magnetization data and first-principles calculation. We also applied our PEEM technique to characterization for the chemical states of ferromagnetic nanosheets with different compositions and their superlattices.

[1] M. Osada et al., Adv. Mater. 18, 295 (2006); Phys. Rev. B, 73, 153301 (2006).

[2] Y. Kotani et al., Appl. Phys. Lett. 93, 093112 (2008).

Dynamic Observation of Magnetic Domains with Novel Spin-polarized LEEM

T. Koshikawa, M. Suzuki, M. Hashimoto, T. Yasue, Y. Nakagawa [1], A. Mano [1], N. Yamamoto [1], M. Yamamoto [1], T. Konomi [1], M. Kuwahara [1], S. Okumi [1], T. Nakanishi [1], X.G. Jin [2], T. Ujihara [2], Y. Takeda [2], T. Kohashi [3], T. Ohshima [3], T. Saka [4], T. Kato [5], H. Horinaka [6] and E.Bauer [7]

Fundamental Electronics Research Institute, Osaka Electro-Communication University, Neyagawa, Osaka 572-8530, Japan, 1 Graduate School of Science, Nagoya University, Nagoya 464-8602, Japan, 2 Graduate School of Engineering, Nagoya University, Nagoya 464-8603, Japan, 3 Central Research Laboratory, Hitachi Ltd., Kokubunji, Tokyo 185-8601, Japan, 4 Electrical and Electronics Engineering, Daido University, Nagoya 457-8530, Japan, 5 Daido Steel Co. Ltd., Nagoya 457-8545, Japan, 6 Graduate School of Engineering, Osaka Prefecture University, Sakai 599-8531, Japan, 7 Department of Physics and Astronomy, Arizona State University, Tempe 85287-1504, USA

A novel spin-polarized LEEM (SPLEEM) has been developed, which has high spin polarization, very high brightness and a long life time of the cathode and dynamic images of the magnetic domain can be accumulated in 20ms/frame. The following development has been carried out.

1. The strained superlattice (GaAs/GaAsP) has been newly developed as the cathode, which has high spin polarization (90%) and can make the back side illumination of the laser possible because GaP materials (transmitted with 780 nm laser beam) was used as the substrate [1-3].
2. The back side illumination has been adopted, which gives us high brightness (1.3×10^7 A/cm^2 sr) because the lens position of the laser can be located at the close place of the cathode (less than several mm) which is totally different from that of the commercial one (several tens cm) [1-4].
3. A new electron optics has been designed, which transfers 100 % electrons emitted from the cathode to the next optics possible.
4. Extreme high vacuum (XHV, $2\text{-}5 \times 10^{-10}$ Pa) at the electron gun can be kept even during electron emission [1-4] and the cathode has long life time (about 2 months).
5. After the above development has been completed, an accumulation time of a SPLEEM image needs less than 20ms/frame, which makes us the dynamic observation possible [4].

Some examples of dynamic images will be presented in the workshop.

The project has been supported with the JST (Project on the Development of System and Technology for Advanced Measurement and Analysis).

[1] X. G. Jin et. al.,: Appl. Phys. Express **1**, 045002 (2008).
[2] N. Yamamoto et. al.,: J. Appl. Phys. **103**, 064905 (2008).
[3] X. G. Jin et. al.,: J. Cryst. Growth **310**, 5039 (2008).
[4] M.suzuki et. al.,, Appl. Phys. Express **3**, 026601 (2010).

Fe nanowires on ZnS(100)

K.M. Man[1], A. Pavlovska[2], M.S. Altman[1], E. Bauer[2], S.K. Lok[1], I.K. Sou[1], G. Wong[1], A. Locatelli[3], T.O. Menteş[3], M.A. Niño[3]

[1]Department of Physics, The Hong Kong University of Science and Technology, Clear Water Bay, Kowloon, Hong Kong, PR China, [2]Department of Physics, Arizona State University, Tempe, AZ 85287, USA, [3]Sincrotrone Trieste, Basovizza, Trieste 34149, Italy

Nanowire growth on semiconductor surfaces is a subject of considerable current interest. Most of the work has been concerned with Si surfaces, but recently nanowire growth has been reported also on ZnS(100) surfaces [1]. We have studied the growth of Fe on this surface with LEEM and LEED for structural characterization, with XPEEM for chemical characterization and with XMCDPEEM for magnetic characterization. The results show a complex, strongly temperature-dependent growth behavior with an initial reaction layer, followed by the growth of Fe nanowires with different orientations together with small crystals. The growth at different temperatures will be illustrated by movies.

[1] S. K. Lok, S.K. Chan, G.K.L. Wong, I.K. Sou, J. Cryst. Growth **311**, 2208 (2009)

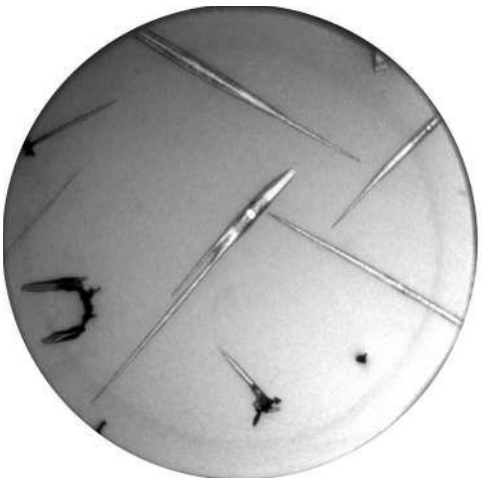

Fig.1. LEEM image of Fe nanowires on ZnS(100). Energy 10 eV; FoV 34 µm

Fig.2. LEEM image of a Fe nanowire on ZnS(100), showing the reaction layer. Energy 10 eV; FoV 12 µm.

The Magnetic Stripe Phase in Fe/Ni/Cu(100): Reversible Transition and Domain Wall Spin Structure

Adrian Quesada[1], A.K. Schmid[1], G. Chen[2], J. Li[2], Y. Z. Wu[2]

[1]NCEM, Lawrence Berkeley National Laboratory, Berkeley, California 94720, USA
[2]Department of Physics, Applied Surface Physics State Key Laboratory, and Advanced Materials Laboratory, Fudan University, Shanghai 200433, P. R. China

The study of the long-range order in two-dimensional (2D) magnetic systems, intimately related to the understanding of magnetic domains structure, earned the interest of experimentalists with the development of growth methods that enabled true 2D magnets in the form of ultrathin-films. The motivation was triggered by the fact that the spin structure characterization of the domains is fundamentally important to the comprehension of the 2D magnetic nature. Under specific conditions, a magnetic stripe phase with out-of-plane magnetization appears near the spin reorientation transition (SRT) of ultrathin magnetic films. This domain structure forms as a consequence of the competition between anisotropy, exchange and magnetostatic energy contributions. However, the spin structure of the domain wall could as well play a key role.

We present in this contribution our experimental study of the spin structure of the domain wall in the stripe phase. Moreover, by tuning the different contributions to the magnetic free energy, we experimentally demonstrate the reversibility of the SRT.

By means of Spin-Polarized Low-Energy Electron Microscopy (SPLEEM), which enables both in-plane and out-of-plane imaging of magnetic domains, we have investigated *in situ* the formation and evolution of the stripe phase in Fe/Ni/Cu(100) ultrathin-films as a function of the Fe thickness. In most cases, a Néel-type domain wall is observed in the stripe phase as shown in Fig. 1, in contradiction with previous theoretical models. Nonetheless, Bloch-walls have been occasionally detected. After the SRT has taken place, the magnetization lies in the plane of the film. Upon CO adsorption, the perpendicular magnetic anisotropy is enhanced and we observe that the stripe phase is restored. The SRT becomes then reversible.

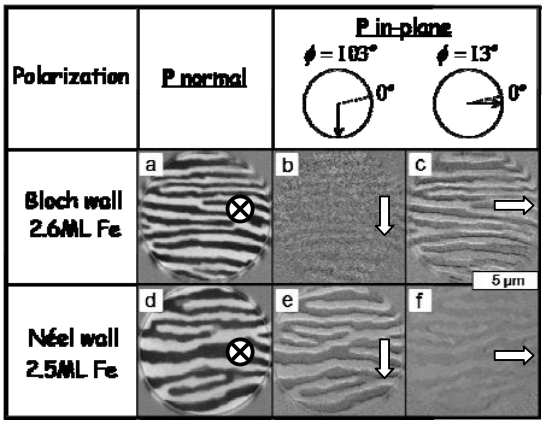

Fig. 1. Magnetic stripe domains with (a-c) Bloch-type and (d-e) Néel-type domain walls imaged with different magnetization components in Fe/Ni/Cu(001) system. The arrows show the measured magnetization directions.

The authors acknowledge support from the U.S. Department of Energy under Contract # DE-AC02-05CH11231 and the support from NSFC and MOST of China.

Layer-specific magnetization dynamics in spin-valve systems revealed by time-resolved PEEM

A. Kaiser[1], C. Wiemann[1], S. Cramm[1], C. Tieg[2,3], C.M. Schneider[1]

[1] Institut für Festkörperforschung IFF-9, Forschungszentrum Jülich, Germany
[2] ESRF, Grenoble, France
[3] present address: Helmholtz-Zentrum Berlin für Materialien und Energie, Berlin, Germany

Email: a.kaiser@fz-juelich.de

The study of processes determining the dynamics of magnetization on short time scales is a hot topic for scientists working in fundamental research as well as application-related fields. Since it's development in 2003 time-resolved photoemission electron microscopy (PEEM) based on synchrotron radiation has been established as a powerful tool for studying such processes due to the unique combination of elemental selectivity, magnetic sensitivity and spatial resolution [1].

In this contribution we present time-resolved and layer-selective PEEM studies of the magnetodynamics of pseudo-spin valve elements of the CoFe/Cr/NiFe type. The material system is characterized by different magnetic properties of the individual layers and a weak parallel interlayer exchange coupling through the Cr interlayer. Under the influence of a sub-nanosecond magnetic field pulse both layers exhibit a complex inhomogeneous reaction.

The usage of X-rays as a photon source with variable polarization and photon energy allows us to probe the magnetization of the invidual constituents. In combination with the spatial resolution of the PEEM technique we are able to study the temporal behaviour of the different processes involving magnetization rotation, domain wall motion and domain nucleation in both layers independently. We observe an inhomogeneous influence of both material-specific parameters such as damping, anisotropy and coercive field and a locally varying strength of the coupling.

In particular we find qualitatively similar magnetodynamic processes in both layers with a short lag of the rotation of the CoFe magnetization compared to that of the NiFe magnetization. This effect is interpreted in terms of an empirical model of the magnetic switching time [2] and can be attributed to the difference of the coercive fields of both layers. However, regarding domain wall motion we find a synchronous reaction in both films due to a local enhancement of the magnetic coupling by domain wall stray fields [3]. The findings of the TR-PEEM measurements will be discussed in terms of the magnetodynamic and –static properties of the individual materials that have been derived from independent studies by XMCD and FMR.

[1] G. Schönhense, H.J. Elmers, S.A. Nepijko, and C.M. Schneider, Adv. Im. El. Phys. **142**, 159 (2006).

[2] W.D. Doyle, S. Stinnett, C. Dawson, and L. He, J. Magn. Soc. Jap. **22**, 91 (1991).

[3] L. Thomas, M.G. Samant, and S.S.P. Parkin, Phys. Rev. Lett. **84**, 1816 (2000).

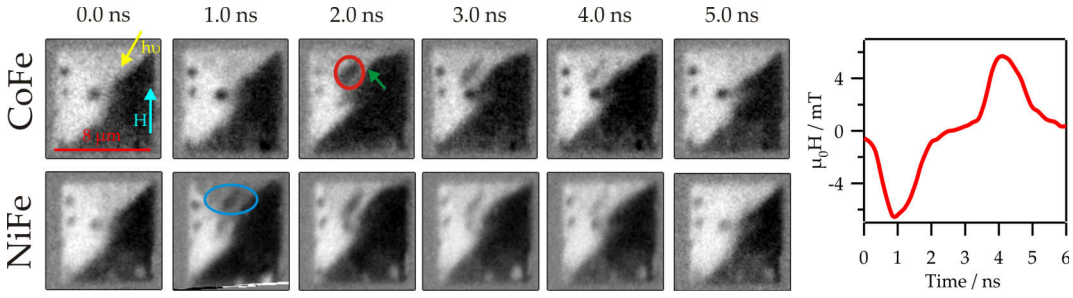

Figure 1: XMCD Pictures showing the magnetic domain structure of both ferromagnetic layers under the influence of the magnetic field pulse shown on right. Three different processes can be identified: magnetization rotation (blue oval), domain nucleation (red circle) and domain wall motion (green arrow).

Combined PEEM, LEEM and XPS Studies of III-V Semiconductor Nanowires

Martin Hjort[1]*, A. A. Zakharov[1], M.T. Borgström[1], R. Timm[1], J.N. Andersen[1],
E. Lundgren[1], L. Samuelson[1] and A. Mikkelsen[1]
1: Lund University, Box 188, 221 00 Lund, Sweden. *martin.hjort@sljus.lu.se

The PhotoEmission Electron Microscope and the Low Energy Electron Microscope (PEEM/LEEM) are powerful instruments enabling surface studies using a wide variety of contrast mechanisms. When studying III-V semiconductors they have the possibility to reveal both surface morphology and work function differences at the same time as chemical and doping induced contrast can be observed. We have studied nanostructures both by LEEM and by PEEM using synchrotron x-rays which are tunable over a large wavelength range.

Combining PEEM/LEEM imaging with high resolution X-ray Photoelectron Spectroscopy (XPS) gives us a more in depth understanding of surface chemistry and its implications for the electronic properties of the nanostructures examined. Further on it makes it possible for us to connect the different contrast mechanisms in the microscope with a complete understanding of the surface chemistry of our samples.

We have examined 80 nm wide untapered InP nanowires with up to two axial pn-junctions using an energy filtered Elmitec LEEM III connected to the MAXII synchrotron storage ring in Lund, Sweden. In addition XPS measurements of doped wires have been performed at beamline i311 located at MAX-lab.

Low energy electrons were used in the SPELEEM to get a good understanding of the morphology of the nanowires and their orientation, figure 1c. When x-rays were incident on the sample and secondary electrons (SE) used to form the image we observed a doping induced contrast along the nanowires with the n-part of the nanowires emitting the most SE, figure 1 a,b. The dopant induced shift of the SE yield was very small demanding a fine energy slit with a resolution of 200 meV. In conjunction with this, we also tuned in different core levels and observed the distribution of different elements in the nanowires, figure 1 d.

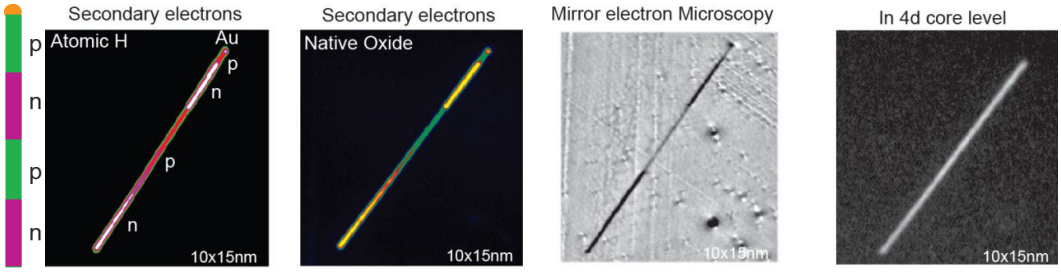

Figure 1. a) Schematic of the npnp-InP nanowire. b) Mirror image of the NW in *a*. c) XPEEM image formed using In4d-electrons. c) XPEEM image of NW with thinned surface oxide after atomic hydrogen treatment. d) XPEEM image of NW covered with native oxide.

The SPELEEM setup is due to its relatively large energy window well complemented by the high resolution XPS measurements which has orders of magnitude better resolution. Something that is absolutely crucial when the surface chemistry is to be determined. From the XPS measurements we find that the native oxide present on the nanowires behaves as a highly n-doped layer leading to not only axial but also radial pn-junctions in the case of uncleaned nanowires which affects the SE emission.

Tuesday August 10 – Grand Hyatt Hotel

Morning Session 2: Poster Session (Chair: J. Sadowski)

P1. A.M. Clausen, C.S. Ritz, C. Euaruksakul, K. Saenger, D. Savage, M.G. Lagally; Probing Local-Stressor Induced Conduction Band Changes in Si Nanoribbons and Membranes

P2. E. Starodub, N.C. Bartelt, K.F. McCarty; The Reaction of Oxygen with Graphene on Ir and Ru

P3. R. van Gastel, I. Sikharulidze, S. Schramm, J.P Abrahams, B. Poelsema, R.M. Tromp, S.J. van der Molen; Medipix 2 Detector Applied to Low Energy Electron Microscopy

P4. A. Locatelli, T.O. Menteş, M.A. Niño, E. Bauer; Space Charge in XPEEM under Micro-focused Illumination with Synchrotron Radiation

P5. F. Nickel, A. Kaiser, I. Krug, S. Cramm, C. Wiemann, A. Schmid, A. Berghaus, O. Schaff, and C.M. Schneider; Commissioning af the New Aberration-Corrected, Energy-Filtered PEEM/LEEM Endstation at BESSY

P6. H. Setoyama, D. Yoshimura, T. Okajima; Installation and Obtained Performance of PEEM System at the BL10 of SAGA-LS

P7. S.M. Kennedy, C.X. Zheng, W.X. Tang, D.M. Paganin, D.E. Jesson; Laplacian and Caustic Imaging of Surface Topography in Mirror Electron Microscopy

P8. R.M. Tromp; Aberrations of a Cathode Objective Lens

P9. B. Borkenhagen, H. Döscher, G. Lilienkam, Th. Hannappel, W. Daum; Anit-Phase Domain Inspection of III-V on Silicon by Low Energy Electron Microscopy

P10. H.M. Ghomi, U. Lanke, A. Odeshi; XPEEM Investigation of Adiabatic Shear Bands in Metallic Alloys

P11. J.I. Flege, A. Meyer, B. Kaemena, S. Senanayake, F. Alamgir, F. Falta; In-situ Characterization of Bimetallic Oxidation and Oxide Thin-Film Growth using Intensity-Voltage Low Energy Electron Microscopy

P12. T. Nakagawa, T. Yokoyama; Magnetic Domain Imaging by Laser PEEM_ Two Photon Photoemission and Energy Dependence

P13. U.D. Lanke, T. Walker, V. Olorunda, M. Stauffer, A. Odeshi, M. Quann, A. Trevors, S. Mason, A. O'Reilly, P. MacDonald, T. Saulnier, A. Riebel, J. d'Entremont, E.Flett, K. Cripps; Detection of Magnetic Circular Dichroism in an Extraterrestial Object_ X-ray Photo Emission Electron Microscopy Study of an Iron Meteorite

P14. Q. Wu, Y.R. Niu, R. Zdyb, A. Pavlovska, E. Bauer, M.S. Altman; SPLEEM Investigations of Fe Films on the W(111) Surface

P15. Shuaihua Ji, J. B. Hannon, R. M. Tromp, A. W. Ellis, M. C. Reuter and F. M. Ross; Surface Electrochemical Potential Mapping of Graphene on SiC(0001)

P16. S. Oida, F.R. McFeely, J.B. Hannon, R.M. Tromp, M. Copel, Z. Chen, Y. Sun, D.B. Farmer, J. Yurkas; Decoupling Graphene from SiC by Oxidation

P17. Stephen Christensen, Brian Haines, Uday Lanke, Stephen Urquhart; Secondary Electron Emission Microscopy and Partial - Yield X - ray Absorption Spectromicroscopy with an Energy Filtered PEEM Microscope

P18. S. Günther, M. Kronseder, G. Woltersdorf, C.H. Back; Threshold photoemission magnetic circular dichroism of Ni(001) films: theory and experiment

P19. Hongwen Liu, N. Fukui, H.T. Yuan, L. Zhang, Y. Iwasa, T. Hitosugi, M.W. Chen, T. Hashizume, Q.K Xue; Growth of topological insulator Bi2Te3 ultrathin films on Si(111) investigated by LEEM

P20. W. Swiech, E Samman and C. P. Flynn; Pulse-probe studies using delayed LEEM and LEED following an ion beam pulse

P21. R. Yamaguchi, K. Terashima, K. Fukumoto, Y. Takada, M. Kotsugi, Y. Miyata, K. Mima, S. Komori, S. Itoda, Y. Nakatsu, M. Yano, N. Miyamoto, T. Nakamura, T. Kinoshita, Y. Watanabe, A. Manabe, S. Suga, S. Imada **;** Magnetic domain and chemical structures of Dy-doped Nd-Fe-B permanent magnet studied by PEEM and XMCD

Probing Local-Stressor Induced Conduction Band Changes in Si Nanoribbons and Membranes

Anna M. Clausen, Clark S. Ritz, Chanan Euaruksakul, Katherine Saenger[1], Don Savage, Max G. Lagally
University of Wisconsin-Madison, Madison WI 53706 [1]IBM Research Center, Yorktown Heights NY

We use X-ray absorption spectroscopy (XAS) and photoelectron emission microscopy (PEEM) to investigate changes in the conduction band resulting from local strain in very thin Si(001) sheets and ribbons. Biaxial strain in Si(001) breaks the six-fold degeneracy of the conduction band minimum which shifts and splits the absorption edges.[2] The magnitude of the shift is proportional to the magnitude of the strain.

Local strain on the 100nm scale can be induced in Si nanomembranes by growing Ge quantum dots because of the 4% lattice mismatch with Si. When using chemical vapor deposition (CVD), these quantum dot stressors arrange themselves into rows on both sides of freestanding Si nanoribbons. The Ge dot growth is monitored to inhibit dislocations, which can form as the dot size reaches a critical height.[3] Dislocation formation is undesirable because less strain is transferred to the Si

When nanostressors are grown, the stochasticity of the growth process leads to some disorder in the arrangement of the nanostressors. There are many reasons why improved order in the nanostressors is desirable. For example, a highly periodic strain lattice could produce a periodic band gap variation in Si. Silicon nitride (SiN_x) has long been used in semiconductors to induce uniaxial strain in field effect transistor channels.[4] It can be deposited with either compressive or tensile stress. We grow SiN_x stripes using plasma-enhanced CVD. A uniform film is deposited, patterned, and etched leaving periodic or aperiodic (depending on choice) stressor arrays. Raman spectroscopy by Saenger et al. has shown that such patterns can locally strain the underlying Si.[5] Closely spaced stressors may have an enhanced effect because of the superposition of strain fields from adjacent stressors.

XAS and PEEM using synchrotron radiation are combined to probe the empty states by observing the turn-on of the absorption spectrum. The detection method, total electron yield based on Auger deexcitation, assures high near-surface sensitivity. We are able to observe shifts in the absorption spectrum for both SiN_x stripes and Ge quantum dots, although the lateral resolution is not sufficient to observe changes due to individual Ge dots.

Research supported by DOE.

[1] Rim et al. Electron Devices, IEEE Trans **47**, 1406 (2000).
[2] Euaruksakul et al. Phys Rev Lett **101**, 147403 (2008).
[3] Teichert, C. Physics Reports **365**, 335 (2002).
[4] Lu et al. Solid State Elect **52**, 1584 (2008).
[5] Saenger et al. App Phys Lett **92**, 124103 (2008).

The reaction of oxygen with of graphene on Ir and Ru

E. Starodub, N.C. Bartelt and K.F. McCarty
Sandia National Laboratories, Livermore, CA 94550

We use low-energy electron microscopy to investigate how graphene is removed from Ru(0001) and Ir(111) by reaction with oxygen. We find two mechanisms on Ru(0001). At short times, oxygen reacts with carbon monomers on the surrounding Ru surface, decreasing their concentration below the equilibrium value. This undersaturation causes a flux of carbon from graphene to the monomer gas. In this initial mechanism, graphene is etched at a rate that is given precisely by the same nonlinear dependence on carbon monomer concentration which governs growth. That is, during both growth and etching, carbon attaches and detaches to graphene as clusters of several carbon atoms. At later times, etching accelerates. We present evidence that this process involves intercalated oxygen, which destabilizes graphene. On Ir, this mechanism creates observable holes. It also occurs most quickly near wrinkles in the graphene islands, depends on the orientation of the graphene with respect to the Ir substrate, and, in contrast to the first mechanism, can increase the density of carbon monomers. We also observe that both layers of bilayer graphene islands on Ir etch together, not sequentially.

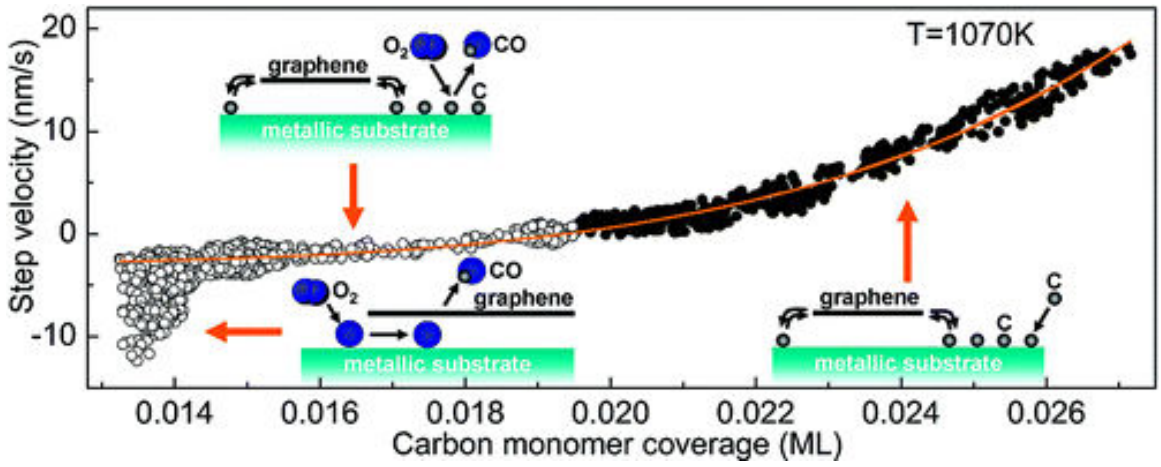

Work at Sandia was supported by the Office of Basic Energy Sciences, Division of Materials Sciences, U. S. Department of Energy under Contract No. DE-AC04-94AL85000.

Medipix 2 detector applied to Low Energy Electron Microscopy

R. van Gastel[1], I. Sikharulidze[2], S. Schramm[3], J.P. Abrahams[2],
B. Poelsema[1], R.M. Tromp[3,4], and S.J. van der Molen[3]

1 University of Twente, MESA+ Institute for Nanotechnology,P.O. Box 217, NL-7500AE, Enschede, Netherlands
2 Leiden University, Leiden Institute of Chemistry, P.O. Box 9502, NL-2300RA, Leiden, Netherlands
3 Leiden University, Leiden Institute of Physics, P.O. Box 9504, NL-2300RA, Leiden, Netherlands
4 IBM Research Division, T.J. Watson Research Center, P.O. Box 218, Yorktown Heights, NY 10598, U.S.A

LEEM and PEEM rely on Micro Channel Plates (MCP) to convert electrons, backscattered or photo-emitted from a sample, into an image. Unfortunately, MCP-units suffer from several drawbacks that limit both the detector resolution and the total electron current handled. Here, we report on a successful test to acquire LEEM and PEEM images using a solid state hybrid pixel detector: Medipix 2 [1]. Medipix 2 is a background-free detector with a large dynamic range, making it very promising for both spectroscopy and real-space imaging. Figure 1 shows PEEM images that were acquired with both a Medipix detector and an MCP unit on the same graphene flake, grown on Ir(111) through thermal decomposition of ethylene [2]. The Medipix images clearly show a significant enhancement in both image contrast and resolution.
Since Medipix 2 was originally designed for the detection of high-energy subatomic particles and photons, it was not a priori clear how efficient it would be for lower energy electrons. For this reason, we have also characterized the detector count rates in PEEM, whilst changing the microscope potential in the range from 10 kV to 20 kV [1]. We find that Medipix 2 is well-suited for detecting low-energy electrons, albeit that further improvements can be made by optimizing the sensor layer on the Medipix chip.
With new interfaces becoming available for Medipix 2 (USB 2.0 and Ethernet), its acquisition rate will far exceed that of MCPs shortly. Since aging is also negligible for low electron energies, we expect Medipix to become the detector of choice for a new generation of LEEM/PEEM-systems.

[1] R. van Gastel *et al.*, *Ultramicroscopy,* **110**, 33 (2009).
[2] J. Coraux *et al., New J. Phys.*, **11**, 023006 (2009)

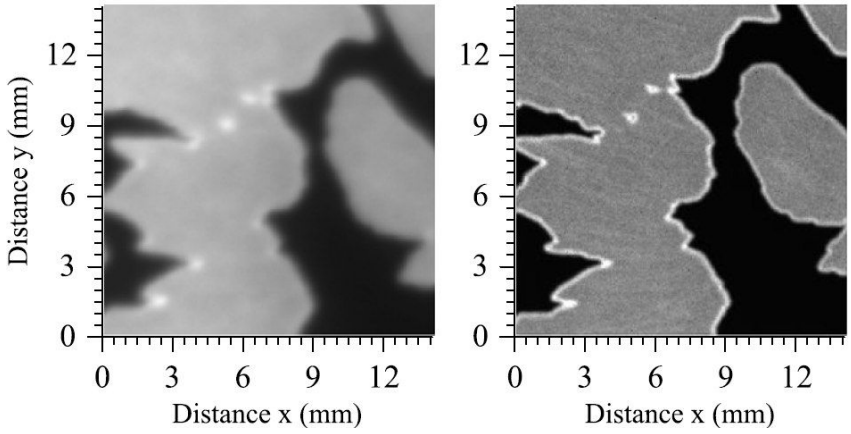

FIG. 1*. Comparison of PEEM images (FOV: 15.5 μm) of graphene flakes on Ir(111) as taken with a MCP detector (left) and a Medipix 2 detector (right). The uncovered Ir appears dark and the graphene appears bright as a result of the difference in work function between the two surfaces. Note that the full detector area is larger for the MCP than for Medipix. The left image was therefore cut from a 50 μm FOV MCP image. The axes in the Figures denote the dimensions at the detector itself.*

Space charge in XPEEM under micro-focused illumination with synchrotron radiation

Andrea Locatelli[1], T. Onur Menteş[1], Miguel A. Niño[1], Ernst Bauer[2]

[1]*Sincrotrone Trieste S.C.p.A., Basovizza, Trieste 34149, Italy (andrea.locatelli@elettra.trieste.it)*
[2]*Department of Physics, Arizona State University, Tempe, Arizona 85287-1504, USA*

The availability of beamlines delivering highly monochromatized light together with progress in electron analyzer design has lead to tremendous improvements of the energy resolution of the most popular experimental methods based on photoemission. The parallel development of brighter and more powerful light sources, such as pulsed lasers and FELs, has raised concerns of space charge effects. A recent study reports that line broadening up (to 10 meV) and other artifacts (such as Fermi level shift) already occur with synchrotron radiation [1]. Due to the limited energy resolution of most XPEEM and SPEM microscopes, space charge effects in spectro-microscopy have so far received little attention. The most recent literature however suggests that space charge can become a major issue in time resolved PEEM with atto- of femto-second resolution, due to the extremely high flux of the illumination [2,3]. Most relevantly, it is expected that space charge effects are especially important in the presence of photon beam micro-focusing. The SPELEEM microscope available at Nanospectroscopy (Elettra Synchrotron Laboratory) was recently employed in a proof-of-principle imaging experiment using the storage ring FEL as photon source [4]. Using coherent harmonic generation (CHG) of vacuum ultraviolet ultra-short pulses we recorded topographic images of a patterned SiO_2 sample, demonstrating the feasibility of CHG-PEEM, at least at intermediate lateral resolution. During the experiments severe space charge effects were observed, which compromised both the lateral resolution and the spectroscopic ability of the microscope (broadening of Fermi Edge up to more than 1eV). The investigation on space charge effects was then extended to the operation with synchrotron radiation. Our results demonstrate that at photon fluxes above 10^{13} photons per second both the energy resolution and the lateral resolution of the XPEEM microscope are considerably degraded. As shown in the Figure below, the lateral resolution of the microscope is degraded to more than 60 nm when imaging core level electrons at high photon fluxes; much larger effects have been observed in XPEEM with secondary electrons.

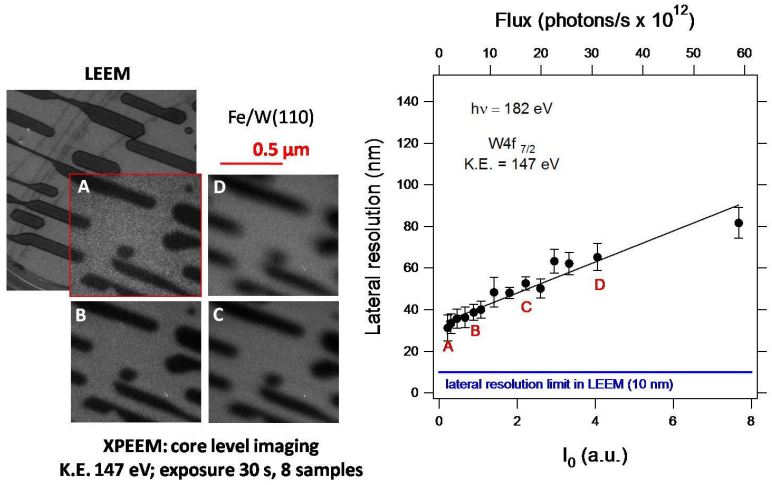

Figure. Degradation of the lateral resolution of the SPELEEM versus increasing photon flux on the sample.

References

[1] X.J. Zhou et al, Journal of Electron Spectroscopy and Related Phenomena **142**, 25-38 (2005).
[2] A. Mikkelsen et al, Review of Scientific Instruments **80**, 123703 (2009).
[3] N.M. Buckanie, et al, J. Phys.: Condens. Matter **21,** 314003 (2009).
[4] G. De Ninno et al, Physical Review Letters **101**, 053902 (2008).

Commissioning of the new aberration-corrected, energy-filtered PEEM/LEEM endstation at BESSY

F. Nickel[a], A. Kaiser[a], I. Krug[a], S. Cramm[a], C. Wiemann[a], A. Schmid[b], A. Berghaus[c], O. Schaff[c], and C.M. Schneider[a]

[a] Forschungszentrum Jülich, Institut für Festkörperforschung IFF-9, and JARA-FIT, 52425 Jülich, Germany
[b] Materials Sciences Division, Lawrence Berkeley National Laboratory, Berkeley, California 94720, USA
[c] SPECS GmbH, Voltastrasse 5, 13355 Berlin, Germany

E-mail: fl.nickel@fz-juelich.de

Since Brüche invented the photoemission electron microscope in 1933 [1] the imaging quality of immersion lens microscopes continuously improved, and has now approached the limit in lateral resolution for non-aberration-corrected designs (3-10 nm for LEEM [2]). It is therefore desirable to further push the limits in resolution and microscope transmission by applying some kind of aberration-correction approach. To exploit and characterize the capabilities of the latest instrument generation, we built up a state-of-the-art PEEM/LEEM endstation at the soft x-ray beamline UE56/1-SGM at BESSY in spring 2010.

This microscope, being based on a design by R. Tromp [3] and custom-built by SPECS GmbH [4], comprises an electrostatic electron mirror for aberration correction improving the lateral resolution as well as transmission. Due to the dispersion of the built-in magnetic prism arrays the instrument allows one to perform in-line energy-filtering for laterally-resolved photoemission spectroscopy. The device is operated at the Juelich soft x-ray beamline which provides photons in the energy range from 50 to 1500 eV and with variable linear/circular light polarization. These properties allow element-selective studies of magnetic properties by means of magnetic linear and circular dichroism (XMLD, XMCD). By using the pulsed time structure of synchrotron radiation the instrument is furthermore predestined for stroboscopic (TR) PEEM experiments [5]. Due to superior lateral resolution as well as transmission as a result of aberration-correction, the endstation is ideally suited for this purpose. To further enhance the primary flux in the synchrotron mode, an additional refocusing optics has been developed to provide a small and stable synchrotron light spot adapted to the small field of view of the PEEM.

All features mentioned generate a unique environment for nanospectroscopy studies featuring time and laterally resolved measurements of magnetic excitations in nanostructures such as spin waves or vortex core dynamics, but also electronic dynamics by time-resolved photoelectron spectroscopy.

In order to perform time-resolved pump-probe measurements at arbitrary repetition rates a gating technique is needed. We successfully tested an MCP gating approach in the new instrument with a switching amplitude of several hundreds of volts during a gating pulse of several tens of ns width.

We will show the first results of magnetic imaging with our new instrument. Furthermore, we will present the results of the performance of our MCP gating system in BESSY's hybrid bunch mode. Both the bunch gap and the isolated single bunch in the BESSY hybrid filling mode could be clearly identified using this technique, which is an important step for future TR-PEEM experiments.

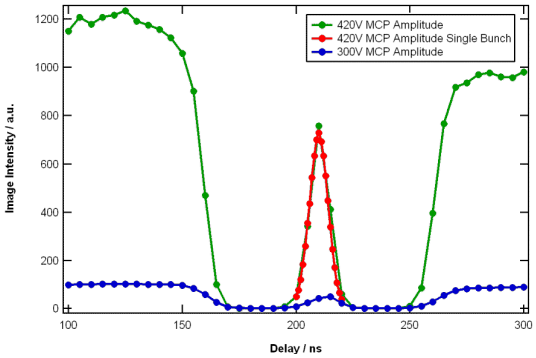

Fig. 1: Varying the delay between gating pulse of 70ns width and BESSY bunch clock clearly shows the hybrid filling pattern (multi bunch – gap – single bunch). Image intensity resulting from the single bunch (red) can be completely isolated with our MCP gating technique.

[1] E. BRÜCHE, *Elektronenmikroskopische Abbildung mit lichtelektrischen Elektronen*, Z. Phys. A Hadr. and Nuclei **86**, 448 (1933)
[2] L.H VENEKLASEN, *The continuing development of low- energ electron microscopy for characterizing surfaces*, Rev. Sci. Instr. **63**, 5513 (1992)
[3] R.M. TROMP, J.B. HANNON, A.W. ELLIS, W. WAN, A. BERGHAUS, O. SCHAFF, *A new aberration-corrected, energy-filtered LEEM/PEEM instrument. I. Principles and design*, Ultramicroscopy, in press (2010)
[4] www.specs.com
[5] G. SCHÖNHENSE, H.J. ELMERS, S.A. NEPIJKO, C.M. SCHNEIDER, *Time-resolved Photoemission Electron Microscopy*, Adv. Im. El. Phys. **142**, 159 (2006)

Installation and obtained performance of PEEM system at the BL10 of SAGA-LS

Hiroyuki SETOYAMA, Daisuke YOSHIMURA and Toshihiro OKAJIMA

Kyushu Synchrotron Light Research Center
8-7 Yayoigaoka, Tosu, Saga 841-0005, Japan

A photoemission electron microscope (PEEMSPECTOR; Elmitec GmbH) has been installed at the beamline BL10 of the SAGA Light Source (SAGA-LS). Using energy tunable soft X-ray as probe, PEEM is a powerful tool for μ-NEXAFS measurements of many applications materials science, such as complex polymer thin films[1], organic thin films[2], etc.

Synchrotron radiation from a variably polarizing undulator (APPLE-II) can be used in this beamline. Various polarized X-rays in the energy range 30 eV to 1200 eV are utilized at this beamline[3]. The X-ray with high photon flux and high energy resolution is monochromatized by a varied-line-spacing plane grating monochromator. The focal position of the X-ray is located 0.8m from a focusing toroidal mirror placed after the monochromator. The sample is illuminated by the X-ray at an incident angle of 30°. The observed spot size evaluated by the PEEM image was about 100 μm (W) × 15 μm (H) (FWHM). According to a field of view of the PEEM, the position of the PEEM system can be adjusted to use the X-ray effectively by a remote moving system along the optical axis. We confirmed that the spatial resolution of the PEEM system was less than 40nm by measuring the patterned Si wafer using a mercury (UV) lamp. The performance of the system and some application examples will be presented.

[1] C. Morin *et. al.*, J. Electron Spectroscopy **137-140** (2004) 785.

[2] Y. Baba *et. al.,* Surf. Sci. **603** (2009) 2612.

[3] D. Yoshimura *et. al.,* AIP conference proceedings (Proceeding of the 10th International Conference of Synchrotron Radiation Instrumentation), to be published.

Laplacian and Caustic Imaging of Surface Topography in Mirror Electron Microscopy

S. M. Kennedy, C. X. Zheng, W. X. Tang, D. M. Paganin and D. E. Jesson
School of Physics, Monash University, Victoria 3800, Australia

Mirror electron microscopy (MEM) is a well-established technique suited to the real-time study of surface phenomena, via the interaction of the reflected electron beam with electric microfields in the vicinity of the surface. Such microfields may arise due to variations in surface height and/or in the potential of the surface itself, and this surface information is contained within the resulting image contrast produced with MEM.

We discuss a new approach to the interpretation of MEM image contrast. For sufficiently small variations in surface topography we show that Laplacian imaging theory is valid and the contrast can be directly related to surface curvature [1]. When Laplacian imaging theory is not valid the image contrast can be interpreted in terms of caustics, and we will discuss a new graphical representation which describes how the caustics contained in images vary with objective lens defocus.

As a specific example we consider the topical case of Ga droplets running across a GaAs (001) surface, leaving behind smooth trails (Fig. 1) [2]. The droplets exhibit caustic image contrast and the trails Laplacian image contrast. We will discuss the inverse problem of how surface topography can be extracted from MEM images in both contrast regimes using a through focus series of images.

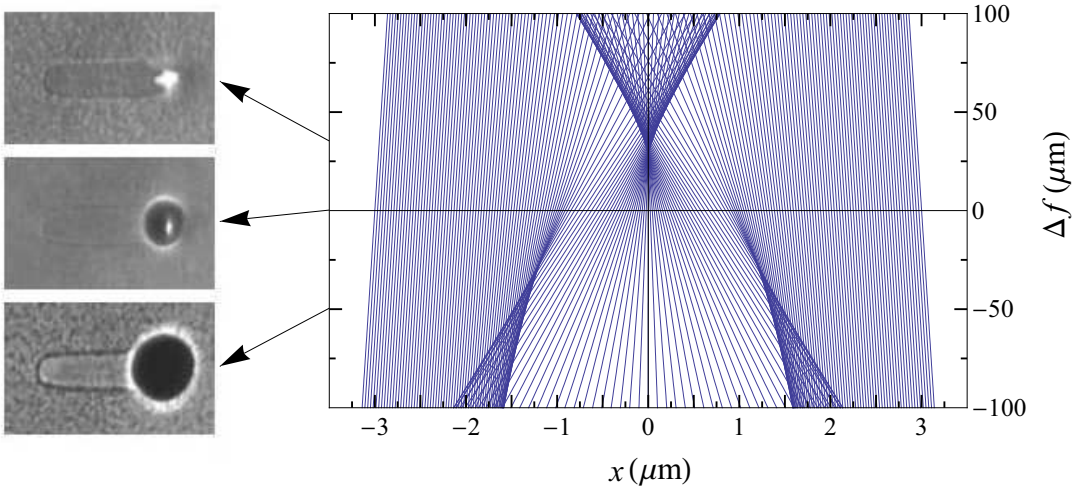

Figure 1: MEM images of a Ga droplet and trail on GaAs (001), for positive objective lens defocus (Δf), zero defocus, and negative defocus. The droplet contrast may be explained using caustic imaging theory, with corresponding defocus regions for each image indicated.

[1] S. M. Kennedy, C. X. Zheng, W. X. Tang, D. M. Paganin and D. E. Jesson, *Proc. Roy. Soc. A*, published online (2010), doi: 10.1098/rspa.2010.0093.

[2] J. Tersoff, D. E. Jesson and W. X. Tang, *Science* **324** (2009) 236.

Aberrations of the Cathode Objective Lens

R.M. Tromp

IBM T.J. Watson Research Center, P.O. Box 218, Yorktown Heights, NY 10598, USA

I will discuss theoretical and practical aspects related to measuring and correcting chromatic and spherical aberrations of a cathode objective lens as used in Low Energy Electron Microscopy (LEEM) and Photo Electron Emission Microscopy (PEEM) experiments. Special attention is paid to the various components of the cathode objective lens as they contribute to chromatic and spherical aberration, and how they affect practical methods for aberration correction.. The chromatic and spherical aberration coefficients in image space can be captured by simple analytical expressions. Both theoretically and experimentally it is possible to separate the chromatic aberrations of the electrostatic and magnetic fields that make up the cathode lens While the magnetic component is independent of the energy E_0 with which the electrons leave the sample, the electrostatic component varies strongly with E_0. I will show how to measure these aberrations, and how to interpret the results. In aberration-corrected instruments, voltage settings to the electron mirror must be adjusted as the electron energy is changed. Based on a proper understanding of the objective lens aberrations, and with sufficiently accurate control of the mirror optics, it will be possible to make such adjustments 'on the fly.

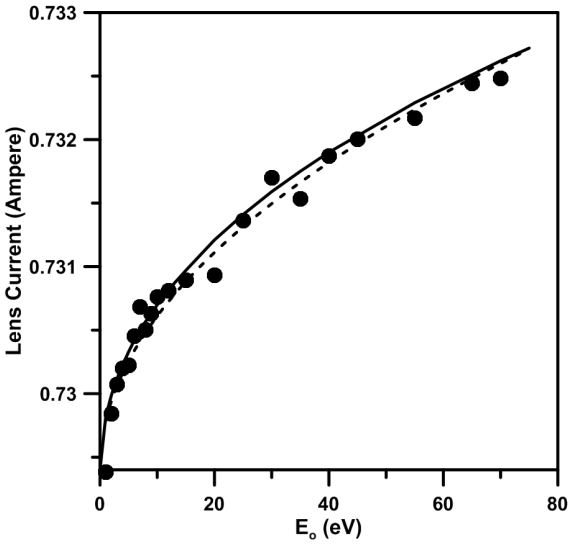

Objective lens current as a function of E_0, keeping the column energy at a fixed value of 15000 eV. The dashed line is a fit of the form $I = I_0 + a.\sqrt{E_0}$. The solid line is the theoretically predicted lens current, based on the analytically known chromatic aberrations of the objective lens.

Anti-Phase Domain Inspection of III-V on Silicon by Low Energy Electron Microscopy

Benjamin Borkenhagen[1], Henning Döscher[2], Gerhard Lilienkamp[1], Thomas Hannappel[2] and Winfried Daum[1]

[1] *Institute of Energy Research and Physical Technologies, TU Clausthal, Leibnizstr. 4, D-38678 Clausthal-Zellerfeld, Germany*
[2] *Helmholtz-Zentrum Berlin für Materialien und Energie, Hahn-Meitner-Platz 1, D-14109 Berlin, Germany*

A major obstacle in the heteroepitaxy of high-quality, lattice-matched III-V semiconductor thin films on Si(100) is the formation of anti-phase domains. We introduce dark-field imaging in a low energy electron microscope (LEEM) as a new, non destructive technique to image the anti-phase domain structure of GaP epitaxial films on Si(100). The high contrast achieved in LEEM is based on the perpendicular orientation of the characteristic P-rich (2x2)/c(4x2) surface reconstruction. Different than transmission electron microscopy (TEM) which also was applied in a specific dark-field mode for comparison, the characterization of the anti-phase domains with LEEM does not require elaborate sample preparation.

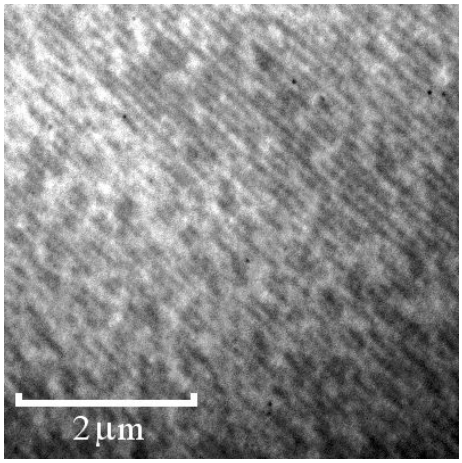

Figure 1: *Typical main phase / anti-phase pattern of a regularly stepped sample, $E_{kin} = 56$ eV (main phase bright, anti-phase dark)*

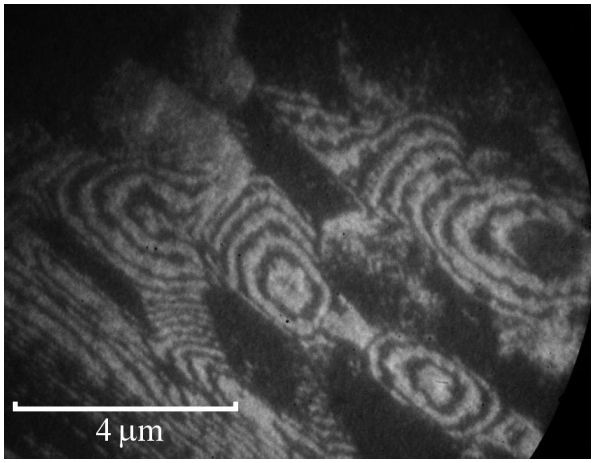

Figure 2: *Phase distribution near defect sites, $E_{kin} = 10.3$ eV (anti-phase bright)*

On a slightly miscut Si(100) substrate terraces are alternately covered with GaP in main phase and anti-phase orientation respectively whereas main phase partially spreads to adjoining terraces. This phase distribution can be observed for the predominant part of the sample surface (fig. 1). Inspection of the sample also yields elliptical defects often surrounded by target pattern like domain distributions (fig. 2). The defects originate possibly from inhomogeneities of a Si buffer layer. Large single domain areas are formed either on equally large terraces or at sites with high step density due to double step formation.

XPEEM investigation of adiabatic shear bands in metallic alloys

Homa Mostaghimi Ghomi[1], Uday Lanke[2] and Akindele Odeshi[1]

[1]*Mechanical Engineering Department, University of Saskatchewan, Saskatoon, SK, Canada*

[2] *Canadian Light Source Inc., University of Saskatchewan, 101 Perimeter Road, Saskatoon, SK, Canada*

Adiabatic shear bands (ASB)[1,2] are regions of intense shear strain localisation in metallic alloys subjected to impact loading. A combined action of adiabatic heating and strain localization results in the formation of these bands, which initiate failure of engineering materials under dynamic shock loading.

We used x-ray photoemission electron microscopy (XPEEM)[3], scanning electron microscopy and atomic force microscopy to study the shear band formed in AISI 4340 steel. XPEEM studies were performed on spectromicroscopy beamline at the Canadian Light Source, while optical and scanning electron microscopies were carried out at the Mechanical Engineering Department. The main motivation behind this study is to find the micro-structural evolution; new phase formation, if any, that may result in the formation of adiabatic shear bands. Our preliminary XPEEM investigations confirmed more Ni (and less Cr) inside the shear band while less Ni (and more Cr) is recorded outside the shear band. Further investigations are underway that will give us quantitative picture and better understanding of the ASB.

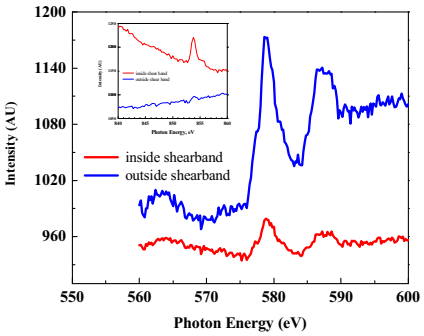

Figure 1. Cr 2p NEXAFS spectra from regions inside and outside the shear band. Inset figure shows Ni 2p spectra from the same region.

References:

1. A G Odeshi and Bassim *Materials Science and Engineering A* **525**, 91-96, 2009
2. Y Xu, J Zhang, Y Bai and M A Meyers *Metallurgical and Materials Transactions A* **39**, 811-843, 2008
3. U D Lanke, A P Hitchcock and S G Urquhart *CLS activity report,* 2009

In-situ Characterization of Bimetallic Oxidation and Oxide Thin-Film Growth Using Intensity-Voltage Low-Energy Electron Microscopy

J. I. Flege[1], A. Meyer[1], B. Kaemena[1], S. Senanayake[2], F. Alamgir[3], and J. Falta[1]

[1]Institute of Solid State Physics, University of Bremen, Bremen, Germany
[2]Department of Chemistry, Brookhaven National Laboratory, Upton (NY), United States
[3]Materials Science and Engineering, Georgia Institute of Technology, Atlanta (GA), United States

The controlled design of multi-component oxide nanostructures has been a long-standing goal in nanoscience due to their wide-spread use in numerous applications, ranging from microelectronics to heterogeneous catalysis. Because of the inherent complexity involving the frequent occurrence of multiple phases and oxidation states, an in-situ characterization during growth is highly desirable. In this contribution, we will show that intensity-voltage low-energy electron microscopy (IV-LEEM) is the ideal tool for this purpose owing to its high sensitivity to oxidation and subsurface oxygen incorporation [1, 2] combined with nanometer lateral resolution and video-rate monitoring capability.

We will illustrate the technique by presenting two studies targeting chemical reactions in model systems relevant to heterogeneous catalysis. In the first example, we investigate the oxidation of well-defined ultra-thin silver films grown on Ni(111) surfaces of few-monolayer thickness (ML) [3]. By I-V analysis, we are able to distinguish between surface and subsurface oxidation as well as subsequent reduction upon ethene exposure, allowing for an identification of the nanoscale surface composition under reaction conditions. In the second example, we study the morphology and atomic structure of ceria films on Ru(0001) by reactive molecular beam epitaxy. Throughout the whole temperature range from about 670 K to 1270 K (fig. 1 (right)), a Volmer-Weber growth mode is identified with average island densities, shapes and thicknesses depending on temperature [4].

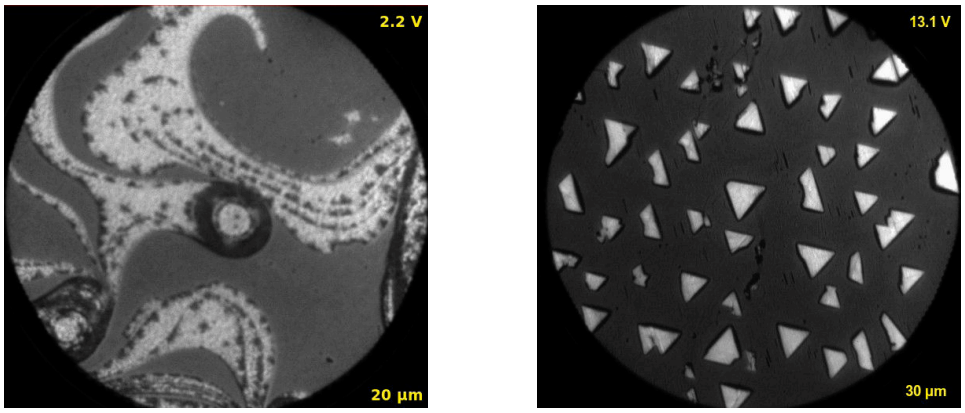

Figure 1: LEEM images showing nanoscale surface morphologies of (left) ultra-thin Ag films (1 ML: bright; 2 ML: dark) during oxidation, which induces the formation of small, dark areas in the monolayer film, and (right) triangular ceria islands grown on Ru(0001) at high temperature.

References

[1] J. I. Flege, J. Hrbek, and P. Sutter, Phys. Rev. B **78**, 165407 (2008).
[2] J. I. Flege and P. Sutter, Phys. Rev. B **78**, 153402 (2008).
[3] A. Meyer, J. I. Flege, R. Rettew, S. Senanayake, Th. Schmidt, F. Alamgir, and J. Falta, submitted (2010).
[4] J. I. Flege *et al.*, in preparation.

Magnetic Domain Imaging by Laser PEEM: Two Photon Photoemission and Energy Dependence

Takeshi Nakagawa, Toshihiko Yokoyama
Institute for Molecular Science

Email: nakagawa@ims.ac.jp

Magnetic domain imaging by PEEM is an inevitable method for studies of magnetic thin films. Whereas magnetic circular dichroism PEEM using synchrotron radiation is prevailing because of its high sensitivity and element specific measurements, magnetic domain imaging in lab using MCD – PEEM is also available using threshold photoemission PEEM[1-3]. Use of two photon photoemission (2PPE) is a merit of laser photoemission, which sometimes gives rather higher MCD asymmetry compared with that by 1PPE.

The threshold photoemission MCD can give enhanced asymmetry, offering well contrasted magnetic domain images in PEEM. The reason is the combined mechanism due to the threshold photoemission in low energy excitation: well filtered energies and restricted initial state momentum for photoelectrons due to the photoelectron refraction at the surface by the potential difference between the solid and vacuum. Figure shows thickness dependent 2PPE MCD asymmetry taken at $h\nu$ = 2.6 eV by increasing the Cu overlayer thickness. The bare Ni film gives 0.28 MCD asymmetry signal, but the one monolayer Cu capping reduces the MCD effect; the MCD asymmetry drops to 0.12, 60% decrease. On the other hand with much thicker Cu capping the asymmetry change shows slow decreasing and the MCD contrast survives above the 3.5 nm capping. The estimated escape depth, 2.3 nm, is in agreement with long mean free path for low kinetic energy electrons [4], but the rapid decrease in the thinner thickness has not been pointed out, which can be explained by the refraction effect.

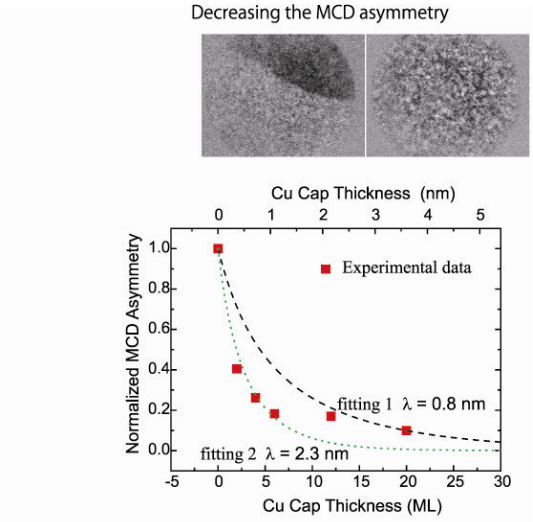

Figure (top) Tow Photon Photoemission MCD-PEEM image on Ni(12 ML)/Cu(001). (bottom) The corresponding MCD asymmetry change as a function of Cu overlayer thickness($h\nu$ = 2.6 eV).

References

[1] T. Nakagawa, and T. Yokoyama, 2006 *Phys. Rev. Lett.* 96, 237402.
[2] T. Nakagawa, T. Yokoyama, M. Hosaka, and M. Katoh, 2007 *Rev. Sci. Instrum.,* 78 023907.
[3] T. Nakagawa, *et al.*, 2009 *Phys. Rev.* B **79** 172404.
[4] G.K.L. Marx, P.O. Jubert, A. Bischof, and R. Allenspach, 2003 *Appl. Phys. Lett.* **83**, 2925.

Detection of magnetic circular dichroism in an extraterrestrial object: X-ray Photo Emission Electron Microscopy study of an iron meteorite

U D Lanke, T Walker and V Olorunda
Canadian Light Source Inc., Saskatoon SK, Canada

M Stauffer
Geology Department, University of Saskatchewan, Saskatoon SK, Canada

A Odeshi
Mechanical Engineering Department, University of Saskatchewan, Saskatoon SK, Canada

M Quann, A Trevors, S Mason, A O'Reilly and P MacDonald
James M Hill High School, Miramichi NB, Canada

T Saulnier, A Riebel, J. d'Entremont, E. Flett and K Cripps
Miramichi Vally High School, Miramichi NB, Canada

Scientist and researchers are always fascinated with the origin of solar system. The study of meteorites is one way to understand how the solar system has been formed. Earth is constantly bombarded with meteorites and every day approximately a billion meteors enter earth`s atmosphere; adding thousands of tons of mass onto the earth annually. Size estimation for typical meteorites is from marble to automobile-sized or even larger. In the present work, we studied a sample collected from Sikhote - Alin[1], an iron hexahedrite meteorite.

We applied a synchrotron based x-ray photoemission electron microscopy (XPEEM) technique to study the iron meteorite. We used an XPEEM microscope mounted on the spectromicroscopy beamline at the Canadian Light Source [2]. Differences in x-ray absorption between left and right circularly polarized light has been exploited resulting in magnetic domain imaging or x-ray magnetic circular dichroism (XMCD). A quantitative XMCD analysis, using circularly polarized light at Fe 2p absorption edge, has been accomplished. This poster shows details of magnetic domain with the smallest features on the order of a few micrometres. We also performed spectromicroscopy at Ni, P and S 2p absorption edges on this sample. To the best of our knowledge, these are the first XMCD results from Sikhote-Alin meteorite on soft x-ray beamline.

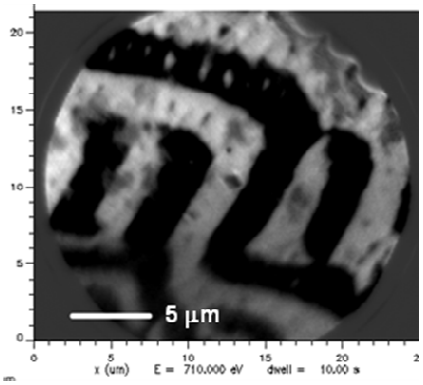

Fe 2p $\longrightarrow$ 3d transition XMCD - PEEM image of an iron meteorite, 25 micron Field of View.

References:

1. *http://en.wikipedia.org/wiki/Sikhote-Alin_Meteorite*
2. U D Lanke, A P Hitchcock and S G Urquhart, *CLS activity report*, 2009

SPLEEM Investigations of Fe Films on the W(111) Surface

Q. Wu[1], Y.R. Niu[1], R. Zdyb[2,3], A. Pavlovska[3], E. Bauer[3] and M.S. Altman[1]
[1]*Department of Physics, Hong Kong University of Science and Technology, Kowloon, Hong Kong*
[2]*Institute of Physics, Marie Curie-Skłodowska University, Lublin, Poland*
[3]*Department of Physics, Arizona State University, Tempe, Arizona, U.S.A.*

The magnetic properties of Fe films on the W(111) surface have been investigated using spin polarized low energy electron microscopy (SPLEEM). Magnetic information is obtained with SPLEEM through the measurement of the reflected intensity asymmetry for incident electron beams of opposite spin polarization [1]. This asymmetry is proportional to the component of the sample magnetization vector that is parallel to the incident polarization direction. The magnetic asymmetry was measured as a function of film thickness, incident electron energy and polarization direction, and temperature. We find that the onset of magnetism occurs at 6 ML coverage during deposition at 300K and that films are spontaneously magnetized in the in-plane direction. The magnetic asymmetry also exhibits a complex variation with increasing thickness (fig. 1). Changes of asymmetry that occur together with a significant modification of the magnetic domain structure at about 12 ML coverage correlate with a structural transformation of the film that was detected previously at the same coverage [2]. Surprisingly, the asymmetry vanishes abruptly at 8 ML and reappears just as suddenly at 9 ML at 300K. The absence of asymmetry at every incident energy, in-plane or out-of-plane polarization direction clearly indicates that magnetism is suppressed in this thickness range. Asymmetry is also detected in an increasingly narrower thickness range centered at 7 ML when film growth is carried out at slightly elevated temperature (fig. 2). This suggests that the ferromagnetic gap at intermediate thicknesses is caused by the suppression of the Curie temperature, although transitory antiferromagnetic ordering cannot yet be ruled out.

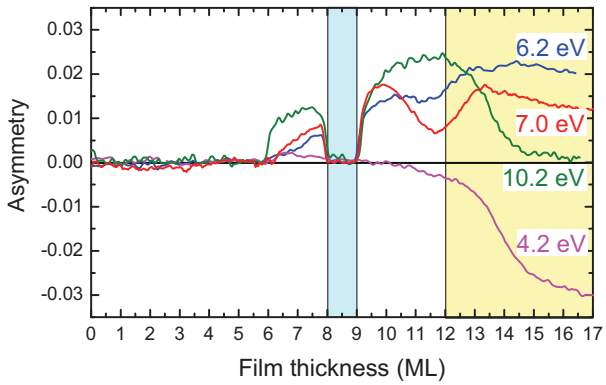

Fig. 1: Magnetic asymmetry vs. film thickness at several incident energies during deposition at 300K.

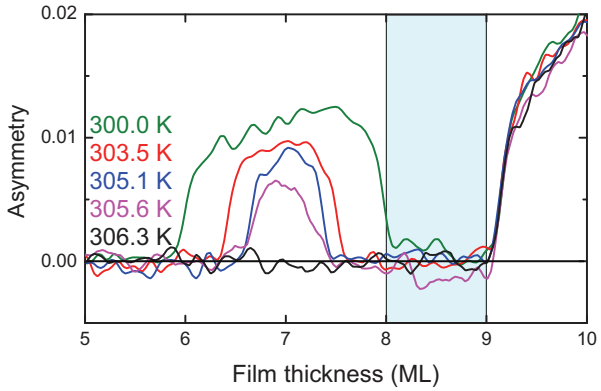

Fig. 2: Temperature dependence of magnetic asymmetry vs. thickness at 10.2 eV incident energy.

References

[1] M.S. Altman, H. Pinkvos, J. Hurst, H. Poppa, G. Marx and E. Bauer, in Magnetic Materials: Microstructure and Properties, ed. T. Suzuki, MRS Symposia Proceedings No. 232 (Materials Research Society, Pittsburgh, 1991) pp.125-132.
[2] J. Kołackiewicz and E. Bauer, Surf. Sci. **420**, 157 (1999).

Surface Electrochemical Potential Mapping of Graphene on SiC(0001)

Shuaihua Ji, J. B. Hannon, R. M. Tromp, A. W. Ellis, M. C. Reuter and F. M. Ross,

IBM Research Division, T. J. Watson Research Center, Yorktown Heights, New York 10598, USA

Thermal decomposition of silicon carbide is one of the most promising ways to achieve high quality wafer-scale epitaxial graphene. Well-controlled thickness and large grain sizes of graphene on SiC(0001) have been realized recently. However, graphene grown on the Si-terminated SiC surface has low mobility, for reasons that are still not clear. Here, low energy electron microscopy (LEEM) and scanning tunneling microscopy (STM) were used in combination to characterize the structure and electronic properties of graphene on SiC(0001). Graphene was grown in a UHV LEEM by annealing SiC above 1300^{o}C in a background pressure of disilane. SiC decomposition creates large graphene domains whose thickness (in the 1-2 ML range) could be determined from the LEEM contrast. After growth, samples were transferred to a UHV low temperature multiprobe system where the structure, defects and step geometry were characterized by STM, and local measurements of the electrochemical potential were made at liquid nitrogen temperature on the graphene sheet. The combination of electrical and structural measurements enabled by LEEM and STM provide information on scattering at steps and terraces at different graphene thickness, helping to understand transport processes at the atomic scale.

Decoupling Graphene from SiC(0001) via Oxidation

S. Oida, F.R. McFeely, J.B. Hannon, R.M. Tromp, M. Copel, Z. Chen,
Y. Sun, D.B. Farmer and J. Yurkas
IBM T.J. Watson Research Center, Yorktown Heights, NY 10598

When epitaxial graphene layers are formed on SiC(0001), the first carbon layer (known as the "buffer layer"), while relatively easy to synthesize, does not have the desirable electrical properties of graphene. The conductivity is poor due to a disruption of the graphene π-bands by covalent bonding to the SiC substrate. Here we show that it is possible to restore the graphene π-bands by inserting a thin oxide layer between the buffer layer and SiC substrate using a low temperature, CMOS-compatible process that does not damage the graphene layer.

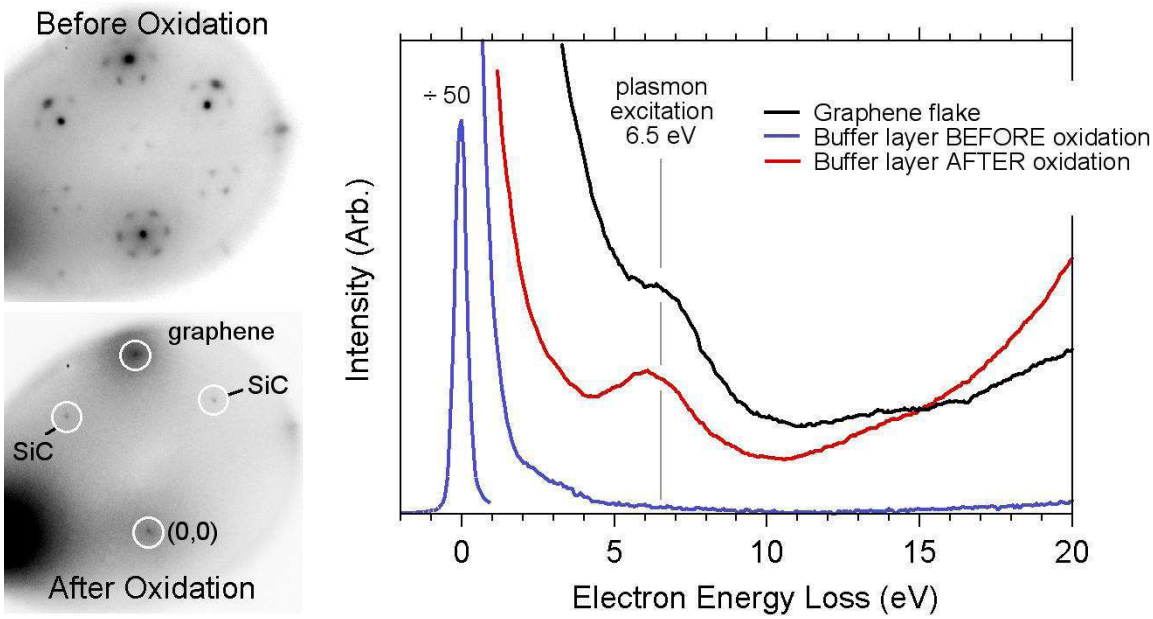

Caption:

LEED patterns recorded before and after oxidation of the graphene buffer layer. Electron energy loss spectra recorded using LEEM from (a) a thick graphite flake placed on SiC(0001) (black), (b) a graphene buffer layer on SiC(0001) before oxidation (blue), and (c) the same buffer layer after oxidation (red). All spectra were recorded using 33 eV electrons at near-normal incidence.

Secondary Electron Emission Microscopy and Partial-Yield X-ray Absorption Spectromicroscopy with an Energy Filtered PEEM Microscope

Stephen Christensen,[1] Brian Haines,[1] Uday Lanke,[2] Stephen Urquhart[1,*]

Department of Chemistry, University of Saskatchewan, Saskatoon, SK, Canada

Canadian Light Source, University of Saskatchewan, Saskatoon, SK, Canada

* Presenter and corresponding author, stephen.urquhart@usask.ca

Energy filtered PEEM microscopes are useful for spatially resolved photoemission spectroscopy measurements. Our observation shows that the energy filter can have an unusual effect on X-ray absorption spectra (e.g. the Near Edge X-ray Absorption Fine Structure, or NEXAFS spectra) of organic thin films.

NEXAFS spectra of solids are often recorded in sample current mode, where the total current of primary and secondary photoelectrons is recorded with a picoameter as a function of photon energy (total electron yield mode; TEY). When NEXAFS spectra is measured in a PEEM microscope, the PEEM imaging optics measure this electron yield with spatial resolution. This detection method is similar to total electron yield, although the signal is weighted by the optic's transmission function. This PEEM signal is dominated by the sample's low energy secondary electron emission band. In an energy filtered PEEM, the energy filter will select a narrow "slice" of this secondary electron emission band to generate the image. When NEXAFS spectra are recorded in an energy filtered PEEM, we find that the spectra are significantly distorted relative to conventional NEXAFS spectra.

This effect is shown in Figure 1 for the carbon 1s NEXAFS spectrum of a polystyrene thin film. Spectra recorded at different relative secondary electron kinetic energies (0 – 4 eV, e.g. partial electron yield) are distorted relative to the conventionally recorded NEXAFS spectrum (TEY). The low energy C 1s → π^*(C=C) feature (285 eV) is broader in most of these spectra and the intensity of the higher energy features varies. This effect is reproducible and is not due to chemical changes induced by radiation damage, as the conventional NEXAFS spectrum remains unchanged over the course of this exposure. The origin of this effect is not clear, although we hypothesize that secondary electron generation, propagation and photoemission leads to differentiation within the secondary electron emission band; while the total band is proportional to the NEXAFS signal, individual energies of this band may reflect propagation differences of specific electronic effects. This observation has consequences for spectroscopic PEEM studies of organic thin films when energy filtering is used.

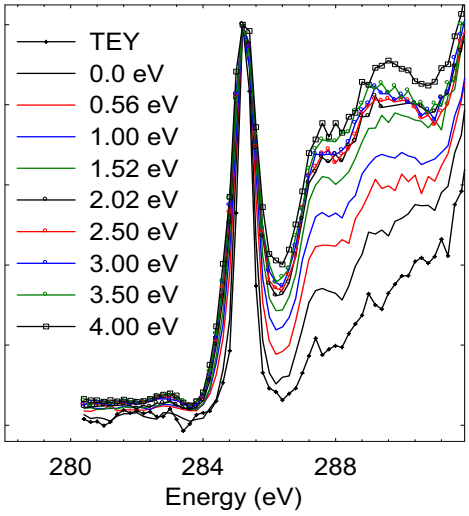

Figure 1: (right) Carbon 1s NEXAFS spectra of a polystyrene thin film, recorded in an energy filtered PEEM microscope (Elmitec GmbH). The spectra are recorded at a range of relative electron kinetic energies (0 – 4 eV) via the imaging energy filter. These spectra differ from the conventional (TEY) NEXAFS spectrum.

Threshold photoemission magnetic circular dichroism of Ni(001) films: theory and experiment

S. Günther[1], M. Kronseder[1], G. Woltersdorf[1], and C. H. Back[1]
[1] *Department of Physics, Universität Regensburg, 93040 Regensburg, Germany*

Threshold photoemission magnetic circular dichroism (TP-MCD) in combination with a photoemission electron microscop (PEEM) allows to image magnetic contrast with high spatial resolution without the need of synchrotron radiation. Due to the fact that perpendicularly magnetized Ni on Cu(001) exhibits a very large MCD-asymmetry this system was used to image magnetic domains and to study the physical origin of magnetic circular dichroism near the Fermi level. We measured the MCD-asymmetry as a function of energy and as a function of polarization state of the incoming photons. A three-step-model ab-initio calculation of the normalized spin-polarization density of Ni(001) can explain the MCD-asymmetry of the TP-MCD. Furthermore the calculated degree of circularity inside the metallic film explains the measured MCD-asymmetry dependence as a function of the incoming polarization state very well.

Growth of topological insulator Bi_2Te_3 ultrathin films on Si(111) investigated by LEEM

Hongwen Liu[1], N. Fukui[1], H. T. Yuan[2,3], L. Zhang[1], Y. Iwasa[2,3], T. Hitosugi[1], M. W. Chen[1], T. Hashizume[1,4], and Q. K. Xue[1,5]

[1]*WPI-Advanced Institute for Materials Research, Tohoku University, Sendai 980-8577, Japan*
[2]*Quantum-Phase Electronics Center, The University of Tokyo, Tokyo 113-8656, Japan*
[3]*Institute for Materials Research, Tohoku University, Sendai 980-8577, Japan*
[4]*Department of Physics, Tokyo Institute of Technology, Meguro, Tokyo 152-8551, Japan*
[5]*Department of Physics, Tsinghua University, Beijing 100084, China*

Some kinds of narrow gap semiconductors Bi_2Te_3 and Bi_2Se_3 are traditional thermoelectric material. Recently, they have attracted great attention as a new class of quantum matter, so called topological insulator (TI), with their gapless metallic properties localized at surface state [1]. The materials for TI investigations are usually prepared in the form of bulk crystals by melt-growth, self-flux method and so on[2-5]. However, to get their exotic TI properties, the crystals have to be heavily doped, thus the unexpected impurity energy bands are introduced. The intrinsic TI thin film growth by molecular beam epitaxy is one answer to overcome this problem [6].

In this work [7], we investigate real time growth of Bi_2Te_3 thin film on Si(111) substrate by low energy electron microscopy (LEEM). In combination with the atomic force microscopy and Raman scattering results, we discuss the growth mechanism and optimal conditions to obtain high quality Bi_2Te_3 films on Si(111) substrate. Transport property measurements prove the insulating behavior of the films grown in this way,

[1] B. A. Bernevig, T. L. Hughes, and S.-C. Zhang, Science, **314**, 1757 (2006).

[2]B.R.Sankapal, R.S.Mane and C.D.Lokhande, Mat.Chem.Phys,**63**,230(2000)

[3] Y. Xia,*et.al,. Nat. Phys.* ***6,*** 398 (2009).

[4] Y. L. Chen.*et.al.*, *Science*, ***325,*** 178-181(2009).

[5] D. Hsieh. *et.al.*, *Nature*, ***452,*** 970-974(2008).

[6] T. Zhang *et.al* , Phys. Rev. Lett. **103**, 266803 (2009)

[7] H.W. Liu et al, Crytal Growth & Design (to be published)

Pulse-probe studies using delayed LEEM and LEED following an ion beam pulse*.

W. Swiech, E Samman and C. P. Flynn,
Physics Dept. and Materials Research Laboratory,
University of Illinois at Urbana Champaign,
Urbana, IL 61801

We are exploring by LEEM and LEED the response of clean surfaces when perturbed by pulses of self-ions. The use of self-ions ensures that the surface remains unaffected by chemical impurities. We have developed equipment and methods that permits resolution of time delay down to the sub-μs regime at temperatures up to 1500K. A variety of phenomena are open to study by this new spectroscopy, using a LEEM or LEED probe, following periodic surface modification by ion pulses from a chopped ion beam. These include, for example: (i) diffusion to and from step edges of adatoms and advacancies selectively created by pulses of irradiation (typical time scale msec or less at relevant temperatures); (ii) local recombination of adatoms and advacancies (typical time scale μsec or less); (iii) regression of island embryos created by irradiation (time scale ~ 10 μsec); (iv) fast recovery at high temperatures of such ion beam damage as amorphization; (v) evolution of surface reconstructions following deposition of excess advacancy or adatom populations (time scale unknown). Using the Pt(111) surface irradiated with Pt^- ions we find a large sensitivity of elastic scattering to surface thermal defects, comparable with values seen by McCarty et al for Ag on W, and C atoms on Ru[1], with sharp peaks of efficiency at 3 eV and 68 eV electron impact energy. Our initial efforts focus on area (i) above, specifically adatom diffusion <u>to</u> steps of adatom excess created by low energy ion irradiation, or <u>from</u> steps to annihilate excess advacancies created by ions of high energy (> 250 eV). Together with the known rate of surface mass diffusion[2] these experiments also access numerous valuable properties, including absolute concentrations of adatoms in thermal equilibrium, adatom formation and hopping entropies, etc. Alternative foci on adatom-advacancy recombination or on transient structure change also appear promising.

* Supported in part by DOE grant DE FG07 08ER46549.

[1] J de la Figuera, N. C Bartelt and K F McCarty, Surf Sci 600, 4062 (2006); E Loginova, N C Bartelt, P J Feibelman and K F McCarty, New J Phys, 10, 093025 (2008).
[2] M Rajappan, W Sweich, M Ondrejcek and C P Flynn, J Phys CM 19, 226006 (2007).

Magnetic domain and chemical structures of Dy-doped Nd-Fe-B permanent magnet studied by PEEM and XMCD

R. Yamaguchi[a], K. Terashima[a], K. Fukumoto[b,c d], Y. Takada[c], M. Kotsugi[b], Y. Miyata[a], K. Mima[a], S. Komori[e,f], S. Itoda[e], Y. Nakatsu[e], M. Yano[e,f], N. Miyamoto[f], T. Nakamura[b], T. Kinoshita[b], Y. Watanabe[b], A. Manabe[f], S. Suga[e], S. Imada[e,a]

[a] *Department of Physical Sciences, Ritsumeikan University, Kusatsu, Shiga 525-8577, Japan*

[b] *Japan Synchrotron Radiation Research Institute (JASRI), Sayo, Hyogo 679-5198, Japan*

[c] *Toyota Central Research & Development Laboratories, Inc., Nagakute, Aichi 480-1192, Japan*

[d] *Department of Materials Science, Tokyo Institute of Technology, Meguro-ku, Tokyo, 152-8550, Japan*

[e] *Department of Materials Physics, Osaka University, Toyonaka, Osaka 560-8531, Japan*

[f] *Toyota Motor Corporation, Toyota, Aichi 471-8571, Japan*

Permanent magnet is becoming much more important than ever particularly as a main part of motor used for hybrid and electric cars. Especially, tolerance to higher temperatures is important in development of permanent magnets. It has been known that Dy-doping makes Nd-Fe-B magnet much more tolerant to heat. It is expected that formation of reversed domains is suppressed by Dy doping. In order to reveal the mechanism for this, it is necessary to observe the formation of reversed domains focusing on the relation between the chemical structure and the magnetic domain structure.

Reversed domains are expected to be formed first on the surface of the permanent magnet. Therefore, photoelectron emission microscope (PEEM) is a powerful tool for the study of reversed domains. Combination of PEEM with monochromatized synchrotron radiation enables x-ray photoabsorption spectromicroscopy, by which chemical distribution on the surface can be measured. Further combination of PEEM with circularly polarized synchrotron radiation enables x-ray magnetic circular dichroism (XMCD) microscopy, by which magnetic domain structure can be observed.

The strong stray magnetic field produced by a magnetized permanent magnet sample, however, has so far disabled the observation by PEEM. In this study, the permanent magnet sample has been attached to a yoke without gaps, so that the stray field on the surface of the sample was reduced to less than 10 gauss. This has enabled the observation of the magnetic domain structure of the fully magnetized Nd-Fe-B magnet by PEEM. Experiments have been performed at BL17SU and BL25SU in SPring-8.

The magnetic domain structures of surfaces parallel to the c axis of $Nd_2Fe_{14}B$ grains in the samples have been studied. We first compared, at the room temperature, the sample without and with Dy doping. On the sample without Dy doping, the observed reversed domains were connected across several grains in the direction of c axis. On the other hand, on the Dy doped sample, the total area of the reversed domains as well as the size of each reversed domain was smaller than those of non-doped sample. More importantly, each reversed domain tended to be confined within a grain. Next, the effect of heat on the Dy doped sample has been studied. When the temperature was raised, the reversed domains became longer in the c axis, growing across grains. Above T = 80 °C, the total area of the reversed domains increased drastically, and the shapes of the reversed domains became much wider and became interconnected. The relation between these changes in domain structures and the chemical distribution will be discussed.

Tuesday August 10 – Grand Hyatt Hotel

Afternoon Session 1: LASER BASED PEEM
Chair: M. Horn von Hoegen

1:30 pm: Erik Mårsell, T. Fordell, M. T. Borgström, A. L'Huillier and A. Mikkelsen; PEEM studies of surface plasmons in nanostructures using femtosecond and attosecond IR/XUV laser pulses

1:50 pm: A.Höfer, S. Förster, K. Duncker, and W. Widdra; Laser - excited PEEM study of the temperature dependent ferroelectric domain structures of BaTiO3(001)

2:10 pm: T. Taniuchi, K. Isogai, Y. Kotani, T. Togashi, H. Akinaga, K. Ono, M. Oshima, S. Shin; Measurement System of UV-PEEM using Wavelength Tunable Femto-Second Laser

2:30 pm: N.M. Buckanie, P. Kirschbaum, S. Sindermann, F.-J. Meyer zu Heringdorf Interaction of Surface Plasmon Polaritons with Ag Islands as Imaged in Two Photon Photoemission PEEM

2:50 pm: Break and Continuation of Poster Session

4:30 pm: End of program for today

Evening Options:

Blue Note

PEEM studies of surface plasmons in nanostructures using femtosecond and attosecond IR/XUV laser pulses

Erik Mårsell[1*], T. Fordell[1], M. T. Borgström[1], A. L'Huillier[1] and A. Mikkelsen[1]

1: Department of Physics, Lund University, Box 118, 221 00 Lund, Sweden. *tn05em1@student.lth.se

PhotoEmission Electron Microscopy (PEEM) is a powerful technique for imaging surface plasmon resonances as it has several suitable and complementary contrast mechanisms. Surface plasmon resonances can be excited by light pulses on rough or structured conductor/dielectric interfaces and can give rise to very large field enhancements. Plasmonic nanostructures have been extensively studied during the last decades and are promising for a wide variety of applications[1, 2]. The ability to achieve time-resolved images of such structures would lead to a more thorough understanding of the ultrafast dynamics of surface plasmons. Time-resolved PEEM imaging can be realised using a pump-probe setup where a pump laser pulse excites a surface plasmon and a second, probe, laser pulse images the charge density variations.

We have combined PEEM with ultrashort laser pulses to image surface plasmons in nanostructures. Surface plasmons are excited by near-infrared femtosecond laser pulses and imaged with multiphoton PEEM using the fundamental wavelength of the infrared laser. The energy of the photons used for excitation is well below half the work function of the materials, leading to multiphoton photoemission.

Since the photocurrent induced by n-photon photoemission is proportional to the nth power of the light intensity, PEEM using an infrared laser as the excitation source can image the enhanced plasmonic field with very high sensitivity. Multiphoton PEEM has previously been used to study surface plasmon resonances[3, 4, 5].

We studied different kinds of samples with nanostructures: Thin metal films with ordered arrays of holes defined by high-precision e-beam lithography, Au aerosol nanoparticles on a Cr film and nanowires of different sizes and materials. All samples are seen to have 'hot spots' of enhanced multiphoton photoemission. We varied the polarisation and the intensity of the laser light. The hot spots are found to be strongly polarisation dependent, with different polarisations being favoured for different samples. For the nanowire samples, the polarisation dependence is found to be material dependent. We also explored space charge effects. All of the structures were also imaged with a standard Hg discharge lamp for reference.

Finally, we have recently shown that PEEM also can be performed in a setup using extreme ultraviolet (XUV) attosecond pulse trains as probe(see [6]). We describe how we will continue to explore pump-probe experiments using both infrared femtosecond laser pulses and XUV attosecond pulse trains, with the aim of achieving time-resolved images of surface plasmons. We discuss this setup, our future experiments and the improvements needed to achieve high spatial and temporal resolution.

References

[1] E. Ozbay. Plasmonics: Merging photonics and electronics at nanoscale dimensions. *Science*, 311:189–193, 2006.

[2] S. Maier. Plasmonics - clear for launch. *Nature Physics*, 3:301–303, 2007.

[3] A. Kubo et al. Femtosecond imaging of surface plasmon dynamics in a nanostructured silver film. *Nano Lett.*, 5(6):1123–1127, 2005.

[4] G. H. Fecher et al. Multiphoton photoemission electron microscopy using femtosecond laser radiation. *J. Electron Spectrosc. Relat. Phenom.*, 126:77–87, 2002.

[5] L. Douillard, F. Charra, and Z. Korczak. Short range plasmon resonators probed by photoemission electron microscopy. *Nano Lett.*, 8(3):935–940, 2008.

[6] A. Mikkelsen et al. Photoemission electron microscopy using extreme ultraviolet attosecond pulse trains. *Rev. Sci. Instrum.*, 80(123703), 2009.

Laser-excited PEEM study of the temperature dependent ferroelectric domain structures of $BaTiO_3$(001)

A. Höfer, S. Förster, K. Duncker, and W. Widdra
Institute of Physics, Martin-Luther-Universität Halle-Wittenberg, Germany

The ferroelectric domain structure of $BaTiO_3$ ceramics and single crystals has been studied since the 1950`s. In many studies bulk-sensitive techniques have been used, like birefringence microscopy, and also in the commonly used piezoresponse force microscopy the signal is dominated by the bulk properties. In contrast, the markedly high surface sensitivity of photoemission electron microscopy (PEEM) enables the observation of the ferroelectric response of the outermost surface layer. The experimental setup used here consists of a femtosecond all-fiber based laser system in combination with two noncollinear optical parametric amplifiers which results in two independently tunable beams. Thus, for sample illumination a photon energy between 1.3 and 2.5 eV with pulse lengths of 20 - 40 fs at a repetition rate of 1.5 MHz is available.

At room temperature, the ferroelectric domain structure of a $BaTiO_3$(001) single crystal is characterized by a stripe-like domain pattern aligned along the [100] direction (see Fig. 1). Following the symmetry of the $BaTiO_3$(001) surface one expects three different domain types, namely a, c^- and c^+ domains. They can be discriminated in laser-excited PEEM by their different photoemission yields. The observed stripe pattern is explained by sequences of 90°-a-c domain walls.

Analysis of the PEEM signal as a function of the incoming UV laser intensity at a photon energy of 4.3 eV shows a linear dependence which indicates that one-photon photoemission is responsible for imaging of the domain structure. Wavelength-dependent measurements of this one-photon process reveal a photoemission onset at 3.8 eV.

In-situ PEEM experiments during heating allow to follow the domain wall dynamics. Between room temperature and 400 K a slight lateral movement of the domain walls takes place. Close to the bulk Curie temperature of 400 K there is an abrupt transition to a new domain configuration consisting of 90°-a-c domain walls, as well. This new surface domain structure persists up to 510 K in the absence of a bulk ferroelectric structure.

The possible time-resolution in fs-pump-probe PEEM experiments will be demonstrated at the first Ag(001) image potential state. In future experiments we will use the femtosecond temporal resolution of the laser excitation to follow the ferroelectric domain wall dynamics at ultrafast time scales.

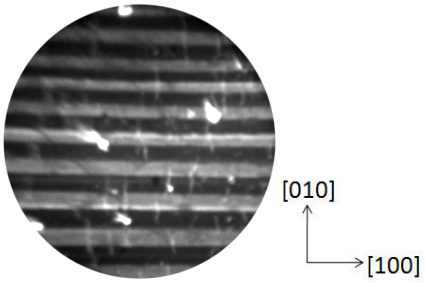

Fig. 1: Ferroelectric domain structure of $BaTiO_3$(001) at room temperature imaged by laser-excited PEEM (hv = 4.43 eV, FOV = 150 µm).

Measurement system of UV-PEEM using wavelength tunable femto-second laser

Toshiyuki Taniuchi[1,2], Kota Isogai[1], Yoshinori Kotani[1,2], Tadashi Togashi[3], Hiroyuki Akinaga[4], Kanta Ono[6], Masaharu Oshima[2,5], Shik Shin[1,2]

[1]*Institute for Solid State Physics, The University of Tokyo, Kashiwa 277-8581, Japan*
[2]*CREST-JST, Honcho 4-1-8, Kawaguchi 332-0012, Japan*
[3]*Japan Synchrotron Radiation Research Institute, Kouto, Sayo, Hyogo 679-5198, Japan*
[4]*National Institute of Advanced Industrial Science and Technology, Tsukuba, Ibaraki 305-8562, Japan*
[5]*Department of Applied Chemistry, The University of Tokyo, Bunkyo-ku, Tokyo 113-8656, Japan*
[6]*Institute of Materials Structure Science, KEK, Tsukuba 305-0801, Japan*

We report the development of the UV laser excited PEEM measurement system using the wavelength tunable laser source with 160 fs pulse width. New methods to control the magnetization by light are important for technological viewpoints. In manganites, for example, photo-induced ferromagnetism was observed in pico-seconds or less [1]. Recently a large magnetic circular dichroism (MCD) was observed near the Fermi level in magnetic thin films [2]. In order to realize the ultrafast observation of magnetic domains, we developed the measurement system for the MCD-PEEM with femto-second UV laser. For this purpose the laser must have an effectively large pulse intensity to pump magnets and a high repetition rate to suppress the space charge effect. Therefore we used a Ti:Sapphire laser and a regenerative amplifier with a 250kHz repetition and 900 mW. We also utilized an optical parametric amplifier for the wavelength tunability, which enables us to measure various magnetic materials without changing their work functions by cesium adsorption. First we present the PEEM images of the Co disk array using the UV sources of the wavelength ranging from 240 nm to 350 nm, corresponding to the photon energy from 3.4 eV to 5.1 eV as shown in Fig.1. The energy resolution is better than 20 meV. This laser system can also switch the circular polarization faster than 5 Hz by a Pockels cell.

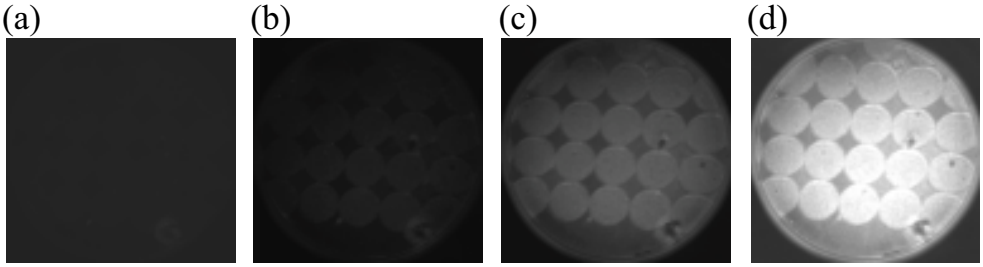

Figure 1. PEEM images of the 5 μm Co disk array obtained with the UV laser of 4.2eV (a), 4.5eV (b), 4.8eV(c) and 5.1eV(d).

References

[1] M. Matsubara *et al*., Phys. Rev. Lett. **99**, 207401 (2007).

[2] T. Nakagawa and T. Yokoyama, Phys. Rev. Lett. **96**, 237402 (2006).

Interaction of Surface Plasmon Polaritons with Ag Islands as Imaged in Two Photon Photoemission PEEM

N.M. Buckanie, P. Kirschbaum, S. Sindermann, F.-J. Meyer zu Heringdorf
University of Duisburg-Essen, Faculty of Physics and Center for Nanointegration (CeNIDE), Lotharstrasse 1, 47057 Duisburg, Germany

Email: meyerzh@uni-due.de

The interaction of light with surface plasmon polaritons (SPPs) provides a way to convert light into electrical signals and back without the need of elaborate light detection or light generation circuitry on the chip. This prospect has inspired a whole area of research that studies the conversion of light into plasmons, uses SPPs to obtain a nano-optical functionality, and finally desires to convert SPPs back into light on a length scale below the diffraction limit. Silver exhibits a surface plasmon resonance in the blue part of the light spectrum, and accordingly, frequency doubled femtosecond laser pulses from a Ti:Sapphire laser make an excellent illumination source for PEEM to study plasmon related phenomena in Ag nanostructures.

After several groups have investigated the moiré-type contrast mechanism of SPP imaging in two photon photoemission PEEM (2PPE PEEM) over the last few years, the observed patterns can by now be quantitatively explained. As such, the technique has matured to a level where the interaction of SPPs with complex islands as well as the manipulation of SPPs by adsorbates can be analysed.

Here we will focus on the modification of the SPP wave during adsorption of C_{60} on Ag islands grown *in-situ* on Si(111). During adsorption of C_{60} the photo emitted electron angular distribution (PEEAD) is changed, and the work function increases. At the same time, the SPP wavelength systematically decreases as a function of C_{60} coverage, reflecting a gradual change of the surface dielectric function. In arbitrarily shaped islands, the incidence direction of the light (projected into the surface plane) and the propagation direction of the SPP wave do not necessarily coincide, since the propagation direction of the SPPs is dictated by Snell's law of refraction. For such cases we also observe a change of the propagation direction of the SPP wave as a function of the C_{60} coverage.

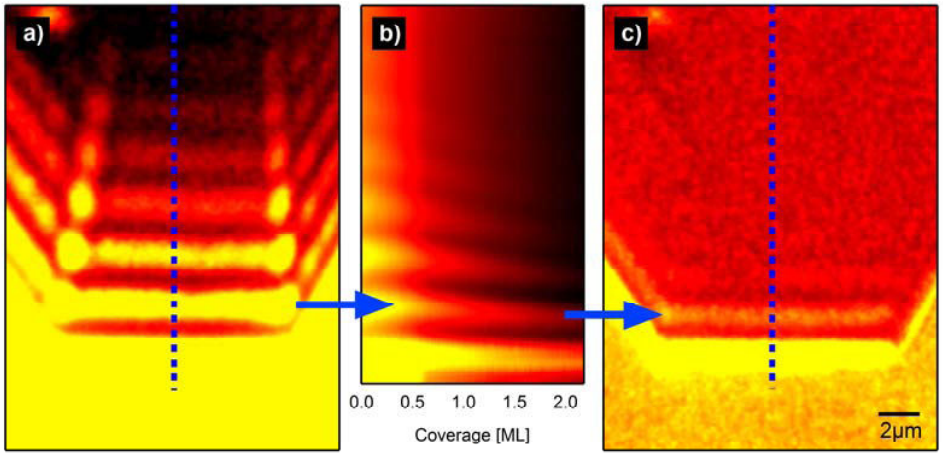

Figure. 2PPE PEEM images of a Ag island on Si(111) before (a) and after (c) deposition of C_{60}. The stripes on top of the islands are explained with a moiré pattern that is formed between the laser pulse and the SPP wave; (b) section along the dotted lines through the stripe-pattern as a function of the C_{60} coverage. Not only does the intensity of the maxima relative to each other change, but also the separation of the maxima varies, indicative of a change of the SPP wavelength.

Wednesday August 11 – IBM T.J. Watson Research Center

7:20 am: Leave Hyatt Hotel by Bus (Breakfast on the Bus)
9:00 am: Arrive at T.J. Watson Research Center

9:30 am: Welcome by Director of Physical Sciences Supratik Guha

Morning Session: GROWTH AND THIN FILMS
Chair: Th. Schmidt

9:40 am: B. Poelsema, G. Hlawacek, F.S. Khokhar, R. van Gastel, C. Teichert; Organic Semiconductor Growth on Graphene Studied by LEEM and μLEED

10:00 am: . A. Al-Mahboob, Y. Tsuruma, J.T. Sadowski, Y. Fujikawa, K. Saiki, T. Hashizume, T. Sakurai, P. Sutter; The Nucleation and Anisotropic Growth of Pn on SiO_2 and FET Structures

10:20 am: M. Vaughn, K.D. Jamison, M.E. Kordesch; Thermionic Electron Emission Microscopy of Ba, Sc, Y, Zr, To and Mg Oxide Multilayers on Tungsten

10:40 am: A. Sala, H. Marchetto, Th. Schmidt, H.-J. Freund; LEEM/LEED Investigation of Fe_3O_4 Thin Film Growth on a Pt(111) Substrate: Morphology and Atomic Termination

11:00 am: T.O. Menteş, A. Locatelli, M.A. Niño, E. Bauer, A. Pavlovska, M. Lewandowski, I.M.N. Groot, S. Shaikhutdinov, H.-J. Freund; The System $Au/Fe_2O_3/Pt(111)$

11:20: I. Krug, N. Barrett, A. Petraru, O. Renault, K. Rahmanizadeh, G. Bihlmayer, L. LeGuyader, A. Besmehn, H. Kohlstedt, C.M. Schneider; Electronic vs. Defect-induced Self-stabilization of Ferroelectric Polarization in Thin PZT Films

11:40 am: Break for Lunch

Organic semiconductor growth on Graphene studied by LEEM and μLEED

B. Poelsema[*], G. Hlawacek[*,†,‡], F.S. Khokhar[*], R. van Gastel[*] and C. Teichert[†]

Organic electronics market is demanding for powerful and flexible devices based on small conjugated molecules. To achieve this, a proper substrate has to be chosen. For para-sexiphenyl (6P), graphene is an ideal substrate for two reasons, namely – its unique properties and the similarity between the structure of the molecule and the graphene lattice. In addition graphene could be used as a transparent and conductive top electrode for OLED applications.

Here, para-sexiphenyl (6P) was deposited at various substrate temperatures onto graphene flakes grown on Iridium (111) [1]. The dynamics of the deposition process and the crystallographic structure were observed in-situ by means of Low Energy Electron Microscopy (LEEM) and micro Low Energy Electron Diffraction (μLEED). Layer-by-layer growth of lying molecules on graphene is observed for low deposition temperatures. After formation of an initial low-density layer, the full first monolayer already shows a bulk like structure. An exceptionally high mobility for 6P on graphene is observed in the initial low density layer. With ongoing deposition the formation of at least 4 smooth layers is observed. The structure of the initial layers as well as of the thick film has been resolved by μLEED.

For room temperature the growth of – for 6P typical – 1D needles on a wetting layer is observed. At elevated temperatures a continuous layer of upright standing molecules on the Ir(111) surface is nucleated by the presence of the graphene flakes.

This work is supported by the FWF project S9707-N08 and FOM project 04PR2318.

[1] Coraux, J. et al., New J. Phys., 2009, 11, 023006.

[*]Solid State Physics, MESA+ Institute for NanoTechnology, University of Twente, Enschede, The Netherlands

[†]Institute of Physics, University of Leoben, 8700 Leoben, Austria

[‡]Email: g.hlawacek@tnw.utwente.nl

The nucleation and anisotropic growth of Pn on SiO_2 & FET structures

A. Al-Mahboob[1], Y. Tsuruma[2], J. T. Sadowski[1], Y. Fujikawa[3], K. Saiki[2], T. Hashizume[4]
T. Sakurai[4] and P. Sutter[1]

[1] *Center for Functional Nanomaterials, Brookhaven National Laboratory, Upton, NY 11973, USA*
[2] *Department of Complexity Science and Engineering, University of Tokyo, Chiba 277-8561 Japan*
[3] *Institute for Materials Research, Tohoku University, Sendai 980-8577, Japan*
[4] *WPI-Advanced Institute for Materials Research, Tohoku University, Sendai 980-8577, Japan*

Pentacene (Pn) is a promising material for organic-based field-effect transistor (FET) applications as it shows highest field-effect mobility among organic thin films. However, the anisotropies in molecular structure and crystal packing complicate nucleation and growth processes in Pn films [1-3]. Here we will discuss in detail the nucleation and growth mechanism of Pn films on native SiO_2 as well as on a FET structure (SiO_2 channel and Au electrodes).

In the in-situ LEEM experiments during the Pn deposition on the native SiO2 we have observed that the crystalline Pn islands grow directly from the first layer, and the nucleation density of a second layer is lower that the first one. The second layer nucleates preferentially at the domain boundaries formed by connections of the 1st layer islands. The 2nd layer overgrows 1st layer with its own initial in-plane crystal orientation regardless of in-plane orientation of the bottom layer. If the 2nd layer nucleates on the terrace rather than the domain boundary, it maintains proper epitaxial relation (i.e. as in the bulk crystal) with the underneath domain. We observed a relative shift in the mirror potential in mirror mode LEEM imaging of 2nd layer such that the relative shift depends on relative orientation of first and second layer. Correlating this shift with azimuthal orientations of Pn domains, we found frequent twining of in the epitaxial 2nd layer, that can be related to mirroring of out-plane, ***c****-axis, or mirroring of molecular tilt with respect to out-plane orientation.

In the case of Pn growth on a FET structure, suppression of nucleation around a Au electrode was found [4]. Here, the mass flow is driven by the difference between the molecular orientations on SiO_2 and Au. Poor connectivity at the channel/electrode boundary causes degradation in the performance of FET, which is found to be improved by self-assembled monolayer treatment on the electrode.

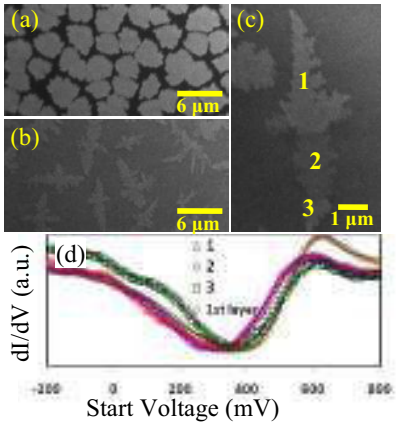

Fig.1. (a)-(b) Time series LEEM images of Pn grown on SiO_2 at 70 ºC (c) 2nd layer Pn island, the contrast within the island is related to its in-plane orientation relative to underneath 1st layer; (d) dI/dV around the SV for mirror imaging.

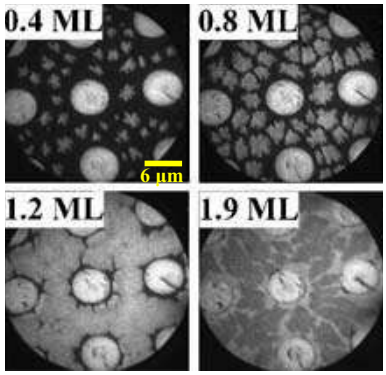

Fig.2. Time series PEEM images of Pn during deposition on SiO_2 substrate with round Au electrodes at 70 ºC.

References

[1] J. T. Sadowski et al. 2007, *Phys. Rev. Lett.* 98, 046104
[2] A. Al-Mahboob et al. 2008, *Phys. Rev.* B77, 035426
[3] A. Al-Mahboob et al. 2010, *Phys. Rev.* B (pending)
[4] Y. Tsuruma et al. 2009, *Adv. Materials* 21, 4996

Thermionic Electron Emission Microscopy of Ba, Sc, Y, Zr, Ti and Mg Oxide Multilayers on Tungsten

Joel M. Vaughn[1], Keith D Jamison[2] and Martin E. Kordesch[1]
[1]Department of Physics and Astronomy, Ohio University, Athens, Ohio 45701-2979
[2]Nanohmics, Inc. Austin, TX

Many theories [1] of work function reduction on Ba activated thermionic cathode surfaces rely on a monolayer surface dipole layer. The charge transfer between the surface atoms, in particular the electron transfer from the barium ion, is the primary agent of work function reduction. A base oxide layer is often added which increases the electron yield at comparable temperatures. We have examined thick (200 nm) layers of reactively sputtered Sc_2O_3, Y_2O_3, TiO_2, MgO and ZrO on tungsten foil activated with a top layer of BaO. Thermionic electron emission microscopy (ThEEM) was used to image the surfaces during electron emission. Current vs. brightness temperature data were used to estimate the work function.

The fabrication method that we have used separates the Ba from the W entirely, and places the Sc-O (or other oxide) to Ba-O interface 200 nm below the surface. As grown, there is no Sc or Ba metal in the cathode structure. The cathodes still achieve low work functions and high emission current densities. A new concept for work function reduction based on the idea of electrostatic compression [2] is consistent with the ThEEM images observed here.

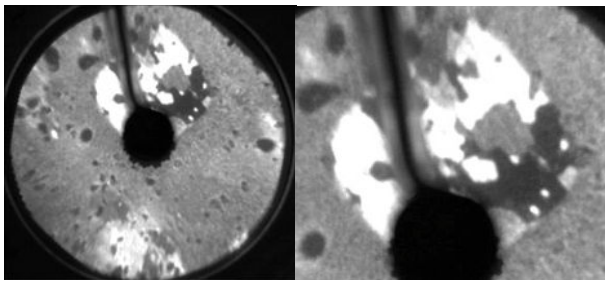

Figure 1. left: ThEEM image of Sc_2O_3 100x100μm square on W foil at 1191K (brightness T), right, same, detail of Sc_2O_3 square.

Sample	Coating	$\phi_{measured}$	$\phi/0.758$	$\phi/1.606$
1	Sc foil	5.62	—	3.50
2	W foil	3.45	4.55	—
3	W foil + Sc_2O_3	3.77	4.97	2.35
4	W foil + Sc_2O_3 + BaO	2.27	2.99	1.41

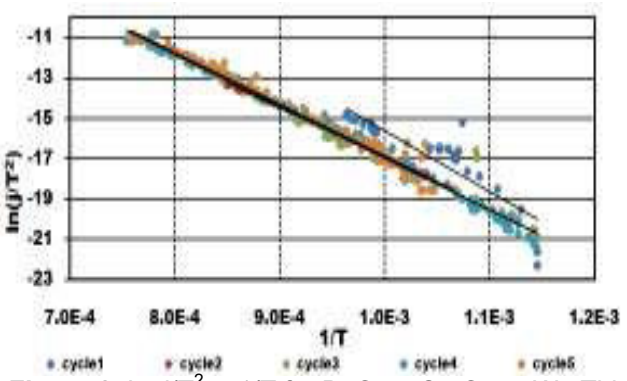

Figure 2. Ln j/T^2 vs1/T for BaO on Sc_2O_3 on W. This type of fit is used to determine work function.

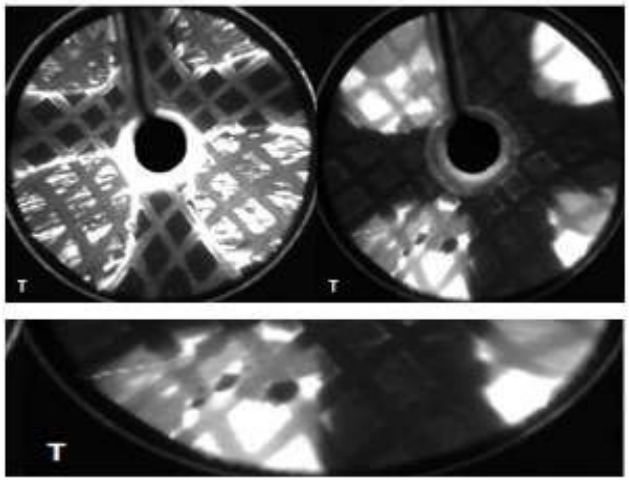

Figure 3. (Left) ThEEM at 1279K of the Sc_2O_3 100x100μm squares with BaO 25x25μm squares on top. Heating cycle 12. (Right) ThEEM at 1303K. Heating cycle 18. (Bottom) detail of right hand image.

This work was supported by Nanohmics, Inc., through the Air Force Office of Scientific Research, contract No. FA9550-09-C-0085.

1. Vlahos, V., Lee, YL, Booske, J.H., Morgan, D, Turek, L.,Kirshner, M., Kowalczyk, R.,Wilsen, C., Appl. Phys. Lett., 84, 184102 (2009).
2. Prada, S., Martinez, U., Pacchioni, G., Phys. Rev. B, 78, 235423 (2008) DOI 10.1103/PhysRevB.78.235423.

LEEM/LEED investigation of Fe_3O_4 thin film growth on a Pt(111) substrate: morphology and atomic termination

Alessandro Sala, Helder Marchetto, Thomas Schmidt, and Hans-Joachim Freund

Fritz Haber Institute of the Max Planck Society, Berlin, Germany

Iron oxide is widely used as a catalyst and as a support for catalytically active systems. Although the system has been intensively studied with various techniques [1], controversies arise in the literature regarding the surface termination [2-4] and structural inhomogeneities. This clearly hinders the direct linking of surface electronic and structural properties to chemical properties. Our aim is therefore a comprehensive and consistent characterization of the Fe_3O_4 film growth on a Pt(111) substrate by using the SMART instrument, specially designed to obtain chemical and structural information with high lateral resolution. In particular, deviating from the optimum preparation conditions [5], the oxide thin film reveals defects like a coexistence of two different stoichiometric phases (Fe_3O_4 and FeO), a Moiré-like patterned morphology with a mesoscopic periodicity and a predominance of one of two possible rotational domains. In addition, a subsequent annealing at 900K changes significantly the IV-LEED spectra and SPA-LEED profiles, which corresponds to different atomic termination of the magnetite surface.

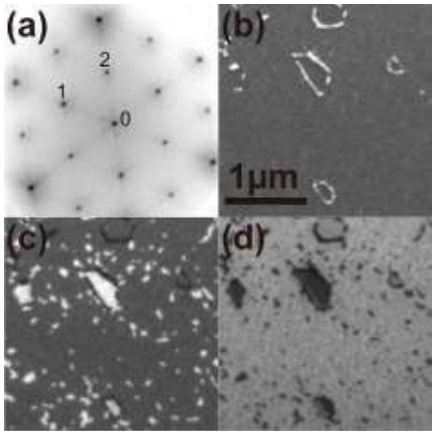

Fig.: Fe_3O_4 film on Pt(111) surface with structural and morphological defects. The LEED pattern (a) shows a superposition of the (2x2) superstructure of the Fe_3O_4 film and additional spots surrounding the central (00) spot resulting from a Moiré pattern of a FeO film. The LEEM images use different LEED spot: (b) shows the bright field image, (c) and (d) are dark-field images using the superstructure spot labeled with '1' and '2', respectively.

[1] W. Weiss and W. Ranke, Prog. Surf. Sci. 70 (2002) 1-151
[2] C. Lemire et al., Surf. Sci. 572 (2004) 103-114
[3] N. G. Thornton et al., Phys. Rev. B 55 (1997) 15885
[4] R. S. Cutting et al., Surf. Sci. 602 (2008) 1155-1165
[5] Z.-H. Qin, M. Lewandowski, Y.-N. Sun, S. Shaikhutdinov, and H.-J. Freund, J. Phys. Chem. C 112 (2008) 10209–10213

The system $Au/Fe_2O_3/Pt(111)$

T.O. Menteş[1], A. Locatelli[1], M.A. Niño[1], E. Bauer[2], A. Pavlovska[2], M. Lewandowski[3], I.M.N. Groot[3], S. Shaikhutdinov[3], H.-J. Freund[3]

[1]Sincrotrone Trieste, Basovizza, Trieste 34149, Italy, [2]Department of Physics, Arizona State University, Tempe, AZ 85287, USA, [3]Fritz-Haber-Institut der Max-Planck-Gesellschaft, Faradayweg 4-6, 14195, Berlin, Germany

The discovery [1] of the high catalytic activity and selectivity of nanoscopic Au supported on a variety of oxides for many reactions, for example for CO oxidation at low temperature, has led to a huge number of studies of oxide-supported Au catalysts. Nevertheless or because of the large number of studies, the structure of the active surface and of the reaction mechanism is still a matter of intense discussion. The present study attempts to get a clearer picture of the nature of the active surface of one of these systems, Au on $Fe_2O_3(0001)$. The oxide films are grown on a Pt(111) surface by stepwise deposition of Fe followed by oxidation via intermediate oxidation states. Growth, structure, chemical and magnetic state are studied with LEEM, LEED, STM, XPEEM and XMC/LDPEEM. Particular attention is given to the so-called Fe_2O_3-biphase surface on which Au grows in a self-organized manner.

[1] M. Haruta, N. Yamada, T. Kobayashi, S. Iijima, J. Catal. **115**, 301 (1989)

Electronic vs. defect-induced self-stabilization of ferroelectric polarization in thin $PbZr_{0.52}Ti_{0.48}O_3$ films

Ingo Krug[1,*], Nick Barrett[2], Adrian Petraru[3], Olivier Renault[5], K. Rahmanizadeh[7], G. Bihlmayer[7], Loic LeGuyader[4], Astrid Besmehn[1,6], Hermann Kohlstedt[3], and Claus M. Schneider[1]

[1] *IFF-9, Research Center Jülich, 52425 Jülich, GERMANY, *i.krug@fz-juelich.de*

[2] *DSM/IRAMIS SPCSI, C.E.A. Saclay, 91191 Gif-sur-Yvette, FRANCE*

[3] *Institut für Elektrotechnik und Informationstechnik/Nanoelektronik, University Kiel, 24143 Kiel, GERMANY*

[4] *Swiss Light Source, Paul-Scherrer-Institute, 5232 Villigen, SWITZERLAND*

[5] *CEA-LETI, MINATEC, 38054 Grenoble, FRANCE*

[6] *ZCH, Research Center Jülich, Leo-Brandt Straße, 52425 Jülich, GERMANY*

[7] *IFF-1 and IAS-1, Research Center Jülich, Leo-Brandt Straße, 52425 Jülich, GERMANY*

Ferroelectrics represent one of the most appealing material classes for the construction of new electronics concepts. Nevertheless, there are some obstacles to overcome when trying to integrate thin films into a real device architecture. One of them is the stability of ferroelectric polarization which naturally breaks down below a certain film thickness due to the increasing depolarization field [1]. Nowadays, there exists a lot of controversy about what mechanisms may stabilize the ferroelectric polarization in real ultrathin films. To elucidate somewhat more the mystery of a stable ferroelectric state in thin films, we present here an energy-filtered PEEM study of polarity-patterned Pb(Zr,Ti) layers with out-of plane polarization. As microscope we used a NanoESCA (LETI group, Grenoble), a fully energy-filtered instrument yielding high transmission for XPS by an aberration-correcting double-hemispherical analyzer. By microspectroscopy we performed polarity-dependent threshold photoemission measurements as well as core-level and valence band XPS. The onset of threshold photoemission is strongly polarity-dependent and reveals a 0.7eV higher work function for a positive than for a negative surface polarity. At the same time, the Pb 4f peak exhibits two components with their ratio dependent on the surface polarity. The high (low) binding energy components can be associated with a positive (negative) surface charge, respectively, a result which is confirmed by DFT calculations as well. Valence band XPS measurements show a reduced oxygen 2p-projected density of states for a negative surface polarity. A comparison to DFT calculations suggests that the valence band electronic structure might be directly altered as a consequence of ferroelectric charge compensation. Another possible mechanism could be simply defect migration, in this case of positively charged oxygen vacancies diffusing towards the negative polarization charge near the surface.

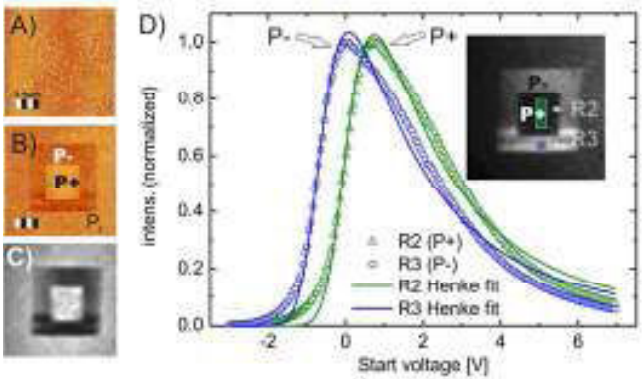

Fig.1: Threshold photoemission spectra with synchrotron excitation (hv=650 eV). The ferroelectric surface potential change creates a shift in the photoelectron kinetic energy range, which can serve as contrast mechanism for energy-filtered PEEM. Fitting by a Henke function yields a surface potential difference of about 0.7eV.

[1] J. Junquera, and P. Ghosez, Nature, **422** 506-9 (2003). [2] M. Escher, N. Weber, M. Merkel, C. Ziethen, P. Bernhard, G. Schönhense, s. Schmidt, F. Forster, F. Reinert, B. Krömker, and D. Funnemann, Journal of Physics: Condensed Matter, **17** S1329-S1338 (2005).

Wednesday August 11 – IBM T.J. Watson Research Center

Afternoon Session: ELECTRONIC STRUCTURE
Chair: A. Locatelli

1:00 pm: Distinguished Guest Lecturer: Dr. E. Rotenberg (Lawrence Berkeley National Laboratory)
(title to be filled in)

1:40 pm: C. Mathieu, N. Barrett, Y. Mi, O. Renault, N. Weber, B. Vilquin; Recent Advances in Bandstructure Imaging by k-PEEM

2:00 pm: N.B. Weber, M. Escher, M. Merkel, K. Winkler; k-Space Imaging in Photoelectron Microscopy: Comparison of Band-pass and High-pass Energy Filter Approaches

2:20 pm: A.A. Zakharov, C. Virojanadara, S. Watcharinyanon, R. Yakimova, L.I. Johansson; 3D (k_x-k_y-E) Band Mapping by using X-ray Photoelectron Emission Microscope

2:40 pm: Break and Conference Photograph

Plans for a 50 nm spatial-resolution ARPES beamline at the Advanced Light Source

Eli Rotenberg*
Advanced Light Source
E. O. Lawrence Berkeley National Laboratory

Angle-resolved photoemission spectroscopy is the premier tool for obtaining not only the momentum-resolved energy bands of conducting materials, but is also able to provide deep insights into many body interactions. This information can be derived when the momentum and energy resolutions do not limit the determination of the linewidths of the ARPES spectral function. Under these conditions, and when the quasiparticle approximation holds, then ARPES can determine the momentum- and frequency-dependent self-energy function of the charge carriers $\Sigma(\boldsymbol{k},\omega)$. This function describes the interaction between an electron and the background excitations such as phonons, magnons, and other electrons.

In this talk I will briefly review some recent determinations of the ARPES spectral function not only for conventional hole-like quasiparticles, but also for new charge-carrying entities we have observed such as spinons, holons, and plasmarons. These and similar studies have motivated us to combine the ARPES technique with spatial resolution, in order to correlate the electronic self-energy with spatial structure for intrinsically or engineered nanostructured materials. Results will be shown for "nanoARPES" measurements with spatial resolutions down to 300 nm, and plans for a dedicated beamline and endstation capable of 50 nm spatial resolution will be presented. This beamline facility, which combines conventional "microARPES", nanoARPES will be called MAESTRO, the Microscopic and Electronic Structure Observatory" will also include provisions for a future LEEM/PEEM instrument.

*In collaboration with A. Bostwick, G. A. Gaines, T. Warwick, and Z. Hussain

Recent advances in band structure imaging by k-PEEM

C. Mathieu[1], N. Barrett[1], Y. Mi[1], O. Renault[2], N. Weber[3], B. Vilquin[4]

[1] *CEA, DSM/IRAMIS/SPCSI, CEA-Saclay, 91191 Gif sur Yvette Cedex, France*
[2] *CEA, LETI, MINATEC, 17 rue des Martyrs, 38054 Grenoble Cedex 09, France*
[3] *FOCUS GmbH, 65510 Hünstetten, Germany*
[4] *Institut des Nanotechnologies de Lyon (INL), 36 avenue Guy de Collongue, 69134 Ecully, France*

The imaging of surfaces using the PhotoElectron Emission Microscopy (PEEM) technique has recently received considerable interest, mainly thanks to the use of high brilliance synchrotron radiation which facilitates the study of surface properties and chemical selectivity [1, 2]. By placing a transfer lens in the optical column of a high transmission and full energy-filtering PEEM, it is possible to image the focal plane, instead of the image plane. Hence, the corresponding image shows the angular distribution of the emitted photoelectrons, for a given kinetic energy. By varying the kinetic energy, the complete energy filtering provides full 2D cuts of the band structure in reciprocal space, called k-PEEM [3]. This approach has two advantages over classical ARPES measurements. No uncertainty is introduced due to sample rotation and the images obtained are directly $\mathbf{I}(k_x, k_y)$. Therefore, full 2D band mapping is possible, with potential acquisition times considerably shorter than in a classical ARPES set-up.

The k-PEEM technique has been successfully used in studying the band structure of metal and alloy, such as Cu(111) [3], Ag(111) and Ag(001) [4] and Cu_3Pt(111). The 2D mapping of the latter sample has allowed us to achieve high momentum resolution and to clearly observe surface features, demonstrating the performances of this technique [5]. We report some promising preliminary results in k-PEEM on $BaTiO_3$ oxides. The $BaTiO_3$(001) perovskite oxide is ferroelectric at room temperature, which can produce spontaneous ferroelectric domains. By closing the field aperture on a selected area, it is possible to image in the reciprocal space the band structure of different apparent domains. The k-PEEM results of thin films of $BaTiO_3$ on $SrTiO_3$ are presented is the figure 1. The superposition of the band structures calculated by Density Functional Theory (DFT) on our experimental data shows good agreement between theory and experimental.

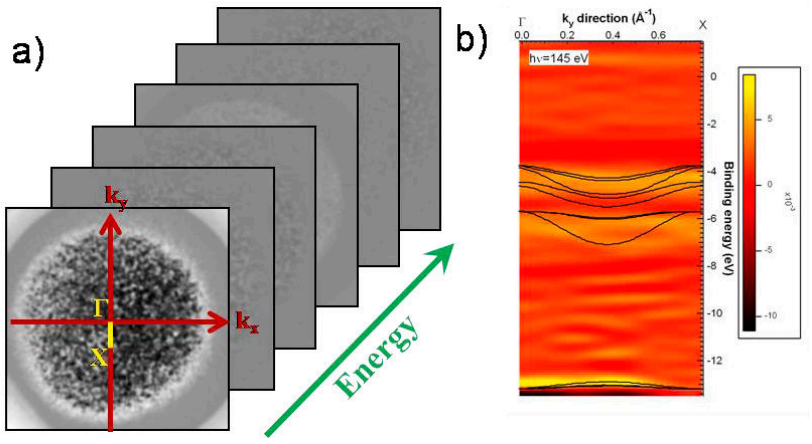

Figure 1: a) Band mapping in the reciprocal space of a 20 nm $BaTiO_3$(001) grown epitaxially on an Nb-doped $SrTiO_3$(001). The stack represents the intensity as a function of both the k_x and k_y directions and the energy.
b) ΓX vertical slice (yellow line crossing the image a)) of the stack.

References:

[1] M. Escher, K.Winkler, O. Renault, N. Barrett, *J . Electron. Spectrosc. Relat. Phenom.* **178–179,** 303 (2010).

[2] E. Bauer, *J. Electron. Spectrosc. Relat. Phenom.* **114–116,** 957 (2001).

[3] B. Krömker, M. Escher, D. Funnemann, D. Hartung, H. Engelhard, J. Kirschner *Rev. Sci. Instr.* **79,** 053702 (2008).

[4] Y. Fujikawa, T. Sakurai, and R. M. Tromp, *Phys. Rev. B* **79**, 121401 (2009).

[5] M. Escher, N. Weber, M. Merkel, B. Krömker, D. Funnemann, S. Schmidt, F. Reinert, F. Forster, S. Hüfner, P. Bernhard, Ch. Ziethen, H.J. Elmers, G. Schönhense*, J. Phys: Condens. Mat.* **17**, S1329 (2005).

k-Space Imaging in Photoelectron Microscopy: Comparison of band-pass and high-pass Energy Filter Approaches

N.B. Weber[1], M. Escher[1], M. Merkel[1], K. Winkler[2]
[1]*Focus GmbH, 65510 Hünstetten, Germany*
[2] *Omicron Nantotechnology GmbH, 65232 Taunusstein, Germany*

Email: m.escher@focus-gmbh.com

Imaging of the angular distribution of photoelectrons becomes more and more important in photoelectron microscopy to obtain information about the structure and electronic properties of small sample regions in the µm-size[1-3]. A prerequisite for k-space imaging is energy filtering of the electron distribution. Here we compare two methods to accomplish the energy filtering: a band-pass-filtering using a double hemispherical analyser in the so-called momentum microcsope [3] and the high-pass double grid energy filter IEF (Imaging Energy Filter) [4] combined with an electrostatic PEEM.

The high-pass analyser IEF is typically mounted to a bolt-on PEEM with a straight column, that can be easily integrated into multi-technique experiments. It is capable for energy resolution <100meV with a geometrical transmission of about 50%. Due to the high-pass behaviour difference images are taken to record an energy stack, thus this energy filter is ideally suited for Fermi-surface-imaging with monochomatic light sources.

The band-pass solution featured by the momentum microscope is a sophisticated instrumental approach capable of PEEM, imaging XPS and k-space imaging with an energy resolution down to 100meV. The double hemispherical analyser ensures a high instrumental transmission as the second analyser compensates the inherent α^2-aberrations originated by the hemispherical field of the first analyser; therefore the energy analyser allows for transmission of a large phase space over the whole energy range [5].

Example images of a Ag(100) single crystal sample using a lab VUV source with and He I excitation (hν =21.2 eV) with both approaches are shown in the figure.

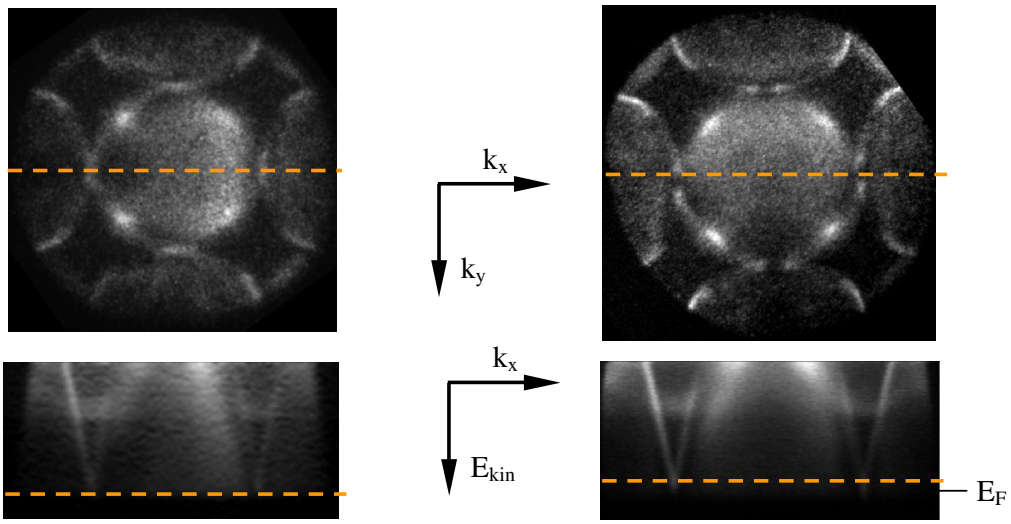

Figure: k-space images (top) and cut through the E-k plane (bottom) of Ag(100) obtained with the IEF-energy filter (left) and the momentum-microscope (right) both excited with He I gas discharge lamp (21.2 eV). The acquisition time was 130sec and 50sec per image respectively. The dashed lines indicate the cut through the data stack.

References

[1] Th. Schmidt et al.Surf. Rev. Lett. **5** (1998) 1287-96
[2] Tromp et al J. Phys.: Condens. Matter **21** (2009) 314007
[3] Krömker et al., Rev. Sci. Instrum. **79**, 053702 (2008)
[4] N. B. Weber et al., J. Phys. conference series **100** (2008) 072031
[5] Escher et al., J. Electron Spectrosc. Relat. Phenom. **178–179** (2010) 303–316

3D (k_x-k_y-E) band mapping by using X-ray photoelecton emission microscope

A.A.Zakharov[1], C.Virojanadara[2], S. Watcharinyanon[2], R.Yakimova[2] , L.I.Johansson[2]

[1] *MAX-lab, Lund University, S-22100, Lund, Sweden*
[2] *Dept. of Physics, Chemistry and Biology, Linköping University, S-58183, Linköping, Sweden*

In this contribution we demonstrate the unique potential and the versatility of the energy filtered photoelectron emission microscope where it is possible to obtain spatially resolved microscopic images of the sample surface and in addition, the photoelectron angle distribution pattern from a small (≤1μm) area of the sample. Experiments were performed at a LEEM/PEEM III instrument (Elmitec GmbH) installed at the undulator beamline I311 of the synchrotron radiation facility MAX-lab in Lund. Linearly s-polarized radiation of the first harmonics of the undulator was used for the excitation, normal incident to the sample surface (light goes through the beam separator of the microscope). The energy filtering function is realized by insertion of a hemispherical analyser in the electron optical path and the lenses of the image column transfer independently the image plane and the back focal plane of the objective through the system. We have applied the technique to observe the 3D (E,k_x,k_y) electronic band structure of 1.5ML of graphene (2ML islands on a 1ML surface) grown *ex-situ* on a 6H-SiC(0001) substrate and quasi free-standing graphene obtained by Li intercalation. Fig.1a shows a surface LEEM image and (b-d) energy resolved (k_x,k_y) maps from a 0.8μm 1ML area for chosen electron kinetic energies, the last frame is taken close to the Dirac points. Acquisition time for one energy slice is within several minutes depending on the energy resolution. The energy resolution of 0.15eV and momentum resolution of 0.03$Å^{-1}$ can be estimated as an upper bound from the data set for a 2ML graphene island where two π bands of graphene near the K-point are clearly distinguished.

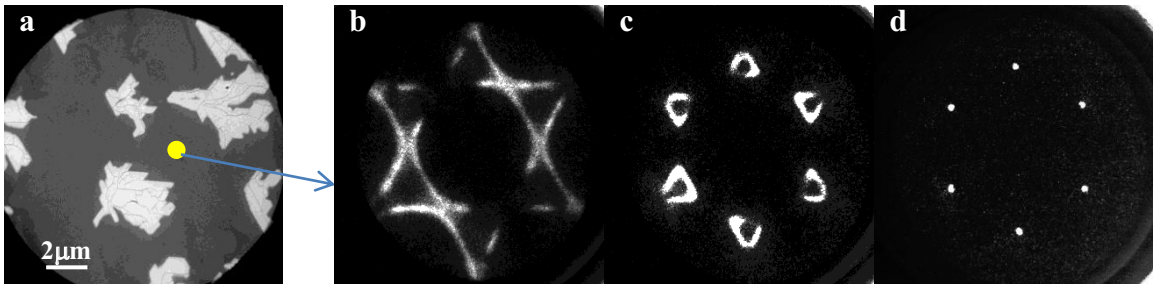

Fig.1. (a)LEEM image of 1ML graphene with 2ML islands, 0.8μm area in the image is the sampling area for band mapping. (b-d) Photoelectron (hν=35eV) angle distribution pattern for electron energies 4eV (b), 2eV (c) and 0.3eV(the Dirac points) (d) below the Fermi level.

Thursday August 12 – Grand Hyatt Hotel

Morning Session: GRAPHENE
Chairs: B. Poelsema, M.Altman

8:20 am: Distinguished Guest Lecturer: Dr. Phillip N First; STM Studies of Graphene Thin Films

9:00 am: Qiang Fu, Yi Cui, Hui Zhang, Xinhe Bao; Dynamic Characterization of Graphene Growth on Ru(0001)

9:20 am: A.T. N'Diaye, R. van Gastel, A.J. Martínez-Galera, J. Coraux, H. Hattab, D. Wall, F.-J. Meyer zu Heringdorf, M. Horn-von Hoegen, J.M. Gómez-Rodríguez, B. Poelsema, C. Busse, Th. Michely; Steering the Growth and Watching the Strain of Epitaxial Graphene on Iridium(111)

9:40 am: P. Sutter, J. Sadowski, E. Sutter; Graphene on Transition Metals – Growth and Interface Physics

10:00 am: J. Sun, J.B. Hannon, R.M. Tromp, P. Johari, A.A. Bol, V.B. Shenoy, K. Pohl; Spatially Resolved Structure and Electronic Properties of Graphene on Polycrystalline Ni

10:20 am: Break

10: 50 am: A.A. Zakharov, K.V. Emtsev, U. Starke; Decoupling Epitaxial Graphene from SiC(0001) Surface by a Germanium Buffer Layer

11:10 am: S. Nie, J.M. Wofford, N.C. Barlelt, K.F. McCarty, O.D. Dubon; Real-time Analysis of Graphene Growth on Polycrystalline Copper Foils

11:30 am: K. McCarty, A.L. Walter, E. Starodub, S. Nie, K. Thürmer, K. Horn, A. Bostwick, N.C. Bartelt, E. Rotenberg; Second-layer Graphene on Ir(111) –Relating Growth Mechanism to Physical and Electronic Structure

11:50 am: T. Ohta, N.C. Bartelt, S. Nie, K. Thürmer, G.L. Kellogg; The Role of Carbon Surface Diffusion on the Growth of Epitaxial Graphene on SiC

12:10 pm: FINAL REMARKS AND CONCLUSION

Spectroscopy and Mapping of Landau Levels in Graphene

Phillip N. First[1*], David L. Miller[1], Kevin D. Kubista[1], Gregory M. Rutter[2], Ming Ruan[1], Walt A. de Heer[1], Markus Kindermann[1], Joseph A. Stroscio[2]

[1]*School of Physics, Georgia Institute of Technology, Atlanta, GA 30332-0430, USA*
[2]*Center for Nanoscale Science and Technology, NIST, Gaithersburg, MD 20899, USA*

LEEM has played a substantial role in recent studies of epitaxial graphene growth on SiC and on metal substrates. However, graphene first became familiar to most people after measurement of its transport properties in regimes inaccessible to LEEM: large magnetic fields and liquid-helium temperature. Scanning tunneling microscopy/spectroscopy (STM/STS) is a technique that can bridge the gap between high resolution microscopy of virgin samples and transport characterization of lithographically-defined devices.

I will present cryogenic STM/STS measurements of graphene grown on silicon carbide. In an applied magnetic field, we directly observe the unconventional spectrum of Landau levels that underlies graphene's half-integer quantum Hall effect [1], and use this information to extract the dispersion $E(k)$ with high resolution. Quantized Hall resistance implies magnetically-induced confinement of charge carriers, which also is unconventional in graphene. We probe this aspect through maps of local density of states (LDOS), especially for the zero-energy Landau level (LL_0) [2]. Unlike disordered LDOS patterns found for conventional 2D electron systems in the quantum Hall regime, above a threshold magnetic field we find an organized pattern of localized states and extended states. In each localized region, an energy gap associated with lattice-scale spatial variation of the LDOS suggests that the sublattice degeneracy (and LL_0 valley degeneracy) is lifted locally. We propose that this occurs when cyclotron orbits become small enough to sample regions of small symmetry-breaking potential originating from a graphene-on-graphene moiré. Such moiré alignment is characteristic of multilayer graphene grown on C-terminated SiC$000\bar{1}$). Our results have interesting implications for transport through this growth-induced physical structure.

[1] D. L. Miller and K. D. Kubista et al., *Science* **324,** 924 (2009).
[2] D. L. Miller et al., *Nature Physics* (in press).

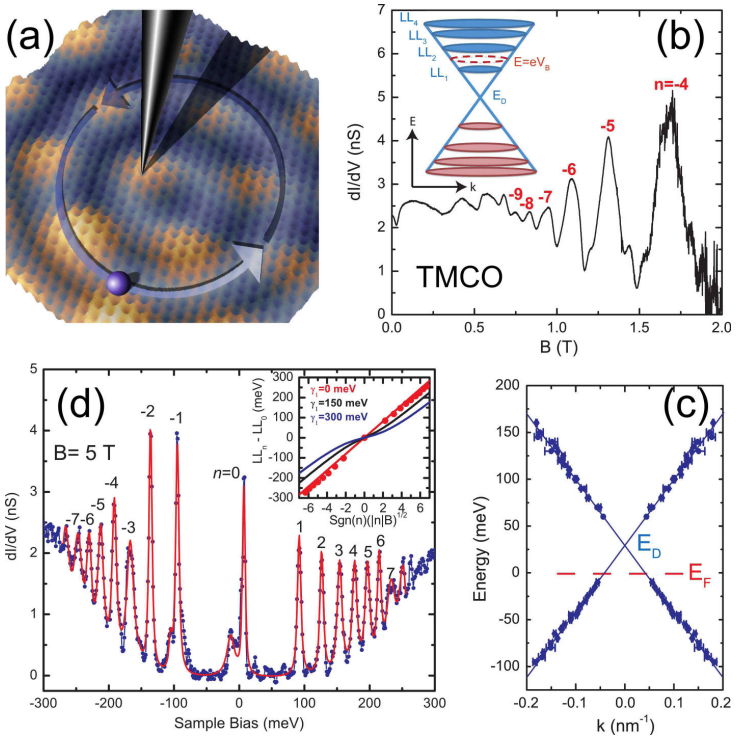

FIG 1: (a) Cartoon of STM tip and a cyclotron orbit over an STM topograph of top-layer graphene from a moiré-aligned multilayer sample grown on 4H-SiC(000$\bar{1}$). (b) Tunneling magnetoconductance oscillations (TMCO) from sweeping the magnetic field at fixed tunnel bias. (c) Graphene dispersion from a set of TMCO measurements. (d) Tunneling density-of-states spectrum at B = 5 T. Inset: the Landau level spectrum is fit by zero interlayer coupling.

*first@gatech.edu

Dynamic characterization of graphene growth on Ru(0001)

Qiang Fu, Yi Cui, Hui Zhang, Xinhe Bao

State Key Lab of Catalysis, Dalian Institute of Chemical Physics, the Chinese Academy of Sciences, Zhongshan Road 457, 116023, Dalian, China
Email: qfu@dicp.ac.cn

Both fundamental research and potential applications of graphene are calling for the controllable synthesis of this new two-dimensional (2D) carbon material. Here, we present the synthesis of graphene with controlled lateral size and thickness via epitaxial growth on Ru(0001). Either ethylene (C_2H_4) or coronene ($C_{24}H_{12}$) was used as the precursors for graphene growth. The mechanism of how 2D graphene overlayers evolve from the hydrocarbon precursors was investigated by high resolution electron energy loss spectroscopy (HREELS), scanning tunneling microscopy (STM) and photoemission electron microscopy (PEEM). We found that identical-size graphene nanoclusters with the 3-C6 ring (C24 cluster) and 7-C6 ring (C13 cluster) structures form on Ru(0001) after pyrolysis of both C_2H_4 and $C_{24}H_{12}$ at elevated temperatures (around 900 K). The nanographene can be regarded as building blocks, and large size graphene structures form through coalescence of these graphene nanoflakes. Via controlling of growth temperature, well-defined graphene overlayers ranging from nanographene to millimeter sized continuous graphene films have been obtained [1, 2]. Besides the lateral size of graphene layer, thickness is another important structural character of graphene. The growth of multilayer graphene was attempted on Ru(0001) surface. In-situ low energy electron microscopy (LEEM) and PEEM investigations indicate that single layer graphene forms on bare Ru(0001) via the surface segregation of carbon, and the second layer starts to appear after the completion of the first layer. The topmost surface of the multilayer graphene is physically continuous as indicated by the STM images. Accordingly, a bottom-up growth mechanism, in which the newly formed graphene layer locates underneath the previously formed graphene layer rather than on its top, was proposed for graphene growth on metal surfaces through the surface segregation route. [3, 4].

1. Hui Zhang, Qiang Fu, Yi Cui, Dali Tan, Xinhe Bao, "Growth mechanism of graphene on Ru(0001) and O_2 adsorption on the graphene/Ru(0001) surface", **Journal of Physical Chemistry C** 113 (2009) 8296-8301.
2. Yi Cui, Qiang Fu, Hui Zhang, Dali Tan, Xinhe Bao, "Dynamic Characterization of Graphene Growth and Etching by Oxygen on Ru(0001) by PEEM", **Journal of Physical Chemistry C** 113 (2009) 20365-20370.
3. Yi Cui, Qiang Fu, Xinhe Bao, "Dynamic observation of layer-by-layer growth and removal of graphene on Ru(0001)", **Physical Chemistry Chemical Physics** 12 (2010) 5053-5057.
4. Yi Cui, Qiang Fu, Dali Tan, Xinhe Bao, "Temperature dependence of the formation graphene and subsurface carbon on Ru(0001) and its effect on surface reactivity", **ChemPhysChem**. 11 (2010) 995-998.

Steering the growth and watching the strain of epitaxial graphene on Iridium(111)

Alpha T. N'Diaye[1,5,*] , Raoul van Gastel[2] , Antonio J. Martínez-Galera[3] , Johann Coraux[1,6] , Hichem Hattab[4] , Dirk Wall[4] , Frank-J. Meyer zu Heringdorf[4] , Michael Horn-von Hoegen[4] ,José M. Gómez-Rodríguez[3] , Bene Poelsema[2] , Carsten Busse[1] and Thomas Michely[1]

[1] II. Physikalisches Institut, Universität zu Köln, • [2] MESA+ Institute for Nanotechnology, University of Twente, The Netherlands • [3] Departamento de Física de la Materia Condensada, C-III, Universidad Autónoma de Madrid, Spain • [4] Institut für Experimentelle Physik, Universität Duisburg–Essen, Germany • [5] Permanent Adress: National Center for Electron Microscopy, Lawenece Berkeley National Lab, USA • [6] Permanent address: Institut Néel/CNRS-UJF, France.

[*] E-mail: ndiaye@ph2.uni-koeln.de

Graphene, a two dimensional layer of sp^2 bonded carbon, is a material receiving vast amount of interest mainly for its unusual electronic, structural and chemical [1, 2, 3] properties.

This contribution addresses the growth and strain evolution of epitaxial graphene on Ir(111). This system is prototypical for a metal with a low solubility for carbon at the preparation temperature. We show with low energy electron microscopy (LEEM), photo emission electron microscopy (PEEM) and scanning tunneling microscopy (STM) in ultra high vacuum, how graphene can be grown with chemical vapor deposition (CVD) of ethylene and observe this growth *in situ*. [4]

Graphene on Ir(111) can grow in different epitaxial relations [5,7]. It is shown how the growth process can be guided, so that only one epitaxial orientation of graphene can be selected: (a) The etching speed upon exposure to oxygen at elevated temperature varies between the rotational variants, so that one phase can be predominantly etched while the other persists on the surface. (b) In a two stage growth process, the nucleation of rotational variants is inhibited by precovering the substrate with small epitaxial graphene flakes prior to CVD growth. Thus macroscopically coherent domains of single layer graphene sheets can be grown. [6]

The growth takes place at high temperatures of around 1000°C. Upon cooling compressive strain builds up. This strain is partly relieved through the formation of nanometer wide and micrometer long wrinkles. With LEEM it is possible determine the position and size of the area in which the formation of these very localized defects has an effect. At room temperature some residual inhomogeneous strain remains in the graphene layer. [7]

The research presented here is directed to understanding and steering the epitaxial growth of graphene on metals and monolayer epitaxial graphene sheets extending over millimeters have been grown. Furthermore wrinkle formation is observed during cooling and it is linked to the partial relief of compressive strain.

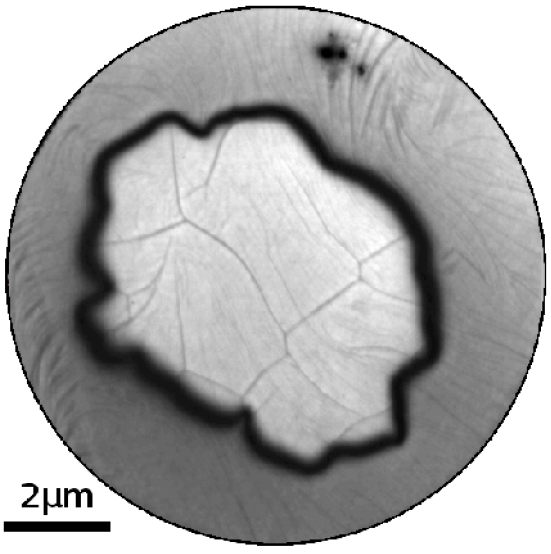

FIG. 1: *LEEM image of a graphene flake (bright) grown on Iridium(111) by high temperature chemical vapor deposition of ethylene in UHV. During cooling to room temperature strain has led to dark wrinkles on the flake.*

References

[1] A.H. Castro Neto, F. Guinea, N.M.R. Peres, K.S. Novoselov and A.K. Geim, *Rev. Mod. Phys.*, 81 (2009) 109

[2] C. Lee, X. Wei, J. W. Kysar, J. Hone, *Science*, 321, (2008) 5887, pp. 385 – 388

[3] A.T. N'Diaye, T. Gerber, C. Busse, J. Myslivecek, J. Coraux and T. Michely *New J. Phys.* 11 (2009) 103045

[4] J. Coraux, A.T. N'Diaye, M. Engler, C. Busse, D. Wall, N. Buckanie, F.-J. Meyer zu Heringdorf, R. van Gastel, B. Poelsema and T. Michely, *New J. Phys.* 11 (2009) 023006

[5] E. Loginova, S. Nie, K. Thürmer, N. C. Bartelt, and K. F. McCarty, Phys. Rev. B 80, (2009) 085430

[6] R. van Gastel, A.T. N'Diaye, D. Wall, J. Coraux, C. Busse, N. Buckanie, F.-J. Meyer zu Heringdorf, M. Horn von Hoegen, T. Michely, and B. Poelsema, *Appl. Phys. Lett.* 95, (2009) 121901

[7] A.T. N'Diaye, R. van Gastel, A.J. Martínez-Galera, J. Coraux, H. Hattab, D. Wall, F-J Meyer zu Heringdorf, M. Horn-von Hoegen, J.M. Gómez-Rodríguez, B. Poelsema, C. Busse, T. Michely *New J. Phys* . 11 (2009) 113056

Graphene on Transition Metals - Growth and Interface Physics

P. Sutter, J. Sadowski, and E. Sutter
Center for Functional Nanomaterials, Brookhaven National Laboratory, Upton, New York 11973 (USA)

Graphene, a two-dimensional honeycomb lattice of sp^2 bonded carbon atoms, has shown a wealth of exceptional properties due to charge carriers behaving as massless Dirac quasiparticles. Characteristics such as very high carrier mobilities, long-range ballistic transport, quantum confinement in nanoscale ribbons, and single molecule gas detection qualify graphene as a promising material for large-scale applications in microelectronics and sensing. To realize this potential, reliable and scalable methods for fabricating and processing high-quality graphene are required.

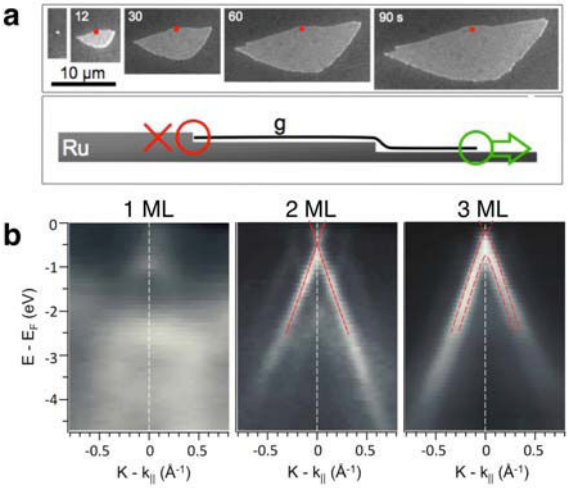

Fig. 1 – Graphene on ruthenium. a – Macroscopic graphene growth by coherent, carpet-like edge flow across substrate steps. **b –** Micro-APRES maps of the electronic band structure of 1, 2, and 3 monolayer (ML) graphene on Ru(0001).

Non-carbide forming transition metals can be used to catalyze and template the assembly of sp^2 bonded carbon into macroscopic graphene sheets [1], required for a wide variety of applications that harness the extraordinary properties of single- and few-layer graphene. We will discuss recent advances in understanding and controlling this synthesis methodology [1-3], derived primarily from real-time, *in-situ* observations of graphene growth by low-energy electron microscopy (LEEM), combined with scanning tunneling microscopy. LEEM and related spectroscopic imaging methods have been used to establish the interfacial interaction between metals and graphene [4, 5], which not only is the basis for large-scale graphene growth but also determines the unique electronic and chemical properties of graphene in the proximity of metals. We find that metal-graphene interfaces offer fascinating opportunities for selective interfacial chemistry, which may be exploited to control transition metal surface chemistry or catalysis and can constitute the basis for novel interfacial processing approaches of future graphene devices [6].

[1] P. Sutter, J.I. Flege, and E. Sutter, Nature Materials **7**, 406 (2008).
[2] E. Sutter, D.P. Acharya, J.T. Sadowski, and P. Sutter, Appl. Phys. Lett. **94**, 133101 (2009).
[3] E. Sutter, P. Albrecht, and P. Sutter, Appl. Phys. Lett. **95**, 133109 (2009).
[4] P. Sutter, M.S. Hybertsen, J.T. Sadowski, and E. Sutter, Nano Letters **9**, 2654 (2009).
[5] P. Sutter, J.T. Sadowski, and E. Sutter, Phys. Rev. B **80**, 245411 (2009).
[6] P. Sutter, J.T. Sadowski, and E. Sutter, J. Amer. Chem. Soc. (online 05-2010).

Spatially-Resolved Structure and Electronic Properties of Graphene on Polycrystalline Ni

J. Sun[1], J.B. Hannon[2], R.M. Tromp[2], P. Johari[3], A.A. Bol[2], V.B. Shenoy[3] and K. Pohl[1]

[1]Physics Department, University of New Hampshire, Durham, NH 03824
[2]IBM T.J. Watson Research Center, Yorktown Heights, NY 10598
[3]Division of Engineering, Brown University, Providence, RI 02912

We have used *in situ* electron spectromicroscopy to correlate the atomic and electronic structure of graphene films on polycrystalline Ni with nanometer-scale spatial resolution. Spatially-resolved electron scattering measurements show that graphene monolayers formed by carbon segregation do not support the π–plasmon of graphene, indicating strong covalent bonding to the Ni. Graphene bilayers have the Bernal stacking characteristic of graphite and show the expected plasmon loss at 6.5 eV. The experimental results, in agreement with first-principles calculations, show that the π-band structure of free-standing graphene appears only in films with a thickness of at least two layers, and demonstrate the sensitivity of the plasmon loss to the electronic structure.

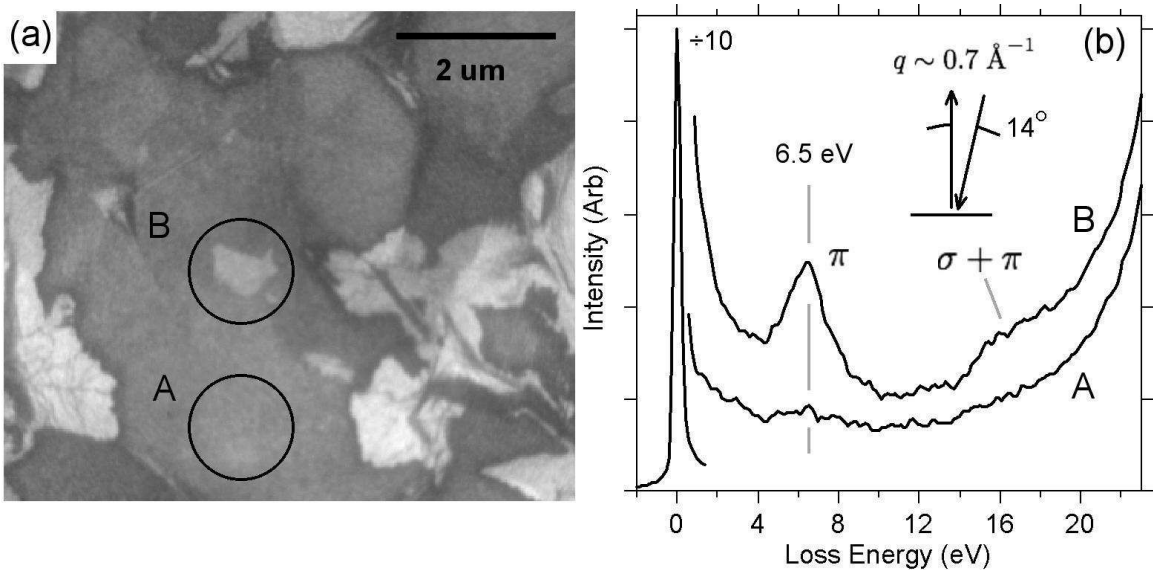

Caption:

(a) Energy-filtered LEEM image. The image is formed from electrons that have lost energy in the range 4 to 7 eV, i.e., from those electrons that have excited a graphene π plasmon at the surface. The incident electron energy was 33 eV. (b) Electron energy loss spectra (33 eV incident energy) recorded from the areas lmarked A and B in (a). Region A has a single graphene monolayer and the EELS spectrum shows no π-plasmon loss feature. Region B corresponds to 2 graphene layers and shows the expected π–plasmon loss at 6.5 eV and σ+π plasmon loss at 16 eV.

Decoupling epitaxial graphene from SiC(0001) surface by a germanium buffer layer

A. A. Zakharov[1], K.V.Emtsev[2] and U.Starke[2]

[1]*MAX-lab, Lund University, Box118, S-22100, Lund, Sweden*
[2]*Max Planck Institute for Solid State Research, Heisenbergstr.1, D-70569 Stuttgart, Germany*

Epitaxial graphene layers formed on SiC surfaces are an appealing material for future electronic applications and currently intensively investigated with respect to their electronic, structural, and electrical transport properties [1]. When epitaxial graphene layers are formed on SiC(0001), the first carbon layer (known as the "buffer or interfacial layer") does not have the desirable electrical properties of graphene due to a disruption of the graphene π-bands by strong hybridization with the SiC substrate. The undesired effects originating from this strong coupling, such as intrinsic n-type doping and degraded transport properties, affect the overlying graphene layers. Most of the remaining problems towards the graphene application are related to the presence of the buffer layer. In this work we demonstrate that the interfacial layer can be converted into quasi-free-standing graphene upon intercalation of Ge atoms at the interface. Initial SiC(0001) samples were annealed ex-situ at high temperatures in Ar atmosphere which results in graphene-like atomic arrangement on the surface with complex $(6\sqrt{3} \times 6\sqrt{3})R30^0$ periodicity [2] and the size of $6\sqrt{3}$ layer domains limited only by the terrace width, i.e. up to 5μm. Few (2-6) monolayers of Ge have been deposited *in-situ* from a Knudsen cell and subsequent annealing steps were carried out in UHV following Kubler et al. [3]. The electronic properties of the surface and the atomic structures of the newly formed interfaces were characterized by low energy electron microscopy (LEEM), X-ray photoelectron emission microscopy (XPEEM) and micro-diffraction (μ-LEED). LEEM imaging at around video frequency allows real time studying of intercalation process at elevated ($\geq 700^0$C) temperatures. The results show that graphene is structurally and electronically decoupled from the SiC substrate by Ge buffer layer and domains of free-standing graphene are of the order of several micrometers and limited only by terrace width of SiC substrate.

1. Th. Seyller et al., Phys. Stat. Sol.(b), **245**, 1436 (2008).
2. K.V.Emtsev et al. Phys.Rev.**B77**, 155303 (2008).
3. L.Kubler et al. Phys.Rev.B72, 115319 (2005).

Real-time analysis of graphene growth on polycrystalline copper foils

S. Nie[a], J. M. Wofford[b], N. C. Bartelt[a], K. F. McCarty[a], and O. D. Dubon[b]

[a]*Sandia National Laboratories, Livermore, CA 94550*
[b]*Department of Materials Science & Engineering, University of California at Berkeley and Lawrence Berkeley National Laboratory, Berkeley, CA 94720*

Despite the potentially significant technological impact of graphene synthesis on Cu, little is understood about both the growth kinetics of this system and the morphology of the resulting heterostructure. We use LEEM to observe directly the UHV growth of graphene on polycrystalline Cu foils by the electron-beam evaporation of carbon. The temperatures required to synthesize highly ordered graphene simultaneously induce significant Cu sublimation and step flow, leading to a dynamic growth surface. As a result a complex interdependence develops between the graphene growth behavior and Cu surface morphology, with the graphene islands limiting Cu step mobility, and Cu step bunching distorting the propagation of the graphene growth front. This interplay becomes increasingly dramatic over time as the inhomogeneous sublimation of Cu leads to considerable surface roughening. The graphene islands are not compact in shape; instead, the islands are ramified, consisting of several distinct lobes extending from a common nucleation site. Diffraction analysis reveals that each constituent lobe has a different in-plane orientation relative to the copper grain below and that the growth velocity of a given lobe depends strongly on its orientation relative to the underlying Cu at the growth front. We will describe the relationship between the orientation-dependent growth velocity and the local atomic geometry at the edge of the graphene sheet. Finally, the implications of this unexpected nucleation and growth mechanism on the formation of high-quality graphene films on Cu foils are evaluated.

Work at Sandia was supported by the Office of Basic Energy Sciences, Division of Materials Sciences, U. S. Department of Energy under Contract No. DE-AC04-94AL85000. Data analysis at LBNL was supported by the Director, Office of Science, Office of Basic Energy Sciences, Division of Materials Sciences and Engineering, of the U.S. Department of Energy under Contract No. DE-AC02-05CH11231, and the National Science Foundation Graduate Research Fellowship Program.

Second-layer graphene on Ir(111) – relating growth mechanism to physical and electronic structure

Kevin F. McCarty,[1] Andrew L. Walter,[2,3] Elena Starodub,[1] Shu Nie,[1] Konrad Thürmer,[1] Karsten Horn,[3] Aaron Bostwick,[2] Norman C. Bartelt,[1] and Eli Rotenberg[2]

[1]Sandia National Laboratories, Livermore, CA
[2]Advanced Light Source, Lawrence Berkeley National Laboratory, Berkeley, CA
[3]Department of Molecular Physics, Fritz-Haber-Institut der Max-Planck-Gesellschaft, 14195 Berlin, Germany

An interesting question is how the second layer of graphene grows on transition-metal substrates. First-layer graphene on Ir(111) [1] exists with four discrete in-plane orientations relative to substrate directions [2]. Thus, this system offers potential to better understand the relationship between second-layer growth and first-layer structure. We use LEEM to characterize where the second-layer graphene forms on Ir(111) covered by domains of differently oriented first-layer graphene. We find that the second layer does not grow easily where the lattice of the first-layer graphene is aligned with the lattice of the substrate. Instead the second-layer graphene forms most easily where the first-layer graphene is rotated, by 30°, for example. Angle-resolved photoemission spectroscopy (ARPES) confirms this strong preference. So how does the orientation of the first layer control the growth of the second layer? ARPES and Raman spectroscopy provide insight, revealing that the rotated variants of first-layer graphene are even less strongly bound to the substrate than the more abundant, non-rotated variant [3]. This information suggests the following growth mechanism. Carbon atoms segregating from the substrate build up in concentration under the first layer. The second layer nucleates and grows where it is easier to debond the first layer from the substrate, that is, under the rotated first-layer domains. Electron diffraction also reveals that the second graphene layers are usually but not always aligned with the first-formed layer. Finally, we will discuss the doping of the different types of second-layer graphene, as revealed by ARPES.

This work was supported by the Office of Basic Energy Sciences of the US DOE under Contracts No. DE-AC04-94AL85000 (SNL) and No. DE-AC02-05CH11231 (LBL).

[1] A. T. N'Diaye, J. Coraux, T. N. Plasa, C. Busse, and T. Michely, New J. Phys. 10, 16 (2008).
[2] E. Loginova, S. Nie, K. Thürmer, K., N. C. Bartelt, and K. F. McCarty, Phys. Rev. B 80, 085430 (2009).
[3] I. Pletikosic, M. Kralj, P. Pervan, R. Brako, J. Coraux, A. T. N'Diaye, C. Busse, and T. Michely, Phys. Rev. Lett. 102, 056808 (2009).

The role of carbon surface diffusion on the growth of epitaxial graphene on SiC

Taisuke Ohta, N. C. Bartelt, Shu Nie, Konrad Thürmer, and G. L. Kellogg
Sandia National Laboratories, Albuquerque, NM 87185 and Livermore, CA 94550

Growth of high quality graphene films on silicon-carbide (SiC) is regarded as one of the more viable pathways toward graphene-based electronics. Graphene films are readily formed on SiC by preferential sublimation of Si at elevated temperature. Little is known, however, about the atomistic processes of interrelated Si sublimation and graphene growth. We have observed the formation of graphene on SiC by Si sublimation using low energy electron microscopy (LEEM), scanning tunneling microcopy, and atomic force microscopy. This work reveals unanticipated growth mechanisms, which depend strongly on the initial surface morphology. Carbon diffusion governs the spatial relationship between Si sublimation and graphene growth. Isolated bilayer SiC steps generate narrow ribbons of graphene by a distinctive cooperative process, whereas triple bilayer SiC steps allow large graphene sheets to grow by step flow. The step-flow growth of graphene is followed using LEEM through imaging the thermionic emission from the sample. We demonstrate how graphene quality can be improved by controlling the initial step structures to avoid the instabilities inherent in diffusion-limited growth. We also show how varying the polytype (6H or 4H) influences the growth front and graphene formation.

This work is supported by the LDRD program at Sandia Labs and the US DOE Office of Basic Energy Sciences, Division of Materials Science and Engineering (DE-AC04-94AL85000), and was performed in part at CINT (DE-AC04-94AL85000). Sandia is a multiprogram laboratory operated by Sandia Corporation, a Lockheed Martin Co., for the U.S. DOE NNSA (DE-AC04-94AL85000).